AD-A062 567 AUSTRALIAN NATIONAL UNIV CANBERRA RESEARCH SCHOOL OF--ETC F/G 4/1
RESEARCH ON LINEAR AND NONLINEAR ATMOSPHERIC WAVES.(U)
AUG 78 D R CHRISTIE, K J MUIRHEAD, A L HALES AFOSR-75-2759
UNCLASSIFIED 78-1 AFOSR-TR-78-1642 NL

1 OF 2
AD
A062567

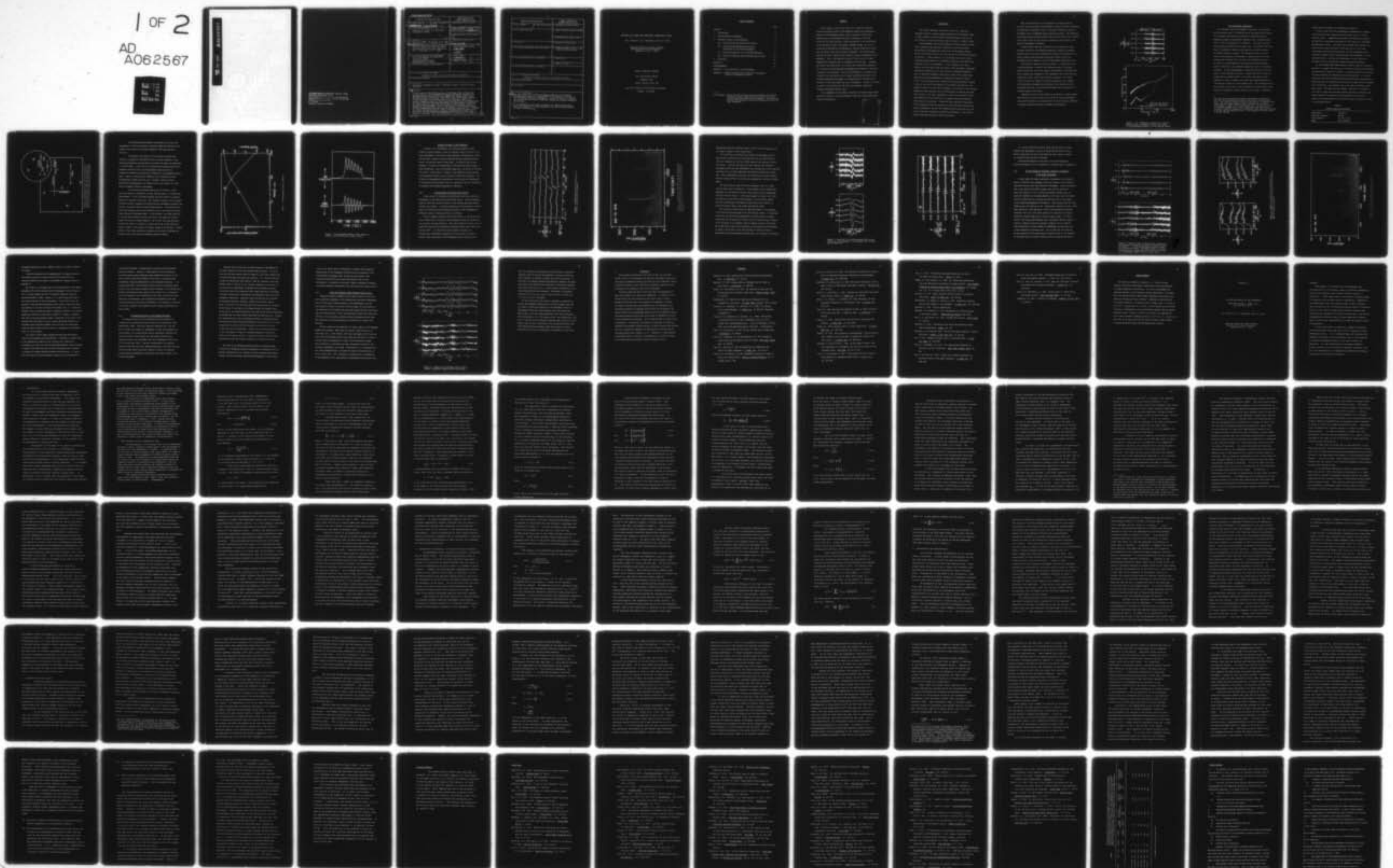

UNCLASSIFIED

i

(19) REPORT DOCUMENTATION PAGE		READ INSTRUCTIONS BEFORE COMPLETING FORM
(18) 1. Report Number AFOSR TR- 78-1	2. Govt Accession No. 642	3. Recipient's Catalog Number (9)
4. Title (and Subtitle) (6) Research on Linear and Nonlinear Atmospheric Waves.		5. Type of Report & Period Covered Final Scientific Report, 30 Period ending ~~August 1,~~ 1978.
(14)		6. Performing Org. Report Number 78-1
(10) 7. Author(s) D.R. Christie, K.J. Muirhead, ~~K.J., and~~ A.L. Hales, A.L.		8. Contract or Grant Number (15) AFOSR-75-2759
9. Performing Organization Name and Address Research School of Earth Sciences The Australian National University Box 4, Canberra, A.C.T. 2600		10. Program Element, Project, Task Area & Work Unit Numbers OTAFUONP 6799
11. Controlling Office Name and Address Air Force Office of Scientific Research, /NP Bolling Air Force Base, WASHINGTON D.C. 20332	(11)	12 Report Date 1 ~~August, 19~~78 (12) 171 p.
		13. Number of Pages 167
14. Monitoring Agency Name and Address		15.

16. & 17. Distribution Statement

Approved for public release; distribution unlimited.

18. Supplementary Notes

19. Key Words

Nonlinear atmospheric waves, Infrasonic waves, Solitary waves, Solitons

20. Abstract

In this report we review the results of a three-year study of linear and nonlinear waves in the atmosphere based on an experimental program at the Warramunga Seismic Station located at 19 deg 56 min S near Tennant Creek in the Northern Territory of Australia. The first section of the report provides a brief description of the installation of the infrasonic arrays, the acoustic sounding system, the array-associated meteorological instrumentation, the data acquisition system and the digital time series analysis techniques. The second section outlines the basic studies of four separate classes of atmospheric wave phenomena. First, a description is given of the discovery of three fundamentally different types of atmospheric solitary wave. Secondly, the results and implications of a study of the evolutionary properties of a new form of soliton-generating propagating disturbance in the lower troposphere are presented. The third investigation is concerned with a study of →

next page

FORM 1473

409 896

sml

REPORT DOCUMENTATION PAGE		READ INSTRUCTIONS BEFORE COMPLETING FORM
1. Report Number	2. Govt Accession No.	3. Recipient's Catalog Number
4. Title (and Subtitle)		5. Type of Report & Period Covered
		6. Performing Org. Report Number
7. Author(s)		8. Contract or Grant Number
9. Performing Organization Name and Address		10. Program Element, Project, Task Area & Work Unit Numbers
11. Controlling Office Name and Address		12. Report Date
		13. Number of Pages
14. Monitoring Agency Name and Address		15.
16. & 17. Distribution Statement Approved for public release; distribution unlimited.		
18. Supplementary Notes		
19. Key Words		

20. Abstract (continued)

cont. the characteristics of acoustic microbarom radiation in the Southern Hemisphere with regard to a determination of the equatorial structure of the stratosphere and lower thermosphere. Finally, an outline is given of the research into the origin of nonlinear long-period irregular atmospheric gravity waves.

In the appendices of this report we present two separate papers which detail the studies of solitary atmospheric waves and soliton-generating intrusive disturbances.

FORM 1473

RESEARCH ON LINEAR AND NONLINEAR ATMOSPHERIC WAVES

D.R. Christie, K.J. Muirhead, and A.L. Hales

Research School of Earth Sciences
Australian National University
Canberra, A.C.T., 2600.

FINAL SCIENTIFIC REPORT

for the period ending

1 August 1978,

under contract with the

Air Force Office of Scientific Research

AFOSR - 75.2759A

TABLE OF CONTENTS

Cover diagram: The two-soliton collision process described by the recently discovered (Joseph, 1977a) N-soliton solution to the nonlinear dispersive Benjamin-Ono wave equation. This equation describes the evolution of long finite-amplitude waves in the lower troposphere.

ABSTRACT

In this report we review the results of a three-year study of linear and nonlinear waves in the atmosphere based on an experimental program at the Warramunga Seismic Station located at 19°56'S near Tennant Creek in the Northern Territory of Australia. The first section of the report provides a brief description of the installation of the infrasonic arrays, the acoustic sounding system, the array-associated meteorological instrumentation, the data acquisition system and the digital time series analysis techniques. The second section outlines the basic studies of four separate classes of atmospheric wave phenomena. First, a description is given of the discovery of three fundamentally different types of atmospheric solitary wave. Secondly, the results and implications of a study of the evolutionary properties of a new form of soliton-generating propagating disturbance in the lower troposphere are presented. The third investigation is concerned with a study of the characteristics of acoustic microbarom radiation in the Southern Hemisphere with regard to a determination of the equatorial structure of the stratosphere and lower thermosphere. Finally, an outline is given of the research into the origin of nonlinear long period irregular atmospheric gravity waves.

In the appendices of this report we present two separate papers which detail the studies of solitary atmospheric waves and soliton-generating intrusive disturbances.

1. INTRODUCTION

This report summarizes the salient results of a three-year atmospheric physics research program undertaken by the Research School of Earth Sciences at the Australian National University for the Air Force Office of Scientific Research under Contract No. AFOSR-75.2759A.

The experimental side of this program is centered around a continuously operating high-resolution infrasonic array and associated meteorological instrumentation installed at the Warramunga Seismic Station near Tennant Creek in the arid interior of the Northern Territory of Australia. A major objective of this program has been to achieve a thorough understanding of the fundamental processes which govern the dynamical state of the atmosphere. It was recognized at an early stage in this work that linear wave theory, while providing a reasonably satisfactory explanation of a wide variety of atmospheric phenomena, gives a completely inadequate description of many of the unique large-amplitude propagating atmospheric disturbances observed at Tennant Creek. This investigation has therefore been directed primarily towards a study of the role of nonlinearity in the general description of the dynamical structure of the lower atmosphere. In particular, this research program has been concerned with an interpretation of observed nonlinear fluid motions in the lower troposphere in terms of the presently understood behaviour of the solutions to the general nonlinear dispersive evolutionary wave equations. Perhaps the most significant achievement of this program has been the discovery of three basically different new forms of atmospheric solitary wave phenomena and the discovery of a new class of nonlinear propagating atmospheric disturbance in the form of soliton-producing interfacial density intrusions.

Many of the features of the observations at Tennant Creek may be seen in the array record section shown in Figure 1(a) which illustrates the differential signatures of both a nonlinear interfacial intrusive disturbance and an independent pure solitary wave packet. The difference in the power spectra evaluated before and after the onset of the intrusive event (Figure 1(b)) may be viewed as a measure of the increase in the degree of atmospheric turbulance.

Further studies have been carried out on the influence of high altitude structure on the observed properties of acoustic microbarom radiation and on the source mechanisms and spectral characteristics of unusual complex large-amplitude long-period irregular shear wave disturbances which commonly occur at the Warramunga experimental site.

This report is organized into two sections. In the first section a brief description is given of the infrasonic array, the acoustic radar installation, the various types of meteorological instrumentation used to measure the parameters of the atmospheric flow field, the data acquisition system and the data analysis techniques. The second section outlines the studies of solitary atmospheric waves, complex soliton-generating atmospheric disturbances, the characteristics of microbarom radiation in the Southern Hemisphere and the properties of nonlinear gravity shear waves.

Appendices A and B of this report are presented as separate papers which detail the initial results of the study of solitary atmospheric waves and the results of an investigation of the evolutionary properties of complex propagating nonlinear atmospheric disturbances.

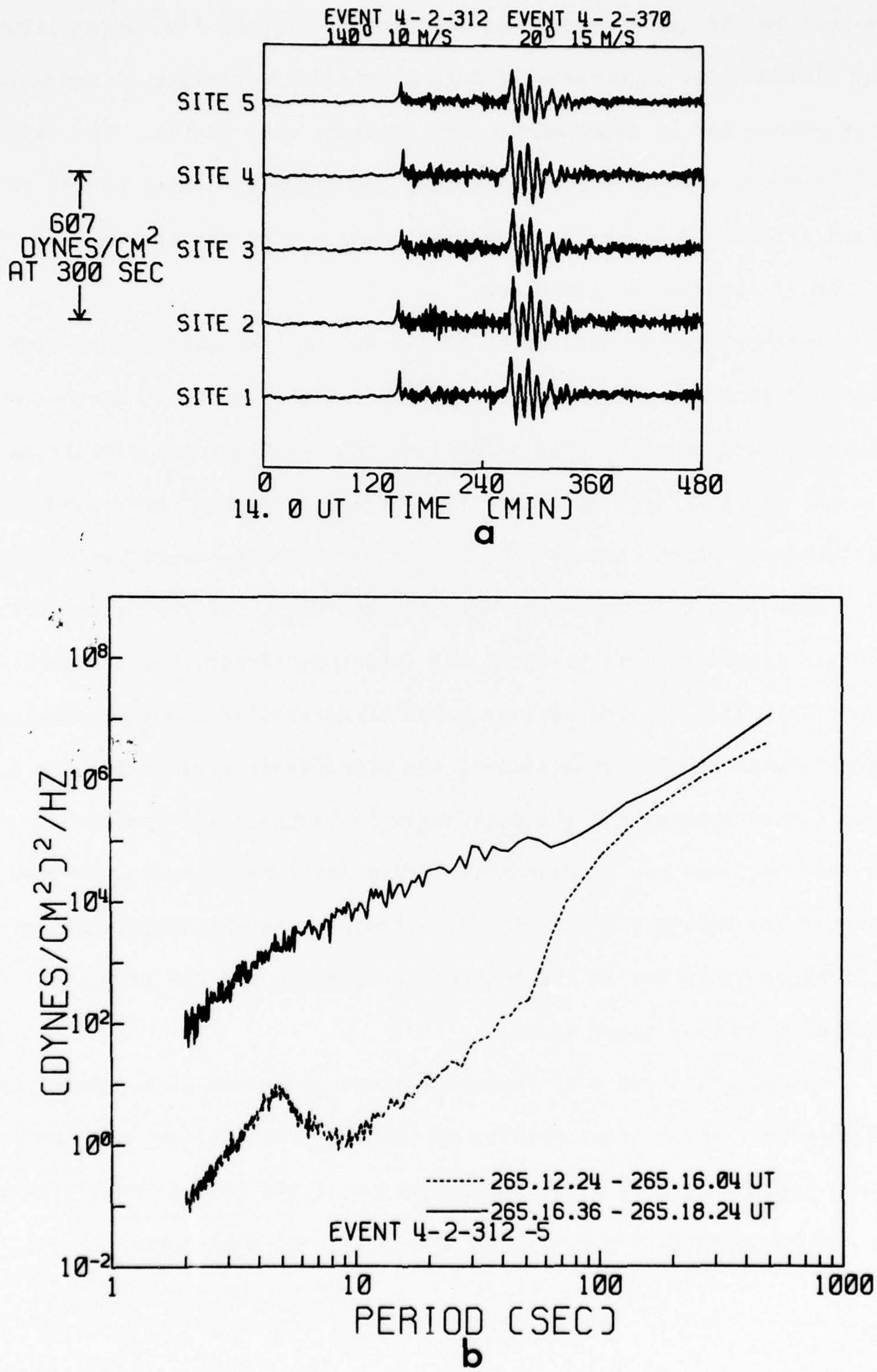

Figure 1. (a) Differential signature of a density intrusion and an independent soliton wave packet. (b) Corresponding estimates of power spectral density.

2. THE EXPERIMENTAL ARRANGEMENT

The infrasonic array at Warramunga is located on an essentially flat semi-desert plain, 37 kilometers SSE of the Tennant Creek airport. In its original form the array consisted of 5 National Bureau of Standards designed microbarometers configured into a centered quadrilateral with a net aperture of 4 kilometers. This main array has been operating continuously since August 1975. In November, 1977, the array was expanded to include a small aperture tripartite subarray of portable infrasonic elements. The operation of this new array serves the dual purpose of furnishing a rigorous field test for the portable array elements and at the same time providing data which is suited to an investigation of high altitude structure through a study of variations in the apparent propagation vector of microbarom radiation. All the microbarograph installations include an efficient Daniels' noise-reducing line filter. Signals from the two arrays are transmitted via overhead lines[†] to the central recording station, sampled at a rate of 2 samples per second, and recorded digitally in IBM-compatable format on 7-track magnetic tape. The configurations of the two arrays, the site of a vault containing a Geotech vertical long period S11 seismometer, and the locations of the array - associated

----

[†] The start of the experimental program at Warramunga was delayed by a bush fire which destroyed the original land lines to the main array sites. The original telemetry system was replaced by an overhead system consisting of #8 gauge aluminium signal lines carried on 10 meter poles beneath a single strand of galvanized wire. The galvanized wire is carefully grounded and is used in conjunction with high voltage isolation transformer coupling and conventional surge arresting techniques to protect against lightning strikes. This telemetry system has proven to be very reliable.

meteorological instruments are illustrated in Figure 2.

As can be seen all of the meteorological instruments are located in the vicinity of the long period seismic vault and site 1 of the infrasonic array. Temperature, wind speed, wind direction, rainfall and humidity are monitored continuously at the surface by a SIAP S2000 meteorological station. A 20 meter radio telemetry tower located on a steep 30 meter ridge, 400 meters to the east of site 1, has been instrumented with National Semiconductor LX 5700A integrated circuit temperature tranducers and a high resolution pitot anemometer. At the recording station, a sensitive millibarograph is used to provide a continuous record of the absolute surface pressure perturbations.

An Aerovironment model 300C monostatic acoustic radar was installed near site 1 in August 1977 and has, at the time of writing, been operating continuously for a period of 11 months. During this period a wide variety of unique nonlinear wave disturbances have been observed. It is worth noting that the results obtained during this observational period clearly demonstrate that the combination of the acoustic sounder and the infrasonic array constitutes a very powerful tool in the study of nonlinear atmospheric waves. The output from the acoustic radar, which is recorded in real time on a grey-scale facsimile machine, provides a continuous time-height display of the temperature microstructure over the array. A summary of the specifications of the acoustic radar installation is given in the following table.

TABLE 1.

ACOUSTIC RADAR SPECIFICATIONS

Output power	100 watts
Acoustical frequency	1600 Hz
Pulse duration	50, 100, 200 ms
Range	30 m to 1000 m

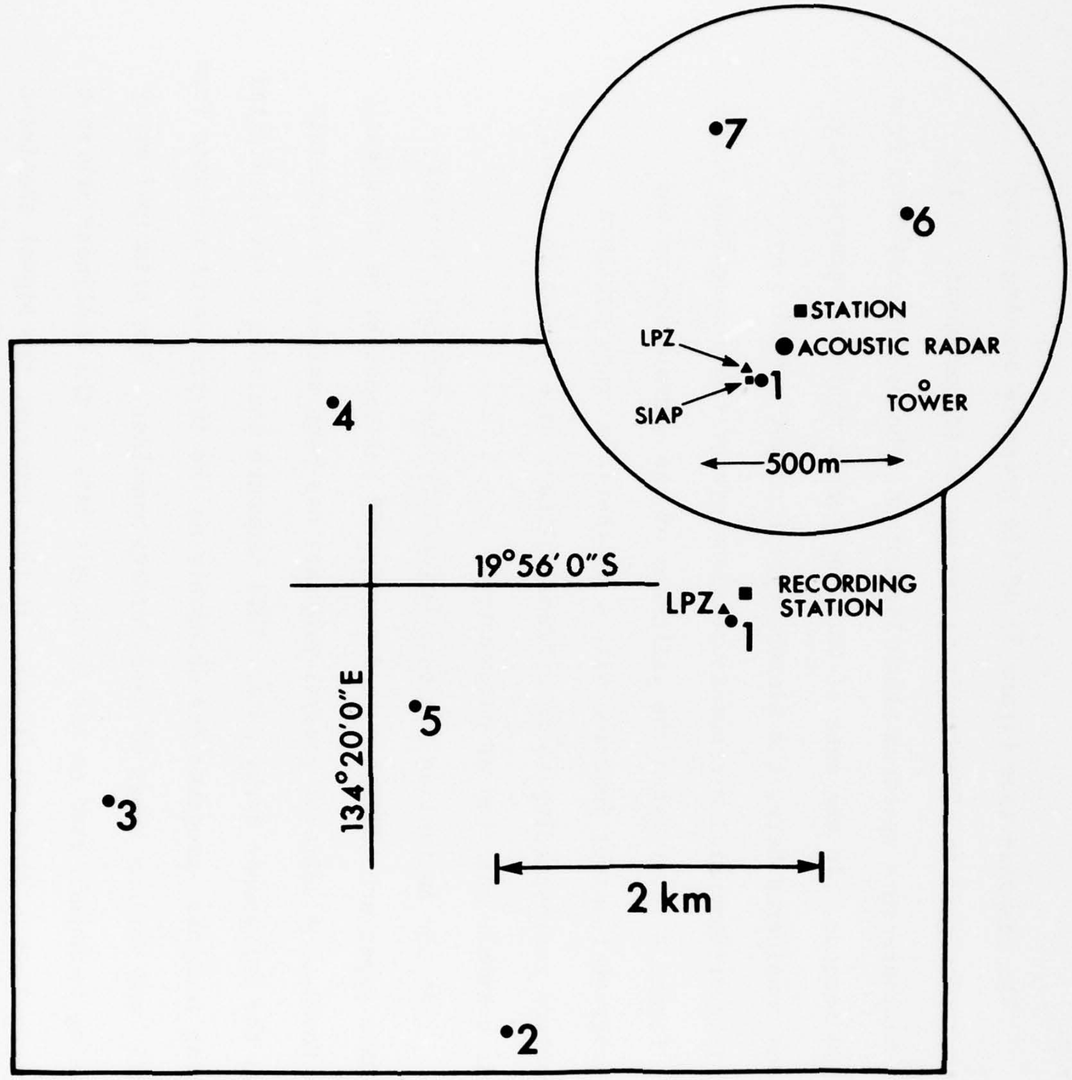

Figure 2. Configuration of the 4 km five-component and the 600 m three-component infrasonic arrays, and the location of the acoustic radar, the long period seismic vault and the associated meteorological instrumentation.

The continuous meteorological observations at the array are supplemented at 6-hourly intervals by balloon flight observations at the Tennant Creek airport of the upper atmospheric wind speed and wind direction.

The response (see Figure 3) of the pressure sensing array elements is designed to effectively filter out those components in the surface micropressure spectrum which lie outside the useful pass-band from 1 to 1000 seconds. In the case of the long-period nonlinear gravity wave phenomena considered here, the microbarograph output provides an essentially differential micropressure signature of the propagating disturbance. Figure 4 illustrates the influence of the convolution of the microbarograph transfer function with a synthetic surface pressure perturbation corresponding to an ordered solitary wave packet in a form which is commonly observed at Warramunga.

At the Australian National University the 556 bpi, 7-track basic data tapes are converted to 9-track, 800 bpi tapes in an efficiently packed format. A suite of general programs has been written to routinely process the infrasonic array data. This sequence includes a set of digital filtering routines, programs for deconvolving the instrumental response from the data and various types of beam-forming routines. The principal array processing technique used on the infrasonic data is the nonlinear Nth-root process devised by Muirhead (1968). In this process, the signal statistic is derived from the phased sum over the array of the digitally filtered output of each array element reduced to the Nth root with sign preserved. The Nth-root process is superior to linear processing in that additional weight is given to the presence of coherent energy in the spectrum. Further details on the signal processing techniques may be found in Muirhead and Ram Datt (1976) and in Christie, Muirhead and Hales (1978a).

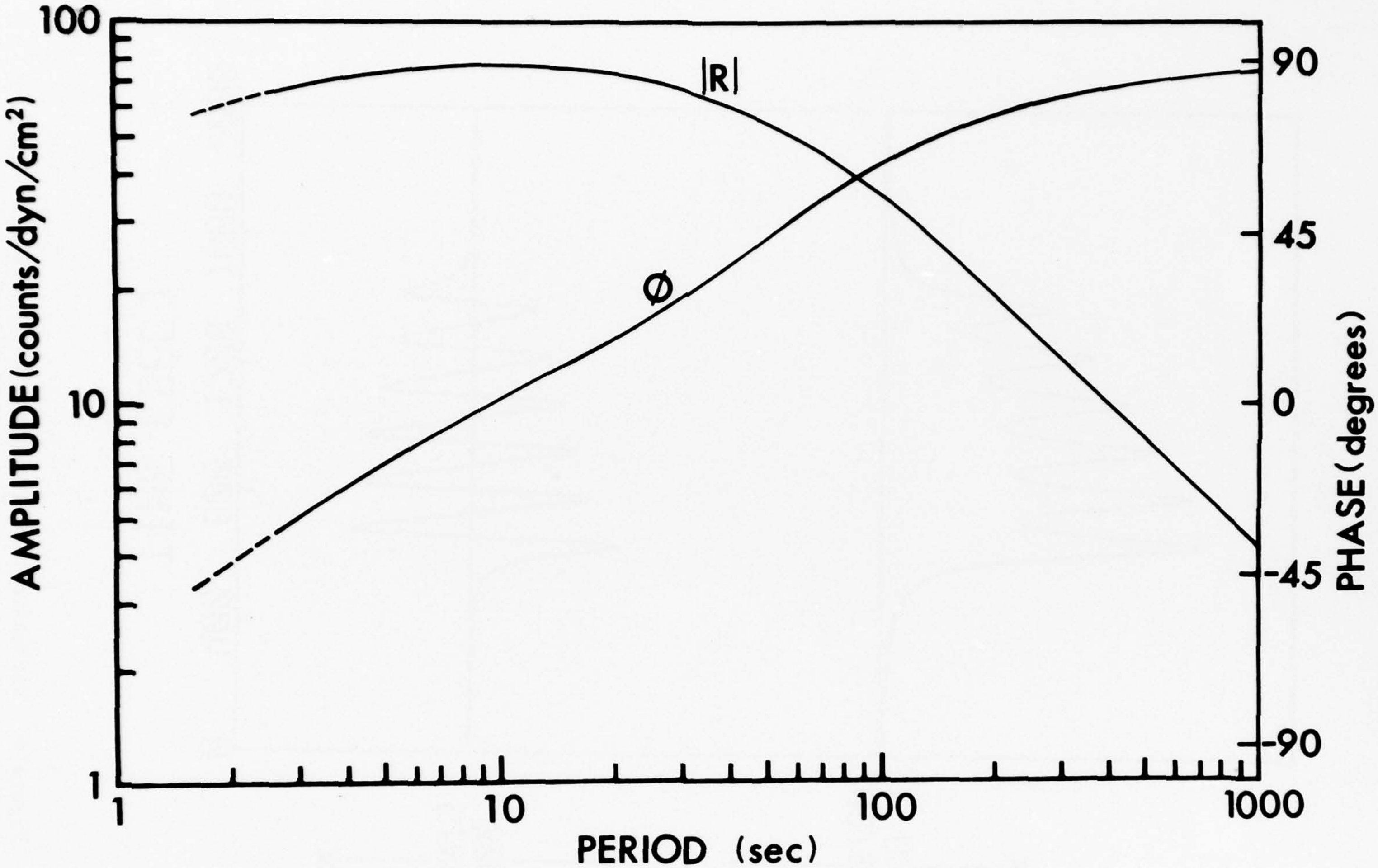

Figure 3. Microbarograph transfer function.

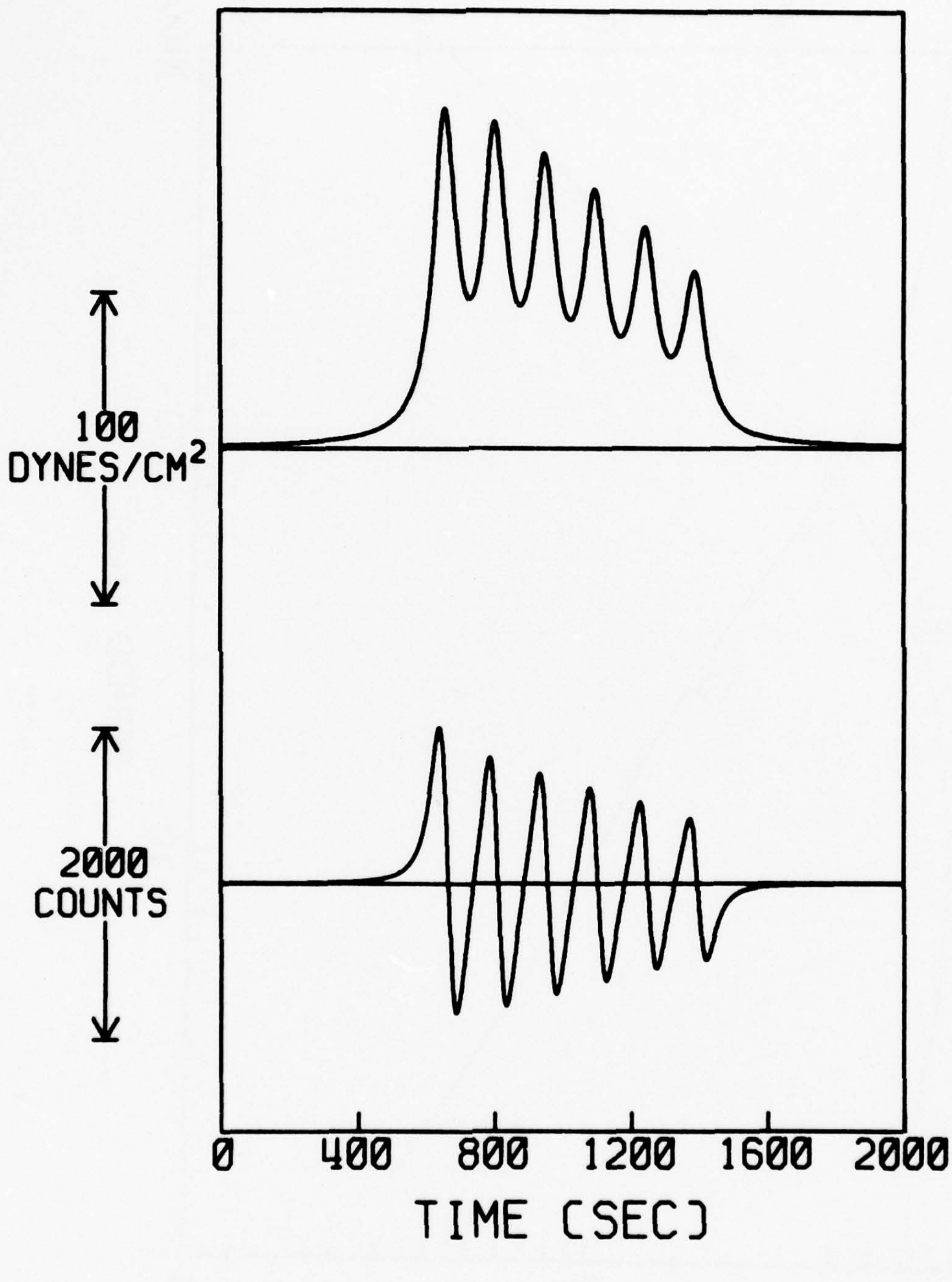

Figure 4. Microbarograph response (lower figure) to synthetic soliton wave packet (upper figure).

3. RESEARCH ON WAVES IN THE ATMOSPHERE

As noted in the introduction, this research program has been primarily oriented towards a study of nonlinear dispersive waves in the lower troposphere in the form of large amplitude, extraordinarily stable solitary waves, complex soliton-producing nonlinear propagating disturbances and nonlinear gravity shear waves. The overall goal of this program is to obtain an understanding of the mechanisms which produce these disturbances, their evolutionary properties, the nature of the asymptotic state - particularly in regards to the underlying reasons behind the exceptional stability of the internal solitary wave component - the influence of topographical perturbations, the form and the consequences of the nonlinear wave-boundary layer jet interaction and the significance of nonlinear wave-generated atmospheric turbulence.

3(a) SOLITARY WAVES AND SOLITARY WAVE PACKETS

A wide variety of solitary wave disturbances have been observed at Warramunga over the three-year observational period. These disturbances range in form from isolated solitons to well-defined amplitude-ordered solitary wave packets. A detailed examination of the properties of these waves has shown that these disturbances belong to three fundamentally different classes of internal solitary wave motion.

The most commonly observed solitary wave form is a relatively small scale isolated wave of elevation which propagates along the interface of the nocturnal radiation inversion; these waves belong to the new class of deep fluid solitary wave considered by Benjamin (1967) and by Davis and Acrivos (1967). An array record section which illustrates the characteristic differential signature of a wave of this type and an acoustic radar observation of two independent stable solitary waves

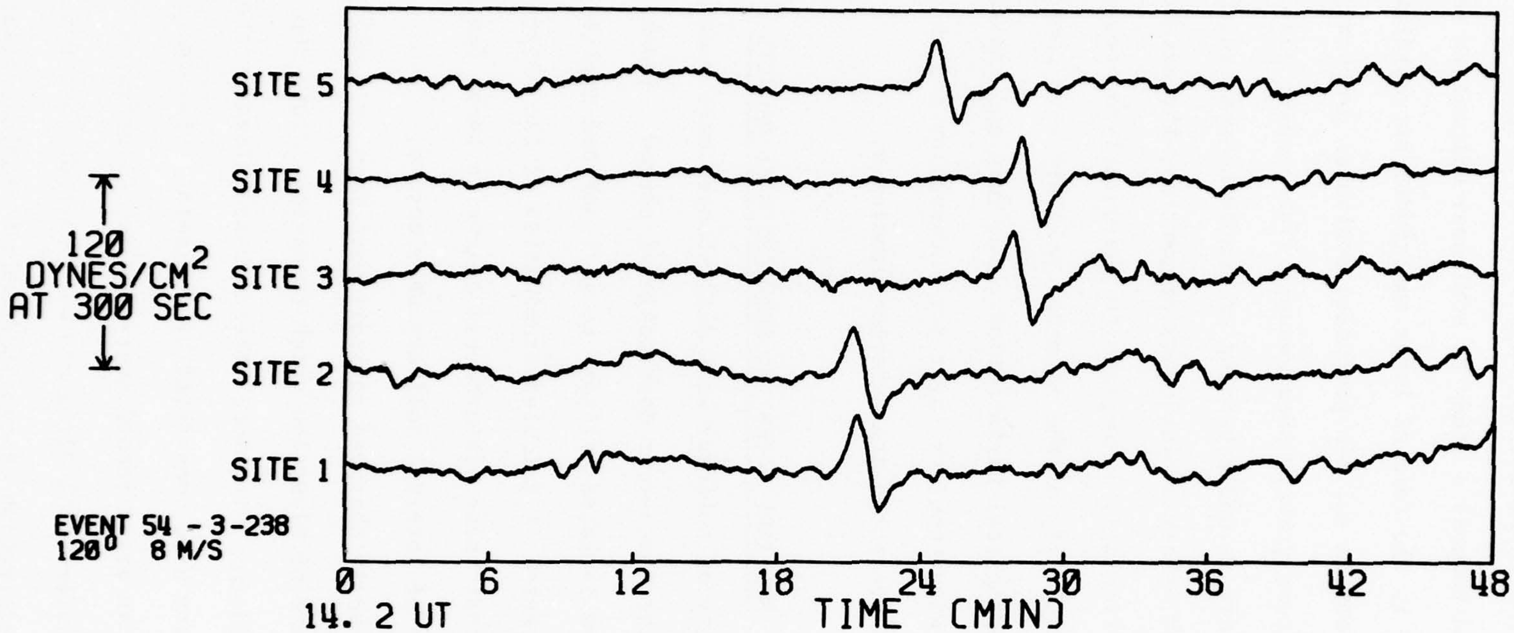

Figure 5. Microbarograph array observation of an isolated solitary wave of elevation.

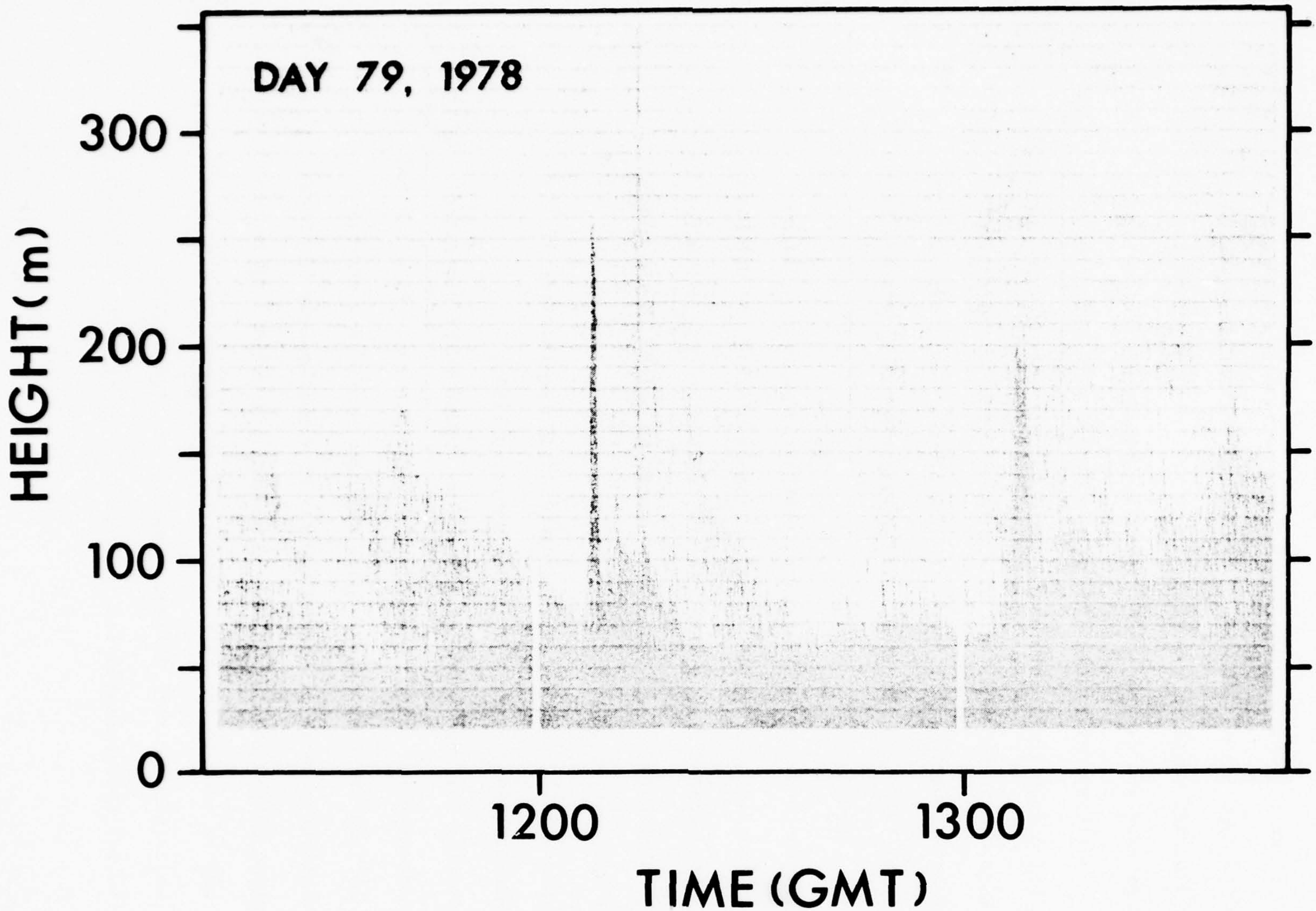

Figure 6. Acoustic radar facsimile record illustrating two deep-fluid solitary waves of elevation propagating along the disturbed surface of the nocturnal radiation inversion.

propagating along the disturbed surface of the nocturnal boundary layer are shown in Figures 5 and 6 respectively.

The second type of solitary wave observed at Warramunga occur as large-scale isolated waves of elevation which are best described by a classical (Korteweg and de Vries, 1895) shallow-fluid internal solitary wave theory. Solitary waves have also been observed with effective wavelengths which span the intermediate scale between that of the classical stationary wave of finite amplitude and Benjamin's deep-fluid solitary wave. These intermediate-scale waves are described by the new solution found by Joseph (1977b) for solitary wave propagation in fluids of finite depth.

The third distinct type of solitary atmospheric wave is a large-scale solitary wave of depression. A good example of this unusual wave phenomena is illustrated in the array record section and corresponding inversion shown in Figure 7. These waves appear to belong to the class of classical solitary waves which propagate in a fluid whose density decreases exponentially with height as described by the theories of Peters and Stoker (1960), Long (1965) and Benjamin (1966).

The classical solitary waves of depression appear to be generated in the final dissipating stage of dry cold frontal systems. As described in the next section existing experimental evidence provides a strong indication that the genesis of solitary waves of elevation may be traced to the evolution of the commonly observed complex intrusive disturbance This aspect may be seen in the infrasonic array record section presented in Figure 8 which shows a well defined group of isolated solitons preceeding the soliton-dominated leading edge of an intrusive disturbance.

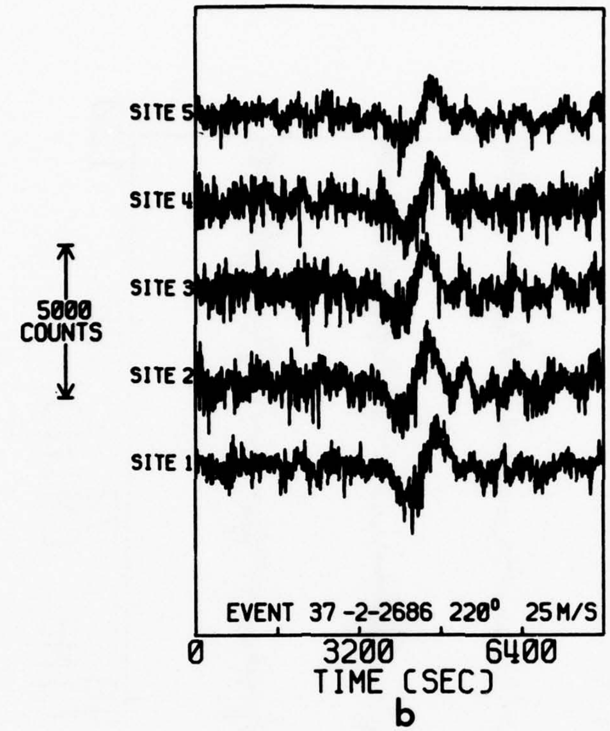

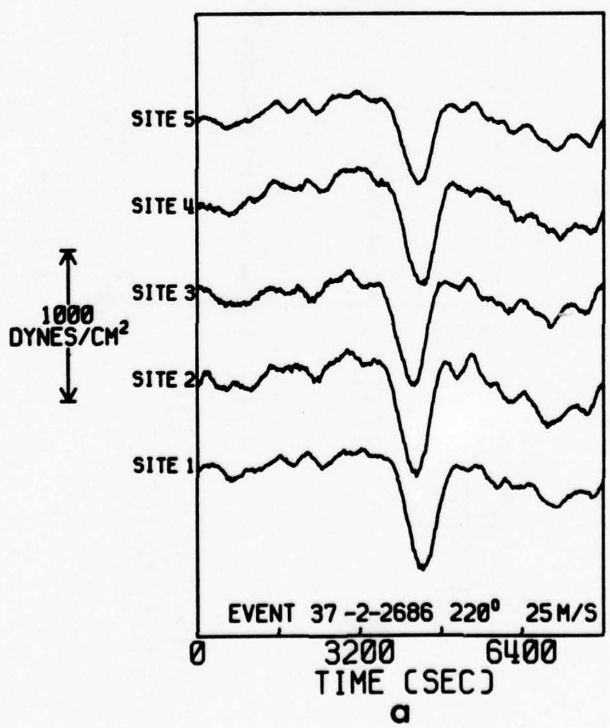

Figure 7. Inversion (a) of microbarograph array record section (b) corresponding to a good example of a solitary wave of depression.

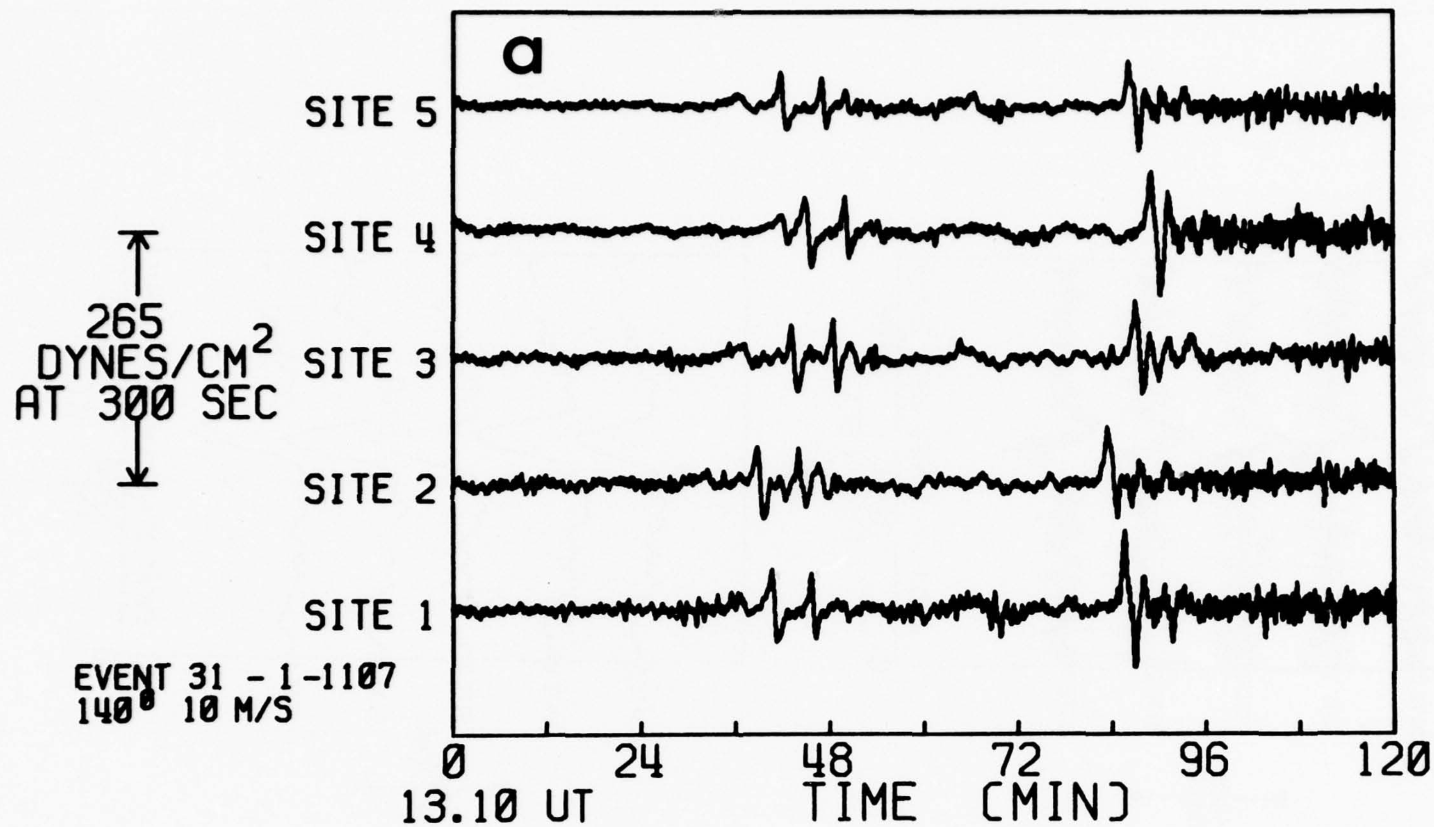

Figure 8. Microbarograph array record section showing a family of solitons preceeding the soliton-dominated leading edge of a density intrusion.

It is worth noting that boundary layer solitary waves have been observed with amplitudes in excess of 700 meters and that the fluid motions associated with these large-amplitude waves present a hazard to aircraft during take-off and landing.

A detailed description of the results of an investigation of solitary atmospheric waves is presented as a separate paper in Appendix A.

3(b) SOLITON-GENERATING NONLINEAR INTRUSIVE DISTURBANCES IN THE LOWER TROPOSPHERE

A large number of unusual atmospheric disturbances in the form of density intrusions which propagate along the interface of the nocturnal radiation inversion have been observed at Warramunga. These disturbances span a wide range of horizontal length scales and are observed to occur (see Figures 9 to 11) as relatively smooth internal bores, as spatially extended well developed families of solitary waves associated with the leading edge of a dissipating intrusion, and as very complex soliton-dominated propagating disturbances. These observations have been compared with the behaviour of the nonstationary solutions (Joseph, 1977a; Meiss and Perira, 1978; Maxworthy, 1978) of the Benjamin-Ono equation (Benjamin, 1967; Ono, 1975) which describe the evolution of nonlinear dispersive internal long waves in fluids of great depth. The theory predicts that long smooth boundary layer disturbances should steepen in regions of negative slope and eventually condense into an asymptotic state consisting of a finite number of independent solitary waves and a small dispersive oscillatory tail. This is precisely the behaviour pattern indicated by the observations at Tennant Creek; it may therefore be concluded that the isolated solitary waves of elevation observed at

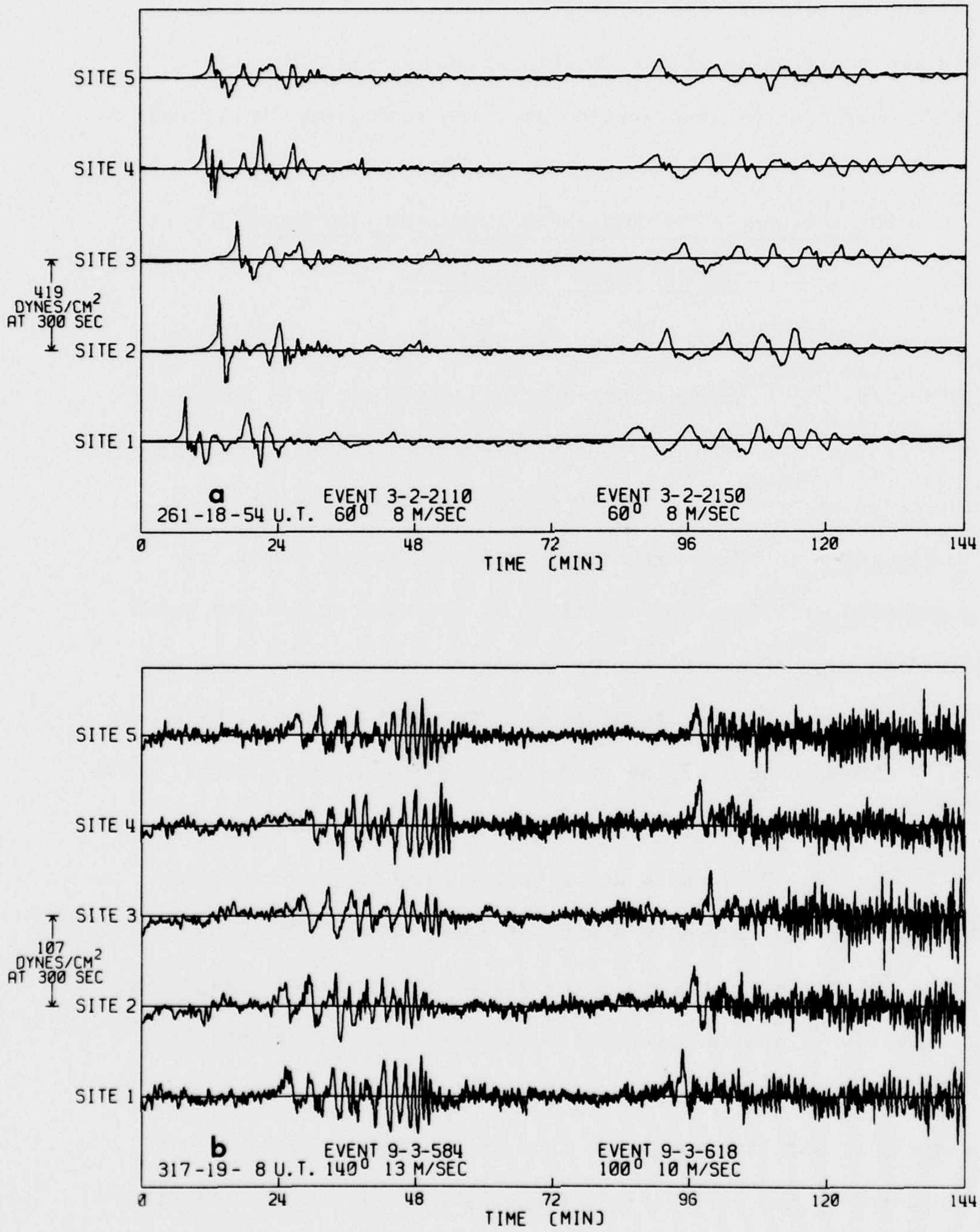

Figure 9. Infrasonic array record sections illustrating the differential signatures of complex elevated intrusive disturbances. (a) Soliton-dominated intrusion followed by a soliton wave packet. (b) Ordered family of solitons arranged along the leading edge of an intrusion followed by an independent simple intrusive density flow.

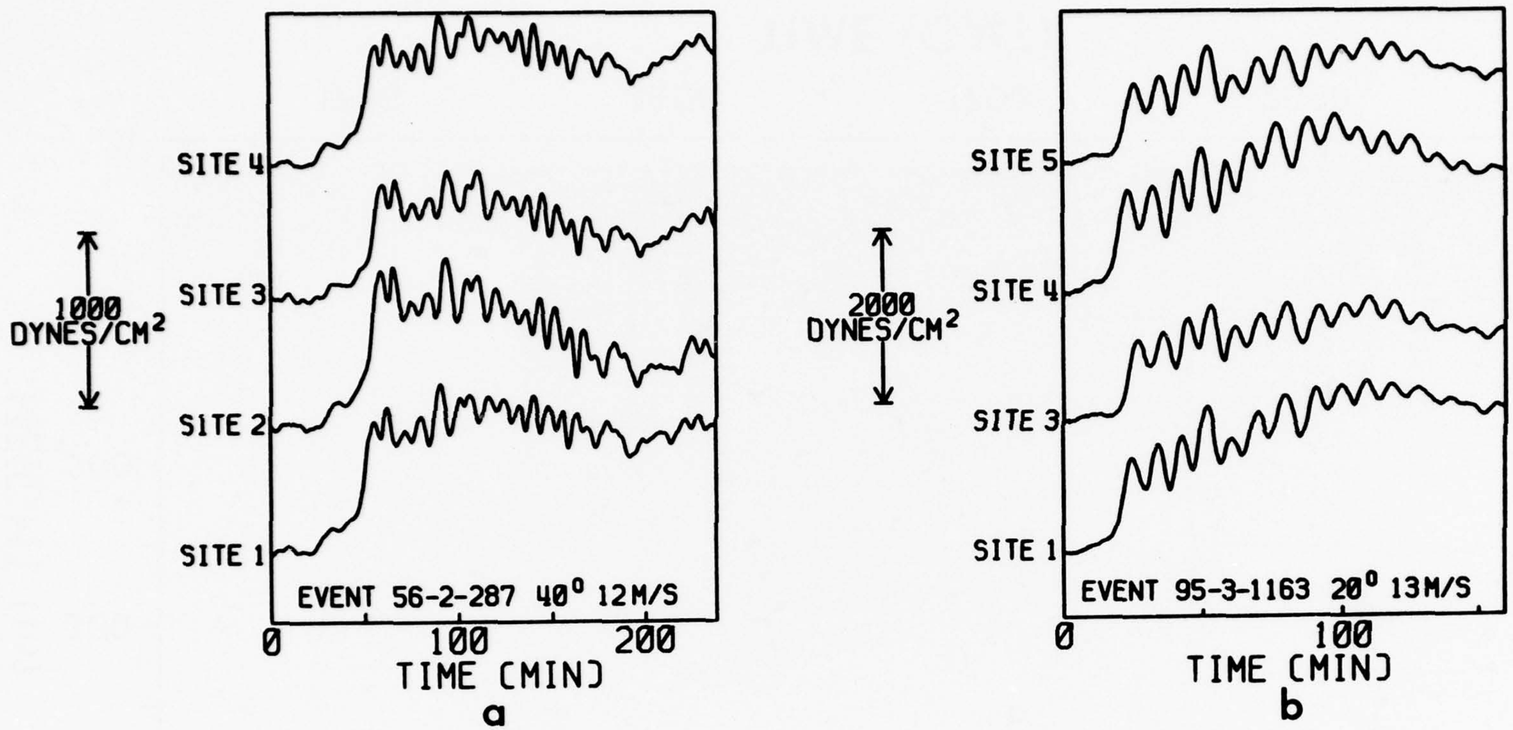

Figure 10. Examples of observations of extensive well-developed families of solitons associated with the leading edge of a density intrusion.

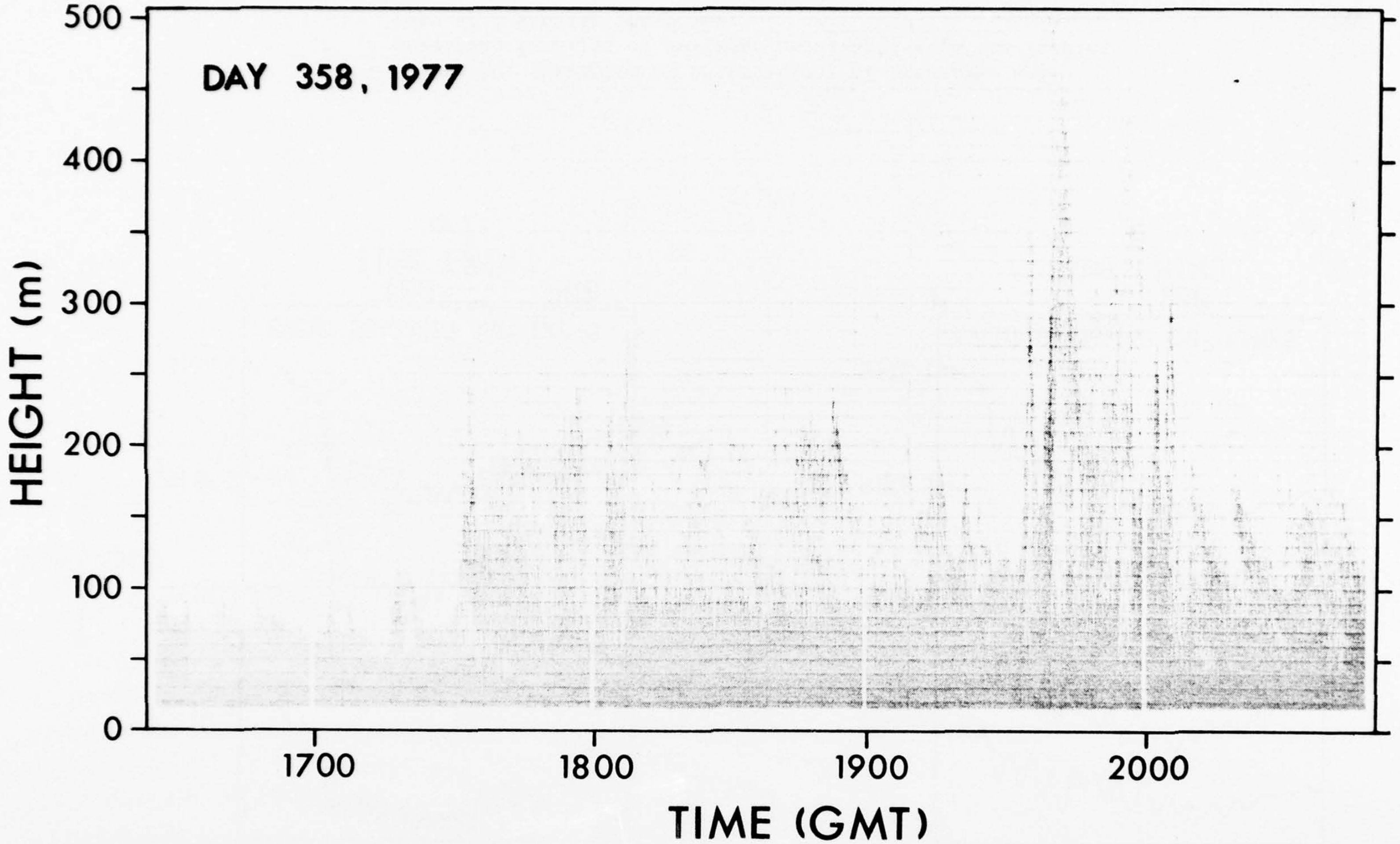

Figure 11. Acoustic sounding record of a complex solitary-wave-dominated intrusive disturbance.

Warramunga represent the time- asymtotic state of interfacial density intrusions.

A detailed comparison of the morphology of the complex intrusive disturbances observed at Tennant Creek with the predictions of nonlinear dispersive wave theory is presented as a separate study in Appendix B.

The results of a thorough study of the perturbations of the ambient atmospheric flow field associated with the passage of these intrusive flows is being prepared and will be published separately (Christie, Muirhead and Hales, 1978b). However, it is worth noting here some of the unusual features of these observations. In the first place, the passage of these elevated disturbances often result in only very minor perturbations to the flow field near the surface (see, e.g., Figure 9a). Secondly, these disturbances produce a temporary increase in the surface temperature which may, in some cases, exceed 5°C. Finally, it appears that some of these disturbances induce a transition in the state of the boundary layer from that of a static stably-stratified inversion to a thoroughly mixed turbulent boundary layer, and that the concomittant change in eddy viscosity leads in turn to a recoupling of the boundary layer jet to the surface.

The origin of these complex propagating nonlinear disturbances remains an outstanding unresolved problem. A theoretical estimate based on the Benjamin-Ono equation of the 'sorting time' required for disturbances to evolve into the well-developed asymtotic states observed at Tennant Creek shows that many of these disturbances must originate at distances of several hundred kilometers from the array. It seems clear that some of these disturbances originate in the interaction of

thunderstorm downdraft - produced density currents with the nocturnal radiation inversion. However, a large number of these disturbances have been observed under conditions where thunderstorm activity is completely absent within 500 kilometers of the array; in addition these disturbances originate predominately in two preferred directions. It is proposed that many of the relatively small intrusive disturbances which arrive at the array from an azimuth of 140° originate in the interaction of katabatic flow from the small range of hills which lie at a distance of about 100 kilometers to the south-east of the array, and that the large-amplitude, well-developed, soliton-dominated disturbances which come from the direction of the Gulf of Carpentaria, 550 kilometers to the north of the array, represent the asymptotic state of deeply-penetrating sea-breeze fronts.

3(c) MICROBAROM RADIATION IN THE SOUTHERN HEMISPHERE

Microbarom acoustic waves are radiated into the atmosphere by standing waves associated with severe storms at sea (Posmentier, 1967; Brekhovskikh, 1968). Their most important characteristic, from the point of view of the studies at Warramunga, is that they propagate over long distances via a high-altitude acoustic atmospheric waveguide and thus they provide a direct means for continuously monitoring the dynamical state of the stratosphere and lower thermosphere (Rind et al., 1973; Rind and Donn, 1975). Previous investigations of microbarom radiation (Donn and Rind, 1972; McDonald and Herrin, 1972; Rind and Donn, 1978) have been almost exclusively limited to studies of radiation propagating along predominately zonal paths from source regions in the Northern Hemisphere.

Acoustic waves of this type are always present at Warramunga and are often observed to occur with unusually high intensity. As can be seen from the power spectra shown in Figure 1b, these waves dominate the low-noise short-period micropressure spectrum. It is worth noting here a number of observations that indicate that the infrasonic array near Tennant Creek is sited in one of the best locations on the surface of the Earth for an experimental investigation of microbarom radiation. In the first place, the essentially flat inland semi-desert environment of Tennant Creek favours long periods of exceptionally stable low-noise atmospheric conditions - conditions which are ideal for the detection of microbarom radiation. Secondly, suitable active source regions exist to the east in the Coral Sea and in the western area of the South Pacific Ocean, to the south in the Tasman Sea and the Southern Ocean, to the west in the Indian Ocean and to the north in the Gulf of Carpentaria, the Arafura Sea, the North Pacific Ocean and the South China Sea. Thirdly, this omnidirectional source distribution provides a unique opportunity for the study of high altitude perturbations associated with microbarom propagation vectors directed both along the axis of zonal flow and in the direction of the meridian. Finally, the low-latitude location of the array permits a study of microbarom propagation along paths which cross the equator and thus a study may be made of high-altitude perturbations which are uniquely confined to the equatorial region.

The study of the microbarom radiation which is currently being carried out at Warramunga therefore encompasses an investigation of the spectral characteristics of a variety of sources ranging from tropical cyclones in both the Southern and Northerm Hemispheres to severe polar

storms in the south, and an investigation of high-altitude dynamical perturbations of the atmosphere associated with the migration of the Inter-Tropical Convergence Zone, diurnal and semi-diurnal tides, equatorial forced Kelvin and mixed Rossby-gravity waves in the stratosphere, the equatorial electrojet, sudden stratospheric warmings, travelling ionospheric disturbances and ultra-long period gravity waves.

3(d) LINEAR AND NONLINEAR SHEAR-GENERATED GRAVITY WAVES

Long-period complex irregular gravity waves constitute one of the most significant components in the micropressure spectrum at Warramunga. Waves of this type are always present at the experimental site and are observed to occur in a variety of forms (Figure 12) with periods in the range from 4 to 40 minutes and with phase speeds between 8 and 50 m/s. They are often observed to occur with amplitudes greater than 1000 dynes/cm^2 and, on a few occasions, periods of greatly enhanced activity have been observed to extend continuously over intervals of several weeks duration.

Previous studies of the properties of similar types of wave phenomena (Madden and Claerbout, 1968; Herron and Tolstoy, 1969; Herron et al., 1969; Donn et al., 1973; Keliher, 1975; Paul and Madden, 1977; Essex and Love, 1978; and Gedzelman and Rilling, 1978) have focussed on a higher-altitude source interpretation in terms of wave generation through shear instability or nonlinear wave-wave interactions associated with the upper tropospheric jet streams. Nevertheless, it is recognized that this source mechanism fails to account for many of the observations of waves in this class. This conclusion is reinforced by an examination of the properties of the wave patterns at Warramunga which indicate that,

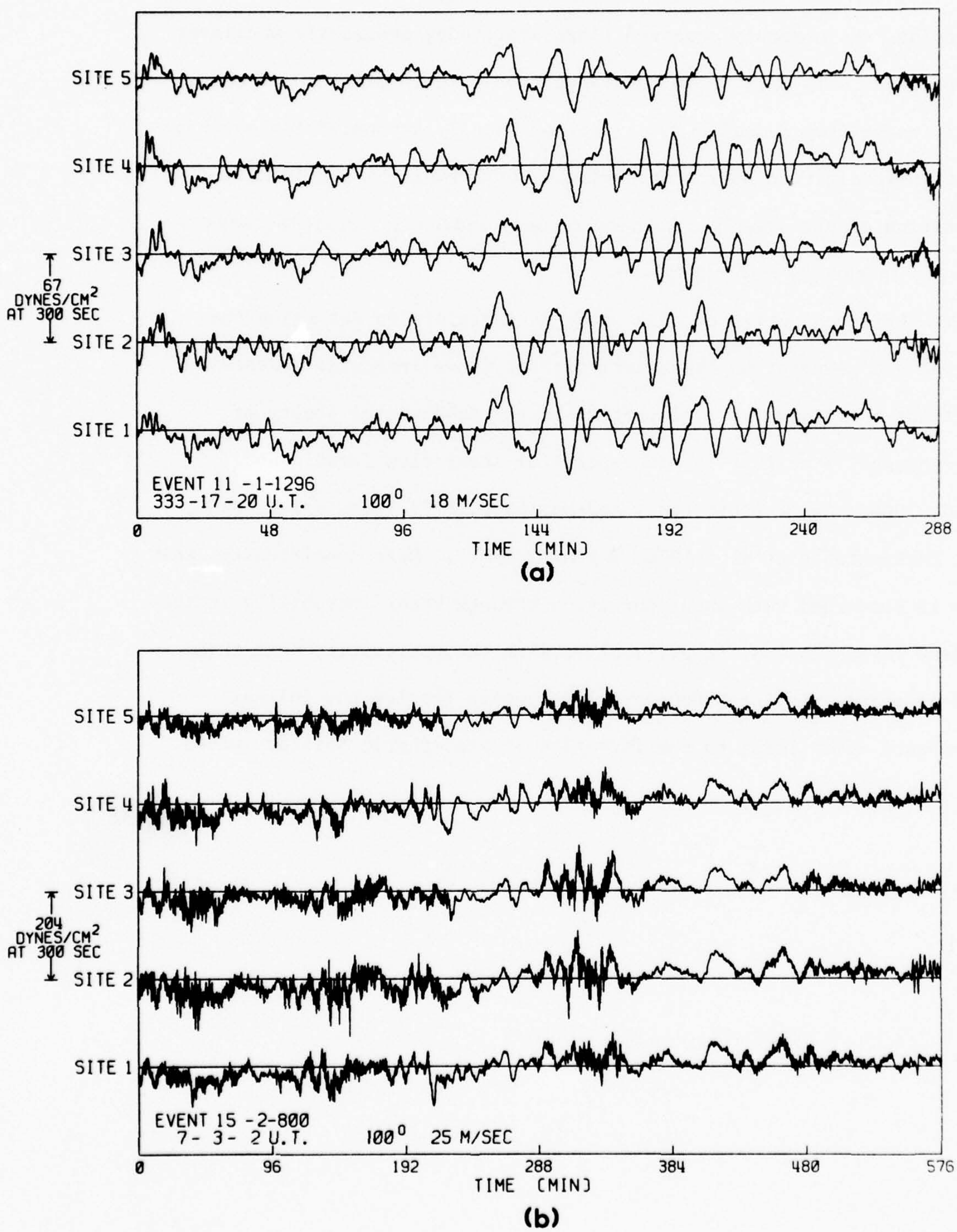

Figure 12. Examples of two different forms of highly-coherent, long-period irregular gravity wave trains.

while the subtropical jet and possibly the polar front jet provide an important source for gravity wave generation, as least one other new source mechanism is required to explain some of the observations. In particular, the commonly observed large amplitude, apparently nonlinear wave patterns with periods in the range from 4 to 10 minutes and phase velocities between 8 and 20 m/s are not usually accounted for by this type of high altitude source mechanism. Furthermore, a preliminary examination of the acoustic sounder records indicates irregular wave activity in the lower troposphere.

The basic objective of this study is therefore to determine the spectral and propagation characteristics of these irregular waves and to attempt to relate these properties to the fundamental theory of hydrodynamical stability in plane-parallel shear flow (Drazin and Howard, 1966; Jones, 1968; Benny and Maslowe, 1975; Lalas and Einaudi, 1976; Mastrantonio et al., 1976; Maslowe, 1977). More specifically, this study is concerned with wave generation through shear instability in the boundary layer jet and, in particular, with the possibility that these shear-generated nonlinear boundary layer waves provide the initial disturbance which leads to the formation of atmospheric solitary waves.

4. CONCLUSION

The principal conclusions of this work are that solitary waves commonly occur in the atmosphere with effective wavelengths which span a wide range of atmospheric length scales, and that these remarkably stable, essentially nonlinear, waves constitute an important component in the description of the dynamical state of the troposphere.

The basic underlying physics which describes the propagation of these waves appears to be fairly well understood. In contrast, at the present time we can only speculate on the various types of source mechanisms which may lead to the production of atmospheric solitons, the nature of the nonlinear wave-boundary layer jet interaction, the perturbing influence of topography and variations in the geometry and density profile of the propagating medium, and on the fundamental energy-dissipating processes which result in the decay of atmospheric solitons and the production of turbulence. All of these problems are under active investigation. In particular, an attempt is being made to accurately determine the atmospheric density profile in order to provide the necessary data for a qualitative comparison of observations with theory and the existing portable array elements will be deployed in a large aperture configuration which is suited to a determination of the precise nature of the mechanisms which generate solitary atmospheric waves.

REFERENCES

Benjamin, T.B. 1966: Internal waves of finite amplitude and permanent form. J. Fluid Mech., 25, 241-270.

Benjamin, T.B. 1967: Internal waves of permanent form in fluids of great depth. J. Fluid Mech., 29, 559-592.

Benney, D.J. and Maslowe, S.A. 1975: The evolution in space and time of nonlinear waves in parallel shear flows. Studies in Appl. Math., 54, 181-205.

Brekhovskikh, L.M. 1968: On the radiation of infrasound into the atmosphere by ocean waves. Izv. Akad. Nauk. U.S.S.R., IV(4), 444-450.

Christie, D.R., Muirhead, K.J. and Hales, A.L., 1978a: On solitary waves in the atmosphere. J. Atmos. Sci., 35, 805-825. (Reprinted in Appendix A).

Christie, D.R., Muirhead, K.J. and Hales, A.L., 1978b: Observations of nonlinear waves in the lower troposphere using an acoustic sounder and a microbarograph array : A study of atmospheric solitary waves and soliton-generating density intrusions. In preparation.

Davis, R.E. and Acrivos, A. 1967: Solitary internal waves in deep water. J. Fluid Mech., 29, 593-607.

Donn, W.L., Gedzelman, S.D. and Balachandran, N.K. 1973: Atmospheric gravity waves and the energy of the jet stream. Bull. Amer. Meteor. Soc., 54, 633-636.

Donn, W.L. and Rind, D. 1972: Microbaroms and the temperature and wind of the upper atmosphere. J. Atmos. Sci., 29, 156-172.

Drazin, R.G. and Howard, L.N. 1966: Hydrodynamic stability of parallel flow of an inviscid fluid. Advances in Applied Mechanics, Vol. 9, Academic Press, 1-89.

Essex, E.A. and Love, G.B. 1978: The occurrence of ground level gravity waves in southeastern Australia as detected by microbarographs. J. Geophys. Res., 83, 1883-1888.

Gedzelman, S.D. and Rilling, R.A. 1978: Short-period atmospheric gravity waves: A study of their dynamic and synoptic features. Mon. Wea. Rev. 106, 196-210.

Herron, T.J. and Tolstoy, I. 1969: Tracking jet stream winds from ground level pressure signals. J. Atmos. Sci., 26, 266-269.

Herron, T.J., Tolstoy, I., and Kraft, D.W. 1969: Atmospheric pressure background fluctuations in the mesoscale range. J. Geophys. Res., 1321-1329.

Jones, W.L. 1968: Reflexion and stability of waves in stably stratified fluids with shear flow: A numerical study. J. Fluid Mech., 34, 609-624.

Joseph, R.I. 1977a: Multi-soliton-like solution to the Benjamin-Ono equation. J. Math. Phys., 18, 2251-2258.

Joseph, R.I. 1977b: Solitary waves in a finite depth fluid. J. Phys.A: Math. Gen., 10, L225-L227.

Keliher, T.E. 1975: The occurrence of microbarograph - detected gravity waves compared with the existence of dynamically unstable wind shear layers. J. Geophys. Res., 80, 2967-2976.

Korteweg, D.J. and de Vries, G. 1895: On the change of form of long waves advancing in a rectangular canal and on a new type of long stationary waves. Phil. Mag., 39 (5), 422-443.

Lalas, D.P. and Einaudi, F. 1976: On the characteristics of gravity waves generated by atmospheric shear layers. J. Atmos. Sci., 33, 1248-1259.

Long, R.L. 1965: On the Boussinesq approximation and its role in the theory of internal waves. Tellus, 17, 46-52.

Madden, T.R. and Claerbout, J.F. 1968: Jet stream associated gravity waves and implications concerning jet stream stability. Proc. Boulder Symposium on Acoustic-Gravity Waves in the Atmosphere, T.M. Georges, ed., U.S. Govt. Printing Office (C52.2:Ac7), 121-134.

Maslowe, S.A. 1977: Weakly nonlinear stability theory of stratified shear flows. Quart. J.R. Met. Soc., 103, 769-783.

Mastrantonio, G., Einaudi, F. and Fua, D. 1976: Generation of gravity waves by jet streams in the atmosphere. J. Atmos. Sci., 33, 1730-1738.

Maxworthy, T. 1978. Private communication.

McDonald, J.A. and Herron, E. 1972: Microbaroms on a northern quarter of the Earth's surface. Nature Physical Science, 238, 86-87.

Meiss, J.D. and Pereira, N.R. 1978: Internal Wave Solitons. Phys. Fluids, 21, 700-702.

Muirhead, K.J. 1968: Eliminating false alarms when detecting seismic events automatically. Nature, 186, 704.

Muirhead, K.J. and Ram Datt 1976: The Nth root process applied to seismic array data. Geophys. J. Roy. Astr. Soc., 47, 197-210.

Ono, H. 1975: Algebraic solitary waves in stratified fluids. J. Phys. Soc. Japan, 39, 1082-1091.

Paul, D.L. and Madden, T.R. 1977: Jet stream gravity generation by nonlinear wave-wave interaction. Trans. Amer. Geophys. Union, 58, 395.

Rind, D. and Donn, W.L. 1975: Further use of natural infrasound as a continuous monitor of the upper atmosphere. J. Atmos. Sci., 32, 1694-1704.

Rind, D.H. and Donn, W.L. 1978: Infrasound observations of variability during stratospheric warmings. J. Atmos. Sci., 35, 546-553.

Rind, D., Donn, W.L. and Dede, E. 1973: Upper air wind speeds calculated from observations of natural infrasound. J. Atmos. Sci., 30, 1726-1729.

Peters, A.S. and Stoker, J.J. 1960: Solitary waves in liquids having non-constant density. Comm. Pure Appl. Math., 13, 115-164.

Posmentier, E.S. 1967: A theory of microbaroms. Geophys. J.R. Astr. Soc., 13, 487-501.

ACKNOWLEDGEMENTS

The authors are indebted to Professor J.S. Turner for many valuable discussions and perceptive observations on the interpretation of complex geophysical fluid motions. His active encouragement and continued interest in this program are greatly appreciated. The authors have also benefited greatly from several stimulating discussions on the nature of solitary waves with Professor T. Maxworthy of the University of Southern California. We would also like to thank M/Sgt. R.L. Chadwick of U.S.A.F. Detachment 421 at J.G.G.R.S. in Alice Springs for his skilled assistance in diagnosing an annoying intermittant problem with the digital recording system. Finally, we would like to express our appreciation to Mr. Paul Le Mesurier, Managing Geologist of Geo Peko Ltd., Tennant Creek, and to Mr. Blair Lade and Mr. Phillip Taylor for their capable efforts in operating and maintaining the Warramunga Seismic Station.

APPENDIX A

ON SOLITARY WAVES IN THE ATMOSPHERE

(Reprinted from J. Atmos. Sci.,
35, 805-825, 1978)

D.R. Christie, K.J. Muirhead, and A.L. Hales

Research School of Earth Sciences
Australian National University
Canberra, A.C.T., 2600.

ABSTRACT

This paper is concerned with a description and interpretation of two unusual types of isolated atmospheric gravity wave observed near Tennant Creek in central Australia. These waves occur in the form of solitary waves of elevation and solitary waves of depression. Comparison of experimental data with theory leads to the conclusion that the majority of the observed isolated waves of elevation belong to the class of deep fluid internal solitary wave considered by Benjamin and by Davis and Acrivos. The second fundamentally different type of large amplitude isolated wave is tentatively identified as a classical solitary wave of depression.

A brief discussion is given of a number of possible source mechanisms which may give rise to internal solitary atmospheric waves. It is proposed that the following two dynamical processes play an important role in the creation of solitary atmospheric waves in the arid interior of Australia: (i) the interaction of nocturnal katabatic density currents with an existing radiation inversion; and (ii) the interaction of a propagating horizontal sea-breeze vortex with the nocturnal inversion.

1. Introduction

It is well known that the creation, propagation and dissipation of gravity waves play an important role in the dynamics of the Earth's atmosphere. The reasons for studying long-period waves of this type are therefore two-fold: in the first place, an understanding of the initial disturbance which gives rise to these waves, the mechanisms by which they propagate and their dispersion characteristics provide insight into the fundamental nature of atmospheric fluid mechanics; secondly, it seems to be equally important to understand the influence that the passage of these waves has on the development of local meteorological conditions - for example, gravity waves may sometimes be correlated with the release of latent atmospheric instabilities which in turn give rise to such diverse phenomena as clear air turbulence, severe convective storms and, possibly, in the extreme case the development of tornado activity.

The purpose of this paper is to present a description and interpretation of the results of an experimental investigation of large amplitude isolated propagating atmospheric disturbances which have been observed, using an array of high sensitivity microbarometers, at the Warramunga Seismic Station located near Tennant Creek in central Australia. It is thought that these unusual phenomena which occur as isolated waves of elevation and isolated waves of depression represent two new types of naturally occurring internal solitary wave. In particular, it will be shown that the properties of the waves of elevation are in accord with the class of deep fluid solitary

wave considered by Benjamin (1967) and by Davis & Acrivos (1967) and that the internal waves of depression appear to be described by the classical solitary wave theories of Peters and Stoker (1960), Long (1965) and Benjamin (1966).

The properties of atmospheric waves have recently been reviewed by Gossard and Hooke (1975). In their most common form, horizontally propagating gravity waves in the troposphere occur as long period, nearly sinusoidal wave trains. This familiar form of atmospheric wave may be contrasted with an example of the specific type of unusual isolated wave considered in this paper as illustrated in the Tennant Creek microbarograph array record section shown in figure 1 for the late evening hours of December 2, 1976. Perhaps the most interesting feature of the observed isolated waves is their unusually large relative amplitude. A study of the properties of these waves therefore encompasses an investigation of the role of nonlinearity in large scale fluid motions and an investigation of the process of wave-induced turbulence. It must be anticipated that this class of waves will prove to be important in other areas of geophysical fluid mechanics.

2. The internal solitary atmospheric wave

The phenomenon of the solitary wave, by its essentially nonlinear nature, occupies a unique place in the development of the theory of wave propagation in fluids. A classical wave of this type is usually defined (Lamb, 1932, §252) as a wave of single elevation which propagates at uniform velocity without change of form. The existence of these stationary waves may be viewed as being the consequence of equilibrium between the competing effects of nonlinearity and dispersion; that is, they arise from a balance between the tendency of waves to steepen ahead of their crests (amplitude dispersion) and the tendency of the longer period Fourier components to propagate at higher velocities (frequency dispersion).

The classical solitary wave of elevation was first observed by Scott-Russell (1837, 1844) on the free surface of shallow water of uniform depth. Subsequently,

Boussinesq (1871) and Rayleigh (1876) independently derived approximations for the speed of propagation, c, and the form, $\eta(x)$, of the wave profile at the free surface. These authors found, to first order in the relative amplitude $\alpha = a/h$, a solitary wave solution described by

$$\eta(x) = a \operatorname{sech}^2 \left\{ \frac{\sqrt{3\alpha K}}{2} \frac{x}{h} \right\} \tag{2.1a}$$

and
$$c = (gh(1+\alpha))^{\frac{1}{2}} \tag{2.1b}$$

where h is the undisturbed fluid depth, a is the maximum amplitude of the wave and g is the acceleration due to gravity. A measure of the effective wavelength of these waves is given by the full width of the wave profile at half maximum,

$$w_{1/2} = \frac{4\ln(1+\sqrt{2})}{\sqrt{3\alpha K}}\, h. \tag{2.1c}$$

In the Boussinesq approximation, the factor K in the argument of the hyperbolic secant takes the value, $K = 1$, while in the solution found by Rayleigh, $K = (1 + \alpha)^{-1}$.

These early investigations revealed an important property of solitary waves; that is, they are always super-critical - the speed of propagation always exceeds the speed

$$c_o = (gh)^{\frac{1}{2}} \tag{2.2}$$

of infinitesimal long waves. This property may be expressed to first order in the dimensionless amplitude as

$$F^2 = 1 + \alpha > 1 \qquad (2.3)$$

where F is the Froude number. It should be noted that all forms of the classical solitary wave are characterized by fluid systems in which the horizontal length scale of the motion is long compared to the total fluid depth.

Korteweg and de Vries (1895) showed that the time evolution of small-but-finite dispersive shallow-water waves is described, in the first approximation, by a non-linear partial differential equation (the KdV equation) which may be written as

$$\frac{\partial \eta}{\partial t} + c_o(1 + \varepsilon\eta)\frac{\partial \eta}{\partial x} + c_o\beta\frac{\partial^3 \eta}{\partial x^3} = 0 \qquad (2.4)$$

where $\varepsilon = 3/2h$ and $\beta = h^2/6$. From this equation they were able to demonstrate the existence of a class of periodic long waves of finite amplitude and permanent form which are described by the square of the Jacobi elliptic function *cn* of modulus k. In particular, they showed that these waves, which they called *cnoidal* waves, reduce to the classical solitary wave of finite extent in the limit as the wavelength goes to infinity. Despite this progress, it was not until relatively recently that Lavrent'ev (1946) and Friedrichs and Hyers (1954) succeeded in rigorously proving the mathematical existence of a solitary wave solution of the full nonlinear equations.

There have been a number of attempts to improve on the first order approximation to the classical solitary wave. The second-order solution was found by Laitone (1960), the third-order by Grimshaw (1971), and a fifth-order

expression for the wave speed has been given by Long (1956b). Much of the recent work on classical solitary waves has concentrated on the determination of the solitary wave of maximum height. Estimates have been obtained from an exact calculation of the position of points on the profile of the wave of maximum amplitude (Yamada 1957; Yamada et al. 1968), from an extrapolation of a ninth-order series approximation for the profile of waves of less than maximum amplitude (Fenton 1972), from an extrapolation of the results of a finite-difference formulation of the problem (Chan 1974), and from the solution of an integral equation (Lenau 1966; Byatt-Smith 1970; Strelkoff 1971). A puzzling aspect of these calculations has been the small, but significant, discrepancy between the various estimates for the wave of maximum amplitude. This problem has recently been resolved by Longuet-Higgins and Fenton (1974) who found that the wave of maximum height does not correspond - as had generally been assumed - to the wave of maximum speed. According to these authors the wave of maximum amplitude is specified by

$$\alpha_{max} = 0.827 \ , \ F = 1.286 \tag{2.5}$$

in good agreement with the results of Yamada (1957) and Lenau (1966) while the wave of maximum speed corresponds to

$$\alpha = 0.790 \ , \ F_{max} = 1.294 \ .$$

It is worth noting that the Boussinesq approximation (2.1) to the shape of the classical solitary wave compares favourably with the exact profiles computed by Yamada (1958)

and by Byatt-Smith (1970) provided the non-dimensional amplitude α is less than about 0.7.

The theoretical study of internal solitary waves, that is, waves which exist as a consequence of internal density stratification, was initiated by Keulegan (1953) who considered a system of two superimposed liquids of different constant densities, bounded above and below by rigid surfaces. Long (1956b) and Benjamin (1966) have also investigated this particular model. Abdullah (1956) obtained, using a systematic perturbation procedure developed by Friedrichs (1948) and Keller (1948), a first order solution for the classical internal solitary wave at the interface of a two-layer atmosphere subject to the condition that the hydrostatic law holds for the upper layer; that is, that motion of the free surface can be neglected. This solution is a supercritical wave of elevation described by the Boussinesq approximation (2.1) with the expression for the phase velocity modified to

$$c = c_o'(1 + \frac{1}{2}\alpha) \tag{2.6}$$

where the infinitesimal internal wave critical speed is now given by the reduced form

$$c_o' = (g'h)^{\frac{1}{2}} \tag{2.7}$$

where

$$g' = \frac{g(\rho_1 - \rho_2)}{\rho_1} \, . \tag{2.8}$$

and ρ_2 and ρ_1 are the densities of the upper and lower fluids respectively.

A more general treatment of internal solitary waves has been given by Peters & Stoker (1960). They examined the full problem of a two-fluid system with a free upper boundary as well as the more difficult problem of the existence of internal solitary waves in a fluid whose density decreases exponentially with height. In the case of the two-fluid problem they found two types of solitary-wave solution corresponding to two critical speeds given by

$$c_o^s = \left(\frac{gh_1(1+R+q)}{2}\right)^{\frac{1}{2}}, \tag{2.9a}$$

and

$$c_o^i = \left(\frac{gh_1(1+R-q)}{2}\right)^{\frac{1}{2}}, \tag{2.9b}$$

with

$$q = \left((1-R)^2 + 4\frac{\rho_2}{\rho_1}R\right)^{\frac{1}{2}},$$

where $R = h_2/h_1$ and h_2 and h_1 are the respective depths of the upper and lower fluids in the region of undisturbed flow. The first of these solutions has maximum amplitude at the free surface and represents the equivalent of the ordinary classical solitary wave of elevation; the second describes an internal solitary wave with a maximum amplitude at the interface much larger than the amplitude at the surface. The internal solitary wave may be either a wave of depression or a wave of elevation. If the difference in the two fluid densities is small, then the streamlines are lines of elevation at the interface if $R>1$ and lines of depression if $R<1$. This form of the two-fluid solution may be suited to a description of large scale internal atmospheric solitary waves.

For this particular model, the wave profile at the interface is given by the usual classical solitary waveform (2.1) with

$$K = \left| \frac{(R-1)}{R^2} \right| \tag{2.10a}$$

and the corresponding internal critical speed reduces to

$$c_o^i = \left(g\left(1-\frac{\rho_2}{\rho_1}\right)\frac{h_1 h_2}{(h_1+h_2)} \right)^{\frac{1}{2}}. \tag{2.10b}$$

In the case of a fluid of finite depth with a density distribution which decreases exponentially upwards, Peters & Stoker found an infinite number of possible internal solitary wave modes corresponding to an infinite spectrum of internal critical speeds. This problem has also been investigated by Long (1965) and, in an elegant and very general treatment of the subject of internal solitary waves in shallow fluids, by Benjamin (1966). The general solitary wave solutions in this case are complicated and will not be given here; it is noted, however, that according to Benjamin, for the case of a free upper boundary, the solitary wave mode corresponding to the highest critical speed - predominantly a wave of depression - is probably the most significant mode in fluids of this type.

Up to this point this discussion has been limited to a consideration of internal solitary waves which can exist in fluids of finite depth. Benjamin (1967) and, independently, Davis & Acrivos (1967) have presented the results of a theoretical and experimental investigation of

an entirely new class of internal solitary waves which can exist in fluids of great depth. These new types of internal waves are shown to exist in regions where the fluid density varies only within a layer of thickness h which is much smaller than the total fluid depth and smaller than the effective horizontal length scale, λ , characteristic of the solitary wave. Thus, in stratified fluids of great depth, the fundamental scale against which wave dimensions are to be measured is the thickness of the region of significant density variation rather than the total fluid depth.

For a two fluid system in which the upper fluid extends to infinity over a lower fluid of depth h resting on a horizontal rigid surface, Benjamin finds a solitary wave solution of the form

$$\eta(x) = \frac{a\lambda^2}{x^2+\lambda^2} . \qquad (2.11a)$$

with

$$c = c_o' \left(1 + \frac{3}{4}\alpha\right)^{\frac{1}{2}} \qquad (2.11b)$$

where

$$2\lambda = w_{1/2} = \frac{8}{3}\frac{\rho_1}{\rho_2}\frac{h}{\alpha} , \qquad (2.11c)$$

c_o' is the reduced internal wave critical speed given by (2.7), and ρ_2 and ρ_1 are the densities of the upper and lower fluids respectively.

Benjamin has also considered the problem of a shallow fluid with an exponential density gradient in contact with a deep fluid of constant density, and, further, the more general problem of solitary waves associated with a thin transition region contained between two homogeneous fluids of substantial depth. In direct analogy with the shallow fluid theory, the continuous variation in density is shown to give rise to an infinite set of solitary-wave modes. For the case of a thin region of sudden vertical density variation in a stably stratified system, the lowest-order mode solitary wave solution takes the form of a bulge which propagates along the interface. This interesting result has been confirmed in the laboratory experiments of Davis & Acrivos (1967) and Hurdis & Pao (1975). The experiments and numerical calculations of Davis & Acrivos are particularly interesting in that they show that solitary waves of this type can exist with dimensionless amplitude near 2.0 and that waves with large amplitudes exhibit an unusual closed circulation in the streamline pattern which suggests the presence of a propagating vortex pair.

It was long thought that solitary waves would only be produced as a consequence of rather specialized initial conditions. The discovery by Zabusky and Kruskal (1965) that the solitary wave or *soliton* solutions of the KdV equation (2.4) possess the remarkable linear property of preserving their form following nonlinear interaction has provided, in recent years, a great deal of impetus to the study of the

general properties of the non-stationary solutions of the KdV equation and other nonlinear wave equations known to admit soliton solutions (see, e.g. Karpman 1975). The importance of these results to the study of atmospheric fluid mechanics stems principally from the fact that soliton production in density-stratified fluids is now known to occur under widely varying initial conditions.

Consider now the existence of solitary-wave motions in the atmosphere. It would seem, on the basis of the atmospheric scale involved, that the deep fluid solitary wave solution (2.11) found by Benjamin (1967) is best suited to a simple description of solitary waves in the planetary boundary layer while classical internal solitary wave theory should provide a reasonable description of higher altitude waves.

In order to clarify the interpretation of experimental data consider the properties, as predicted by both the classical and deep fluid theories, of internal solitary waves associated with a density discontinuity at the 980 mbar (280 m) level corresponding to a temperature inversion of $5^{o}C$. The air beneath the inversion is taken to have a mean temperature of 270 K and the dimensionless amplitude of the wave, α, is chosen to have a value of 0.5, corresponding to a wave with amplitude less than maximum. With these conditions, a classical internal solitary wave as described by the theory of Abdullah ((2.1) and (2.6) with $K = 1$) would propagate along the inversion at a speed of 8.9 m/s with a full width at half maximum, $w_{1/2}$, of 0.81 km and would produce, assuming the hydrostatic approximation, a maximum pressure perturbation, ΔP,

at ground level of 317 dyn cm^{-2}; in contrast, the classical theory of Peters & Stoker ((2.1) and (2.10) with $K << 0.1$) describes an internal solitary wave which propagates with nearly the same velocity but with a much larger effective wavelength. Alternatively, for the same wave amplitude, Benjamin's deep fluid theory (2.11) describes a solitary wave with $w_{\frac{1}{2}} = 1.52$ km propagating at a speed of 8.4 m/s . It is, of course, unlikely that the classical treatment of the theory provides an accurate description of internal solitary waves whose characteristic horizontal dimensions, as in this example, are much smaller than the total fluid depth.

A comparison of the classical and deep-fluid solitary wave profiles for an inversion at the 980 mbar level is shown in figure 2. Note that, as a consequence of an asymptotic exponential behaviour, the influence of the classical wave is much more localized than that of the deep fluid wave of elevation. The shape of both types of solitary wave depends on the value of the dimensionless amplitude α; as α increases the wave profile narrows and the curvature at the crest increases until at maximum amplitude the peak is reduced in accordance with Stokes's (1880) conjecture* to a cusp enclosing an angle of 120°.

---

* This conjecture, which has often been used as a limiting constraint in the mathematical development of large amplitude wave theory, has recently been considered by Byatt-Smith and Longuet-Higgins (1976) as part of a study of the detailed shape of the profile of steep solitary waves. In all cases studied the maximum slope of the wave profile was less than 30°. However, the possibility that the maximum surface slope of the wave of highest amplitude exceeds the limit imposed by Stokes's criterion could not be excluded.

The possible existence of atmospheric internal solitary waves was suggested by Abdullah (1949). The only direct evidence for atmospheric solitary waves appears to be the description by Abdullah (1955) of a large amplitude propagating disturbance which appeared over Kansas during the early daylight hours of June 29, 1951. This disturbance, which produced a ground level pressure perturbation of 3.4 mbar, took the form of an elevated mass of cold air propagating on an inversion at a height of about 2 km. The elevated disturbance appeared to extend over about 150km and was observed to travel with approximately constant form at speeds between 18 and 24 m/s over a distance of about 800km. Abdullah concluded that this disturbance represented a classical internal solitary wave of elevation and attributed its formation to the impulsive movement of a quasistationary cold front into the layer of inversion. As can be seen from the following description, most of the atmospheric solitary waves observed at Tennant Creek which belong to the class of isolated waves of elevation have an effective wavelength of only a few kilometers; they therefore appear to be entirely different from the single observation described by Abdullah. It will be shown that the properties of this new form of isolated wave are best described by the deep-fluid solitary wave theory. In addition, a description will be given of observations of large scale solitary waves of depression. An examination of the properties of this second new type of solitary wave indicates that these waves are probably best described as classical solitary waves which propagate in a stratified fluid whose density decreases continuously with height.

Smart (1966) and Jordan (1972) have reported observations of "exponential pressure pulses" near Denver, Colorado, which may represent a form of internal solitary wave. Additional evidence for the existence of solitary atmospheric waves based on observations of the pressure field is scarce. Philips (1976) has described an interesting example of an isolated propagating disturbance which appeared as an exceptionally large pressure spike of 4 mb amplitude on barograph traces recorded on March 25, 1966 at El Adem and Tobruk in Libya. Apparently this disturbance was vigorous enough to trigger a seiche in Tobruk Harbour. It seems reasonable to assume that this disturbance and other smaller disturbances of a similar nature observed on the same day can be described as large amplitude solitary waves of elevation.

At this point we would like to draw attention to two important acoustic radar studies which were carried out several years ago in areas of Australia with environments which are very similar to the semi-desert environment of the Warramunga Seismic Station. As will be seen, these studies provide considerable insight into the nature of the isolated propagating disturbances observed near Tennant Creek.

In a pioneering atmospheric acoustic sounding study McAllister et al. (1969) described an observation of a "weak, front-like" nocturnal disturbance characterized by the sudden appearance on the inversion level of a well-defined sharp spike in the sounder record. This initial pulse was followed by a rapid buildup of turbulence which, after a period of about 10 minutes, evolved into a pattern of reflections from distinct

slowly ascending strata. A further feature of this record are the clearly visible large amplitude vertical oscillations of the atmosphere in the wake of the initial spike. It is worth noting that the ratio of the amplitude of the initial pulse-like disturbance to the depth of the inversion both ahead of and immediately behind the pulse is at least as high as 1.0. It should also be emphasized that evidence of large-scale vertical atmospheric motions associated explicitly with the spike in the sounder record are provided by the corresponding records from the 75-meter level of an instrumented tower which show that the passage of the disturbance corresponding to the spike produced a simultaneous negative pulse of $4^{o}C$ in the temperature field and a positive pulse of about 6 m/s in the wind speed at this level. These observations were carried out during the month of June at Ivy Tanks on the edge of the arid Nullarbor Plain in South Australia.

A very interesting description of a series of acoustic sounding experiments carried out, again during the month of June, at Julia Creek, Queensland, has been given by Reynolds and Gething (1970). They also observed, usually under clear conditions with light surface winds, several examples of well defined very large amplitude spikes on the interface of the nocturnal inversion. These unusual disturbances appear on the sounder record in two different forms: (a) a single clearly defined pulse with dimensionless amplitude of the order of unity which occurs along or immediately behind the leading edge of a rise in the height of the inversion and which is usually followed by patterns which indicate further wave activity near the inversion level; (b) clusters of particularly large amplitude

pulses on the inversion level which preceed a pattern of lower amplitude wave trains - in this case, the sounder records indicate little evidence for a change in the height of the inversion. Note that the profiles of all of these spikes on the inversion are very similar in form to the profile of a deep-fluid solitary wave.

Reynolds and Gething have also described the corresponding measurements of temperature, wind speed and wind direction recorded at 15 m intervals to a height of 75 m on 3 towers separated by distances of the order of 40 km. A few of the essential features of these measurements are worth noting at this point. In the first place, the sounder measaurement of the inversion height is in good agreement with the value determined from the tower measurements; there would therefore appear to be little doubt that the sounder records provide an accurate picture of the profile of disturbances on the inversion level. Secondly, an examination of the temperature structure associated with the isolated-pulse form of disturbance shows that by far the largest perturbation of the overall temperature field corresponds to the spike in the sounder record. This strongly suggests that this initial transient disturbance may be viewed as a distinct separate phenomenon and, as well, indicates that the dynamical processes associated with the pulse dominate the flow structure of the disturbance. At higher altitudes this initial perturbation takes the form of a strong negative temperature spike similar to that observed by McAllister et al.; at lower heights, the amplitude of the spike decreases steadily with decreasing altitude and has almost disappeared from the trace

recorded at 1.5 m. Note that this temperature distribution is consistent with the perturbations that would occur during the passage of a single large amplitude internal wave of elevation associated with a density profile - as in the examples considered here - which decreases monotonically with height from the surface to the inversion level. Thirdly, the observation of an apparently unattenuated disturbance at sites separated by about 40 km establishes that these pulses propagate over significant distances. These observations also reveal that the thermal structure associated with the spike in an isolated-pulse type of disturbance is identical in form to the structure associated with individual pulses in a cluster type of disturbance - this provides a convincing demonstration that the isolated pulses and the non-isolated pulses possess the same internal morphology; that is, all of these events are manifestations of the same basic phenomena.

The essentially distinct nature of the pulse-like disturbances is further indicated in the 75-meter anemometer records which show a sudden temporary decrease in the wind speed from near 14 m/s to about 7 m/s during the passage of the pulse (in contrast to the observations of McAllister et al. where the pulse-associated wind showed an increase in speed) and a corresponding sudden temporary increase in the wind azimuth by about 60°. Note that this perturbation of the wind vector is significantly larger than any of the perturbations which occurred further on in the disturbance.

Finally, it is worth noting the acoustic radar observation described by Shaw (1971) of a transient isolated disturbance in

the atmospheric boundary layer which occurred near Melbourne in the early morning hours of June 9, 1970. This disturbance, which takes the form of a single symmetrical wave of elevation appears to be very similar to the deep fluid solitary wave described by the theory of Benjamin (1967).

During the course of the experiments at Tennant Creek we have observed a wide variety of unusual propagating lower tropospheric disturbances, many of which bear a close resemblance to the series of observations reported by Reynolds and Gething (1970) and to the events described by McAllister et al. (1969) and Shaw (1971). Observations have been made of disturbances in the form of smooth shallow internal density currents, complex solitary wave families superimposed along the leading edge of sustained internal density flows, isolated clusters of solitary waves of elevation, and disturbances in the form of individual solitary waves which propagate along the nocturnal inversion. It is thought that all of these disturbances belong to the class of deep fluid nonlinear propagating disturbance described by the theory of Benjamin (1967). In particular, we identify all of the boundary layer pulse-like disturbances noted in the acoustic radar records and all isolated waves in the microbarograph array records which correspond to a transient increase in surface pressure as deep fluid internal solitary waves of elevation. Since this paper is primarily concerned with the phenomenon of the atmospheric solitary wave we include here only those observations which clearly illustrate the basic features of isolated solitary waves and isolated

clusters of solitary waves which propagate along an atmospheric inversion. It should be emphasized, however, that the available experimental evidence indicates that the genesis of the deep fluid solitary waves described in this paper may often be traced to the evolution of the observed density-flow disturbances. Since the properties of these complex density currents constitute a separate area of investigation, a detailed description and interpretation of these unusual flow phenomena will be published separately.

3. Experimental arrangement and data processing techniques

The Warramunga Seismic Station is situated 37 kilometers SSE of Tennant Creek. The centered quadrilateral array of microbarometers is located on slowly undulating semi-desert terrain at an elevation of about 410 meters MSL with relief in the area encompassed by the array rising to a maximum of about 6 meters. Probably the most important topographical features, insofar as the location of this array is concerned, are the 600 meter Murchison and Davenport Ranges which run from 20 to 160 kilometers to the SSE and the 1600 meter Macdonnell Ranges, 450 kilometers to the south. All of the area within 400 kilometers to the west of the array can be described as semi-featureless stoney desert and an extensive dry steppe area known as the Barkly Tablelands forms the north-east quadrant.

Each element of the array consists of a National Bureau of Standards designed capacitor microphone which measures variations in pressure relative to a reference volume coupled through a high acoustic resistance to the atmosphere. The

configuration of the infrasonic array along with the location of a vault containing a vertical long-period seismometer which is operated in conjunction with the infrasonic experiment are illustrated in figure 3. An array of Daniels noise reducing space filters arranged in the form of a cross with the microbarograph inlet port at the center has been installed at each site. These filters provide useful suppression of incoherent wind noise in the period range below about 20 seconds. The measured amplitude response of the microbarometers is shown in figure 4.

The response of the differential pressure sensing array elements as a function of period is given by the expression

$$R(T) = \frac{A(T_1+T_2)iT}{T^2+(T_1+T_2)iT-T_1T_2} , \qquad (3.1)$$

with $T_1 = 1.95$ s ,

$T_2 = 48.7$ s ,

and $A = 77.99$ counts/dyne/cm^2.

In this expression the coefficients T_1, T_2 and A have been determined from a least-squares analysis of the measured instrumental response. An examination of this expression shows that wave forms with fundamental components near $T_o = (T_1T_2)^{\frac{1}{2}} = 9.7$s pass through the infrasonic detection filters essentially undisturbed; in contrast wave patterns with fundamental components of the order of T_2 undergo substantial differentiation in the detection process - this latter circumstance dominates the observation of the two types of solitary wave disturbance considered

here. The influence of the instrumental response on the detection of solitary wave surface pressure perturbations may be seen in the computed response to various forms of synthetic solitary wave data illustrated in figure 5. These patterns may be compared with the examples shown in figure 6 of the true surface pressure variation derived from recorded micro-barograph data through an inversion of the instrumental response given by (3.1). As may be seen from these examples, solitary waves are easily identified in the ouput of the microbarograph array by their characteristic differential signature.

The five infrasonic channels and the vertical long-period seismometer channel are sampled at a rate of 2 samples per second, digitized via a 14-bit ADC and recorded in IBM compatible format on 7-track, 556 bpi tape. At the Australian National University these tapes are converted to 9-track, 800 bpi in a compact, 2 data word per 24-bit computer word, format, which conserves magnetic tape and which is suitable for analysis on a 48K Harris Datacraft 6024/4 computer.

A SIAP S2000 meteorological station was installed at site 1 near the end of the recording period spanned by this work. This instrument provides a continuous record of surface temperature, wind speed, wind direction, rainfall and humidity. Accurate timing was achieved through the introduction of a chart marker activated by a pulse derived from the crystal-controlled digital time standard of the seismic station. The analysis of the meteorological data has not yet been completed. However, some of this data which is essential to the interpretation of the phenomena described here is included in this paper.

The main signal processing technique used on the array data consists of a beam-forming program which utilizes the non-linear N-root method devised by Muirhead (1968). The output $e_i(t)$ of the i-th array element is digitally filtered in the bandpass region of interest, properly phased by time shifting to correspond to the passage of a plane wavefront across the array, and then reduced to the N-th root with sign preserved. The resulting product is summed over the n-element array to give

$$R_N(t) = \frac{1}{n} \sum_{i=1}^{n} |\overline{e}_i(t)|^{\frac{1}{N}} \cdot \text{signum } (\overline{e}_i(t)) \qquad (3.2)$$

where $\overline{e}_i(t)$ represents the filter output. This quantity is then raised to the N-th power with sign preserved to provide the signal statistic

$$S_N(t) = |R_N(t)|^N \cdot \text{signum } (R_N(t)) \quad . \qquad (3.3)$$

The principal advantage of this type of automatic infrasonic array processing arises from the fact that this non-linear beam-forming technique gives added weight to the presence of coherent energy in the spectrum. This has proven to be of value in the treatment of data from Tennant Creek due to the prevalence in this semi-desert environment of incoherent, essentially non-Gaussian noise such as that due to dust devils (small whirlwinds called *willy-willies* in Australia) which interact with only one sensor. It can be easily shown that large

events of this type are suppressed in the output of the N-th root process by a factor of approximately n^{-N}.

All infrasonic data is processed for a value of N=2. This output is supplemented by a parallel determination of an integrated polarity stack over the phased array which corresponds to the N-th root process in the limit $N\to\infty$. Further details on the N-th root multi-channel filter may be found in Kanasewich et al. (1973) and Muirhead & Ram Datt (1976).

Power spectral estimates of the data are computed directly using the Fast Fourier Transform. In order to reduce the variance of the estimate the calculations are carried out using the method of time averaging over modified periodograms described by Welch (1967). The digital time series t_r is divided into k portions t_{rj} each of length $M=2^{10}$ points; the elements in each segment j are then weighted according to a cosine taper data window d_r effective over the 10% limits of the segment, as suggested by Bingham et al. (1967), and transformed to the frequency domain to give

$$X_j(f) = \sum_{r=0}^{M-1} d_r t_{rj} \exp\left\{\frac{-2\pi irf}{M}\right\}. \qquad (3.4)$$

The power spectral density is then determined by averaging over the k segments,

$$\overline{P}(f) = \frac{2\Delta t}{kMU} \sum_{j=1}^{k} \left|X_j(f)\right|^2, \qquad (3.5)$$

where Δt is the sampling interval and the factor

$$U = \frac{1}{M} \sum_{r=1}^{M} d_r^2 = 0.875 \qquad (3.6)$$

preserves the invariance of the area under the spectrum to the influence of the data taper window. The power spectral estimates obtained in this way are converted to true spectral estimates by dividing by the square of the microbarograph amplitude response shown in figure 4.

4. Observations and interpretation

Let us first consider the properties of the isolated waves of elevation. A large number of disturbances of this type have been observed in over two years of continuous recording at the infrasonic array near Tennant Creek. These unique waves, which only occur at night, are reasonably well described by the deep-fluid solitary-wave theory outlined above. Consequently, as mentioned in the introduction, these waves are interpreted as being examples of atmospheric internal solitary waves which propagate along the nocturnal inversion.

An examination of the microbarograph record inversions shows that in general these subsonic waves produce a symmetrical pulse-like perturbation in the atmospheric flow field characterized by an initial slow rise in surface pressure over a period of several minutes which gradually develops into an exponential increase leading to a fairly sharp but rounded crest. The microbarograph signatures corresponding to the passage of a wide variety of these commonly occurring buoyancy waves are illustrated in figures 7 to 12. The two relatively

weak but well-defined isolated solitons illustrated in figure 7 are typical of the most commonly observed form of these waves. Occasionally, (see figure 8(b)) large amplitude isolated waves of elevation are observed to pass over the infrasonic array. Almost all of the observed solitary wave microbarometer signatures correspond to pressure distributions which are similar in form to the theoretical soliton profile described by (2.11(a)). The event shown in figure 9(a) is unusual in that this wave of elevation produced, over part of the observational field, a surface pressure distribution in the form of a broad symmetrical pulse with a relatively flat crest. The significance of this peculiar wave pattern will be considered in more detail in the next section. Groups of waves consisting of well separated individual solitons are sometimes observed as illustrated in the record sections shown in figure 10. In contrast, condensed "wave-packets" consisting of two or more closely spaced solitons are frequently observed as shown in the examples in figures 9(b), 11 and 12. It is worth noting that many of these soliton families are composed of waves of unusually large amplitude. These soliton wave packets may be very complex (see figure 12(b)) but they are usually ordered by amplitude with the higher velocity solitons appearing near the forward edge of the wave packet.

The salient features of these atmospheric solitary waves have been determined from an examination of the measured properties of 99 events recorded over a two year period. Waves of this type have been observed with amplitudes as high as 1100 dyn cm^{-2}. They propagate at speeds between 4 and 18 m/sec,

with an effective wavelength, as measured by the full width at half maximum, between 0.4 km and 7.7 km and tend to occur sometimes for four nights in succession. Note that on a few occasions as many as 3 of these waves have been observed to pass over the experimental site from different directions within a period of 12 hours. Even though the available data span a period of only two years, it seems clear (see figure 13) that the frequency of occurrence of these waves is seasonal. In addition, it appears that waves which generate large amplitude ($\Delta P > 300$ dyn cm^{-2}) pressure perturbations at the surface occur most frequently from mid-August to mid-October - a period characterized by the formation of intense stable radiation inversions. Contrary to the observations reported by Smart (1966) and by Jordan (1972), the waves of elevation observed at Tennant Creek do not occur during the daylight hours between 10.00 and 18.00 C.S.T. (see figure 14). A polar plot of the frequency of observation (figure 15) reveals that these solitary waves of elevation originate predominantly to the north and north-east in the directions of the Timor Sea and the Gulf of Carpentaria and to the south-east in the direction of the Simpson Desert. It is worth remarking on the fact that the majority of the larger amplitude solitary waves of elevation detected at Tennant Creek arrive at the experimental site from azimuths between 20° and 60°.

Consider now the infrasonic array observations of atmospheric solitary waves of depression. In contrast to the high frequency of occurance of solitary waves of elevation only 3 waves of depression have been detected during the two year observational period. An example of an isolated wave of depression may be seen in the microbarograph array record section shown in figure 16 for the early morning hours of July 30, 1976.

Despite the scarcity of observations it seems clear that these phenomena represent a completely different form of atmospheric solitary wave disturbance. An examination of the array records indicates that waves of this type propagate with phase velocities between 14 m/s and 50 m/s, that they have effective wavelengths in the range from 8 km to 30 km, that they produce perturbations in the pressure field at the surface of up to 700 dynes/cm^2 and that they originate at an azimuth of 220^o as measured from true north. Note that solitary waves of elevation have never been observed to originate in this direction. These properties suggest that the atmospheric scale of this type of isolated disturbance is substantially larger than the scale associated with the deep fluid solitary waves of elevation. In particular, the unusually high phase velocities indicate that these disturbances are associated with higher altitude atmospheric structure. We therefore tentatively hypothesize that the observed isolated waves of depression properly belong to the classical solitary wave regime, and are in accord with the predictions of the theories of Peters and Stoker (1960), Long (1965) and Benjamin (1966) for classical solitary wave propagation in a fluid whose density decreases exponentially with height.

In the absence of significant gravity wave activity the micropressure spectrum will be dominated by high frequency pressure variations produced by turbulent eddies associated with winds near the surface. The influence of this component is evident in the microbarograph array record sections shown in figures 7 to 12 and in figure 16. For very low wind conditions, a 6 second acoustic microbarom component is clearly evident, at any time of the year, in the Tennant Creek nocturnal micro-pressure spectrum. During the day, buoyant convection of

of unstable turbulent elements created at the surface introduces an additional important component into the micropressure spectrum.

Solitary waves have been observed at Warramunga under a wide variety of meteorological conditions which range from almost totally calm conditions (see figures 8(a) and 10(b)), indicative of a highly stable boundary layer, through light surface wind conditions with speeds from 1 to 2 m/s as in the case of the events shown in figures 1 and 8(b) to higher surface wind conditions with speeds near 4.5 m/s as in the case of the solitary waves shown in figures 11(b) and 16. The solitary wave propagation vector is not necessarily directed along the surface wind vector. For example, the meteorological measurements show that the surface wind vector and the propagation vectors of the wave packet shown in figure 12(a) and the isolated wave in figure 11(b) differ in azimuth by about 15° whereas the difference in azimuth for the soliton family in figure 11(b) and the solitary wave of depression shown in figure 16 amounts to 90° and 115°, respectively. Note that in all of these cases the passage of the solitary wave appears to have had no lasting influence on the surface wind. It is also worth noting that solitary waves have been observed during periods of local thunderstorm activity and also under totally clear conditions where storm activity is completely absent within 500 km of the array.

Perhaps the most significant meteorological observation is the fact that the surface temperature and humidity are not perturbed by the passage of isolated solitary waves and isolated soliton wave packets. An example which illustrates the observations of surface wind speed, wind direction, temperature

and humidity during the passage of a solitary wave of elevation is given in figure 17. This particular event was chosen for illustration since it is well defined (see figure 1) and since it occurred during a period of fairly quiet atmospheric conditions near the surface. As can be seen from the diagram, the wind vector is virtually unchanged by the passage of the wave and no measurable perturbation in either the temperature or humidity can be associated with the main body of the wave or with the region in the wake of the wave. The dynamical properties of the atmosphere in the wake of the wave therefore appear to be almost the same as the conditions which prevailed prior to the arrival of the solitary wave.

5. Discussion and Conclusions.

A detailed comparison of the observed properties of atmospheric solitons with the predictions of solitary wave theory is complicated by the fact that the theoretical treatments have been restricted to static models with simple forms of the vertical density profile. Perhaps the most serious criticisms of the direct application of these models to nonlinear wave propagation in the Earth's atmosphere are the neglect of wind shear (within the limits of dynamic stability) and the over-simplification of the fluid density structure.

In the discussion of the static theories it was noted that the classical solitary wave of elevation is stable to an amplitude of 0.827. The stability limits for other types of classical waves, such as the solitary wave of depression, and for all forms of deep-fluid solitary wave are unknown; it is, however,

clear from the work of Davis and Acrivos (1967) that the limits for deep-fluid solitary waves extend to much larger amplitudes. The fact that solitary waves can exist with very large amplitudes raises the possibility that waves of this type may significantly alter the dynamical properties of the atmosphere. This interaction could result from a tendency of very large amplitude waves to break* - this complicated process can occur in either the forward or backward direction according to the specific form of the wind and density profiles (Long, 1956(a), 1972) - or from a process of turbulent entrainment of fluid near the crest into the circulation pattern associated with the wave thus leading to turbulence in the wake and to further long-period oscillations corresponding to the motion of displaced buoyant fluid elements. A description of a rare observation of an evolving wave of elevation which may represent a breaking internal solitary wave is given below. If the atmospheric solitary waves described here possess an intrinsic turbulent wake then they are rapidly losing energy and it must be expected that they are of limited range.

Consider now the implications of the laboratory observations and numerical calculations of Davis and Acrivos (1967) on solitary waves propagating in a thin layer of fluid contained between two deep fluids comprising a stably stratified system. As has already been noted, these authors found that

---

* The term "wave-breaking" is used here in the general sense of Long (1972) to denote any tendency for the isolated wave to steepen behind or ahead of the crest as it propagates. If this proves to be the case for large amplitude atmospheric solitons then the dynamics of these waves may well be dominated by amplitude dispersion and they must therefore be viewed as quasi-stationary phenomena.

waves of large amplitude develop closed streamlines characteristic of the circulation in a vortex pair and further, that these waves shed semiperiodic waves behind the main disturbance. It follows directly from an argument based on dynamic symmetry (Benjamin, 1967) that a single vortex occurs within large amplitude solitary waves associated with an inhomogeneous shallow layer of fluid lying beneath a much deeper homogeneous fluid and that this internal circulation coupled with the entrainment hypothesis could lead to the development of a turbulent wake.

A measure of the influence of solitary wave propagation on the dynamical properties of the atmosphere is provided by a comparison (figure 18) of the power spectral densities of the surface pressure field evaluated before and after the passage of the wave. Since this technique includes contributions from fluid motions at high altitudes it should be particularly sensitive to changes in the atmosphere flow field induced by the main body of the wave-changes which may not be apparent in the observations of the flow field at the surface. An examination of all of the cases illustrated in figure 18 shows that the spectral character of the atmosphere is largely unaffected by the passage of the wave. In particular, the power spectra shown in figures 18(a) and 18(b) for a solitary wave of elevation and in 18(d) for a solitary wave of depression indicate that the spectral characteristics both before and after the passage of the event are identical. In the case of the event shown in figure 18(c), the wave of elevation appears to be associated with a slight increase in the amplitude of longer period spectral components. It is worth noting that in all of the three examples illustrated for

solitary waves of elevation an identical 4 to 6 second peak due to microbarom activity appears prominently in both the spectrum evaluated ahead of the wave and spectrum evaluated after the passage of the wave. The slight increase in the amplitude of the longer period components in the wake of the event in figure 18(c) - if at all significant - may be a measure of the irregular waves described by Davis and Acrivos (1967) which are shed by large amplitude deep fluid solitary waves or it may merely represent a small amplitude component of the original disturbance which gave rise to the solitary wave.

The fact that an additional high frequency component is absent in the micropressure spectrum corresponding to the wake of these waves suggests that these isolated solitons do not induce turbulence into the atmosphere. The results of this analysis coupled with the observation of an undisturbed surface flow field therefore leads to the conclusion that these disturbances do not significantly perturb the dynamical state of the atmosphere and that they represent essentially pure solitary wave motion.

Solitary waves are normally observed to pass over the experimental site as highly coherent stationary linear wave fronts. The example illustrated in figure 9(a) is exceptional in that this particular wave of elevation was observed to evolve substantially over the 4 km aperture of the infrasonic array. This is the only example of an evolving soliton wave pattern to be observed during the two year experimental period. The degree of evolution may be seen in

the detailed diagrams presented in figure 19 which show both the microbarogram recordings at each array site and the corresponding true surface pressure variation as determined from the measured data through an inversion of the instrumental response specified by (3.1). This wave of elevation first appeared at site 4 and was then observed to propagate along the diagonal of the quadrilateral array to site 2. The evolution of the solitary wave can therefore be followed by examining the sequence of wave patterns at sites 4,5 and 2. As can be seen from the figure, the isolated wave steadily decrease in amplitude over the array and evolves from the unusual symmetric profile with a flattened crest observed at site 4 to the familiar deep-fluid Lorentz soliton profile observed at site 2. This pattern of evolution is further reflected in a steady decrease in the phase velocity from about 4.7 m/s to 4.2 m/s.

There are a number of possible interpretations of this unusual evolving wave pattern. For example, as has already been noted, the form of the pressure distribution in the neighbourhood of the crest of the initially observed wave could indicate an amplitude instability leading to a type of internal wave breaking which might be manifested in the production of turbulence at the crest through the Kelvin-Helmholtz mechanism. However, our current preferred explanation of this evolving wave pattern is that it represents the transition observed in the laboratory by Davis and Acrivos (1967) of a large amplitude deep fluid solitary wave with closed internal circulation to a smaller amplitude wave with an open

streamline flow pattern characteristic of pure wave motion. It is evident that a complete understanding of the dynamical structure of these waves will require further extensive experimental observations of evolving soliton wave patterns.

Consider now some estimates of the intensity, ΔT, and height, h, of the nocturnal inversion and a measure of the dimensionless solitary wave amplitude, α, which may be obtained to a first approximation from measurements of the surface pressure perturbation, ΔP, the effective wavelength, $w_{\frac{1}{2}}$, and the wave speed, c, by applying Benjamin's two-fluid solitary wave solution (2.11) to the lower atmosphere. To this approximation,

$$\alpha = \frac{\Delta P}{\rho_1 c^2 - \frac{3}{4}\Delta P} , \tag{5.1}$$

$$\Delta T = \frac{T}{2} \left(1 - (1 - \delta)^{\frac{1}{2}}\right) , \tag{5.2}$$

and

$$h = \beta \left(1 - \frac{\Delta T}{T}\right) , \tag{5.3}$$

where

$$\beta = \frac{3}{8} \alpha w_{\frac{1}{2}} ,$$

$$\delta = \frac{4\Delta P}{g\beta\rho_1\alpha} ,$$

T is the temperature of the upper fluid and ρ_1 is the density of the lower fluid. In these expressions, the intensity of the inversion and the height of the inversion above the surface are to be regarded as the effective parameters of a two-layer model which provides the simplest

possible description of the complex thermal structure of the nocturnal inversion. In these calculations, T is taken as 280 K and the lower fluid density is held constant at 1.2×10^{-3} gm cm^{-3} corresponding to an inversion near the 980 mb level. The results are presented in Table 1.

The events listed in this table were chosen to illustrate the properties of a wide variety of isolated solitary wave forms. All of these events occurred under low surface wind conditions. It should be noted that the derived parameters corresponding to waves of large amplitude may be unreliable since the theory is valid only to first order in α. As can be seen from the table, this model indicates that solitary wave activity is usually associated with a temperature inversion with an effective depth between 40 to 400 m and with an effective intensity in the range from about 2 to 12°C. The first entries in the table describe solitary wave propagation along a relatively shallow inversion; these events are typical of many of the low amplitude solitary-wave signals which have been observed.

There are, as yet, no suitable measurements of the nocturnal inversion temperature profile with which these results can be compared. Clarke et al. (1971) have reported the results of atmospheric soundings at Hay, N.S.W., 2000 km to the south-east of Tennant Creek, which reveal nocturnal inversion depths from 80 to 200 m and intensities of up to about 5°C. It can be expected that the lower latitude location and semi-desert environment of the Tennant Creek infrasonic array will favour the development of much stronger nocturnal

radiation inversions. This is in agreement with inversion intensities of up to 10°C observed by Reynolds and Gething (1970) at Julia Creek during the course of their acoustic sounding experiments. It seems reasonable therefore to conclude that almost all of the isolated waves of elevation detected at Warramunga are deep fluid solitary waves which propagate along a nocturnally-cooled surface layer.

The very large amplitude event which occurred on day 392 is exceptional in that the scale associated with this particular solitary wave is significantly greater than that of any other wave of elevation detected during the two year observational period. It is therefore suggested, in view of the atmospheric scale involved, that this particular wave may be better described as a classical solitary wave of elevation which is similar - *though* on a smaller scale - to the solitary wave disturbance reported by Abdullah (1955).

It must be emphasized at this point that any discussion of the source mechanisms which excite these solitary waves is largely conjectural since the range and lateral extent of these waves are almost totally unknown. Existing evidence, such as the fact that these waves traverse the 4 km infrasonic array as highly coherent planar wavefronts and the observation, noted above, by Reynolds and Gething (1970) that solitary wave associated disturbances appear to propagate essentially unattenuated over distances of about 40 km, suggests that these waves originate at large distances from the array. However, if the internal morphology of the waves takes the form of a closed circulation which leads to an intrinsic tendency to

shed semiperiodic disturbances behind the main body, or, if these waves are breaking, then they are rapidly losing energy and it must therefore be anticipated that they are of limited range. On the other hand, the experimental observations do not indicate the presence of significant wave-induced turbulence; it therefore appears that the waves of elevation could have a range of up to about 600 km, the limit set by the speed of the wave and the duration of the nocturnal inversion.

Perhaps the first question that should be considered is whether or not the solitary waves observed near Tennant Creek are due to the passage of a frontal system. Dry, cold fronts occur with reasonable frequency over the extreme southern portion of Australia. These fronts seldom reach the center of the continent and are very rare at the experimental site in the Northern Territory. An examination of the isochrones of these cold fronts shows that the few degenerate fronts which extend to Tennant Creek arrive from an azimuth near 220°. It has been established that solitary waves of elevation originate predominantly in directions near 20° and 140° that they never originate in the direction of 220°, that they only occur at night, that they often occur on several nights in succession and that two or more of these waves may pass over the experimental site from different directions during the same night. All of these observations are inconsistent with an interpretation involving the passage of a cold front. In addition, the microbarograph records of these well-defined isolated waves of elevation bear little resemblance to the complex micropressure pattern recorded by McDonald (1974) during the passage of a

frontal system over an array located in northern Texas. It therefore seems very unlikely that cold fronts play an important role in the production of deep fluid atmospheric solitons.

In contrast, the 3 classical solitary waves of depression detected at Tennant Creek do appear to originate in the same direction as atmospheric fronts. However, an examination of the synoptic patterns fails to confirm that these events coincided with the passage of a cold frontal system; nevertheless, the possibility that these large amplitude waves occur in conjunction with weak frontal activity should not be ruled out at this point.

Smart (1966) and Jordan (1972) associate their observed exponential pressure pulses with thunderstorms. The organized, precipitation initiated and maintained downdraft of cold air in severe mature storms is well documented (Wallington, 1961; Browning & Ludlam, 1962; Spillane & McCarthy, 1969). Smart developed a model to describe these pressure pulses by considering the unstable solution of Brunt's well known basic equation of motion (Brunt, 1927) for the vertical displacement (dh) of a parcel of air*:

$$\frac{d^2(dh)}{dt^2} + \frac{g}{T}\left(\beta + \frac{dT}{dh}\right)dh = 0 \qquad (5.4)$$

---

*Priestley (1953) has derived simultaneous equations which describe the vertical motion and temperature of buoyant fluid elements subject to turbulent mixing with the surroundings. A more general theoretical treatment which includes the effect of turbulent fluid entrainment has been given by Turner (1963). In the case of unstable environments solutions exist for both of these models in which the velocity of the fluid element ultimately increases exponentially with time. These models provide a firmer basis for a description of downdraft flow in thunderstorms.

Brunt noted that if the lapse rate, $-dT/dh$, is greater than the adiabatic lapse rate, β, no restoring force exists, and consequently a downwards displaced air parcel will continue to accelerate exponentially. Smart adapted this result to explain the observed form of the pressure pulses by noting that the downwards descending parcel is subject to a constant pressure gradient and thus the density of the parcel increases exponentially with the result that (assuming the approximate validity of the hydrostatic law) the ground level pressure contains an exponentially increasing component. Smart also hypothesized that the downwards motion continues to accelerate in smooth laminar flow until a critical velocity is reached, at which point the flow becomes turbulent and mixes rapidly with nearby warmer air thus causing rapid oscillations behind the pulse, and, eventully, a reduction of the pressure to the ambient level. On the basis of this model, Smart was able to account for 4 out of 10 observations of exponential pressure pulses.

There appear to be a number of difficulties associated with this model, the most serious of which is the fact that this explanation is applicable only to observations recorded directly beneath a thunderstorm downdraft; it must be expected that the ground level pressure distribution outside this very localized region is of a completely different form. Consequently, the observations reported by Jordan (1972) of pressure pulses coming from thunderstorms at distances of the order of 100 km are not accounted for by this model as it stands.

It is an obvious extension of this model to include

the influence of the gravity current of undercutting cold air that advances away from the thunderstorm as the downdraft spreads out at the surface. Wallington (1961) noted an example in which this density current extended over 50 km and the subject has recently been treated in detail by Charba (1974) and by Goff (1976). An interesting description of a Sudanese *haboob*, a downdraft gravity current made visible by its high dust content, has been given by Lawson (1971). A reasonable explanation of long-range thunderstorm-generated pressure pulses is that they represent solitary waves produced by either the direct impulsive interaction of the downdraft on an inversion or the concommitant interaction of the gravity current with an existing inversion. The latter mechanism is closely related to the phenomenon of soliton production in the developing frontal zone of an advancing bore as shown in the numerical studies of Peregrine (1966) and Vleigenthart (1971) on the evolution of non-stationary solutions of the KdV equation.

According to the comprehensive study of Goff (1976), the abrupt transition in surface atmospheric conditions which accompanies the passage of the frontal zone of a well-developed quasi-steady downdraft-produced density current is characterized by a sharp decrease in temperature in the range from 2 to 10°C, a sudden onset of persistent winds and a rapid increase of about 3.4 mb on the average in the surface pressure level. This transition is usually followed by the onset of precipitation. It is clear that a downdraft gravity current interpretation fails to account for the isolated nocturnal disturbances described in this paper since none

of these perturbations of the atmospheric flow field are observed (see figure 17) to accompany these events.

It is possible that some of the solitary waves observed at Tennant Creek during the monsoon season from December to February are due to thunderstorm activity. Note, however, that only one solitary wave has been observed during the month of January. As can be seen from the monthly frequency analysis shown in figure 13, solitary waves are most commonly observed during the period from April to September, a period of very low storm activity. Furthermore, solitary waves have been observed to occur under completely clear conditions when storm activity is absent within several hundred kilometers of the array. We therefore conclude that the thunderstorm source mechanism is of minor importance.

The fact that solitary waves of elevation come from preferred directions suggest that they may be orographic in origin. Consider first the large number of observations of isolated waves which arrive from an azimuth of 140°. These waves are usually detected near midnight but they also occur with reasonable frequency at other times during the night. As one proceeds in the direction of 140° from the infrasonic array the terrain can be described, initially, as a more or less flat featureless plain. At about 10 km from the array a complicated pattern of hills comprising the Murchison Range begins to appear on the right at a distance of about 5 km. This chain of hills, which rises to a maximum elevation of about 200 meters over the surrounding plain, runs parallel to the 140° direction for

a distance of about 100 km. Beyond this point the level plain slowly gives way to the Davenport Range which intersects the Murchison Range at the same altitude at about 140 km from the array. Further afield in this direction the terrain descends to an arid plain which continues uninterrupted and finally merges with the Simpson Desert at a distance of about 460 km.

The presence of these nearby ranges suggests that the origin of solitary waves coming from this direction is to be found in the interaction with an existing inversion of katabatic (down-slope) nocturnal flow of surface-cooled air from these hills on to the surrounding plain. The hypothesis of super-critical katabatic drainage leading to an internal atmospheric hydraulic jump has been employed with considerable success by Ball (1956) (see also, Ball 1957; Lied, 1964) to explain the sudden stationary discontinuity found in surface winds in the Antarctic. Similarly, Clarke (1972) has explained a frequently occurring, sudden, near-dawn squall, accompanied by a spectacular low horizontal roll cloud known as the "morning glory", on the south coast of the Gulf of Carpentaria by evoking the concept of a propagating undular gravity current created in the process of nocturnal surface flow down a 1:1000 slope from the 500 m highlands to the east. Clarke carried out a number of numerical experiments and concluded that internal atmospheric bores and also propagating hydraulic jumps should commonly occur at low latitudes when katabatic flow discharges on to a plain under conditions of a stable radiation inversion.

This conclusion appears to be reinforced by the acoustic soundings at Julia Creek reported by Reynolds and

Gething (1970) which revealed, as has already been noted, the occurrence of a jump in the height of the nocturnal inversions. These authors also hypothesized the existence of katabatic flow aided in part by the geostrophic wind and orographic convergence and concluded that the observed jumps in the inversion level could be attributed to either the head of a gravity current propagating as an internal bore or a travelling internal hydraulic jump.

Since the rise in topography in this direction appears to be sufficient to produce significant nocturnal boundary layer currents, it is proposed that the observed solitary waves coming from an azimuth of 140° are generated in the interaction of katabatic flow with the nocturnal inversion and that they propagate along the inversion to the array. It is premature, without further experimental work, to examine this mechanism in detail but it probably takes one of the following forms:

(a) The direct impulsive interaction of an advancing gravity current impinging on an established inversion;

(b) The disturbance of the atmospheric flow field during the creation (or dissipation) of a hydraulic jump; this may occur at the point where supercritical down-slope flow encounters the horizontal plane - this hydraulic jump may subsequently propagate upstream or downstream as flow conditions vary - or in conjunction with a supercritical-subcritical flow transition in the neighbourhood of a topographic barrier on the horizontal plane;

(c) the momentary transition of a steady advancing bore to a non-stationary flow state upon encountering a topographic obstacle such as a ridge or valley, and

(d) direct soliton production in the evolving frontal zone of a gravity current as described above for downdraft-associated density currents - this is probably the most important mechanism.

The interpretation in terms of katabatic flow at an orographic feature accounts for both the occurrence of waves coming from the direction of 140° and for the scarcity of events originating in the south-west quadrant where orographic features suitable for the production of katabatic flow are absent. However, an attempt to apply an interactive katabatic wind interpretation to account for the source of the large number of solitary waves which originate in the north-east and north-west quadrants is less successful. Consider the waves which arrive from the direction of the Gulf of Carpentaria. In this direction, the elevation decreases steadily from about 410 m MSL to 200 m at a distance of about 150 km from the array. From this point, the land rises slowly to form the Barkly Tablelands at an altitude of about 260 m. At the edge of the Tablelands, about 340 km from the array, the land again rises to about 310 m and then falls continuously to the hot tropical coast of the Gulf 500 km from the array.

It is possible that solitary waves originating in this direction are produced in the dissipation of gravity currents flowing towards the array into the broad shallow valley which separates Warramunga and the Barkly Tablelands. However, in

this case, the topography would not appear to support significant katabatic flow. A katabatic density current interpretation for the source of events originating to the east and north-east can be ruled out for the same reason. A different type of source mechanism is therefore required to explain the solitary waves which originate in these directions.

An indication of the range of isolated waves which originate to the north of the array is given by the observation that the majority of these events are observed to occur between 02.00 and 07.00 CST. This suggests that the source of these waves is to be found at a considerable distance from the array. If it is assumed that these waves are created during or shortly after the formation of a stable inversion then the average measured speed of 10 m/s is consistent with a source in the neighbourhood of the coastal edge of the Barkly Tablelands. This suggests that the solitary waves observed at Warramunga which originate in the directions of the Gulf of Carpentaria and the Timor Sea may represent the final form of deeply penetrating sea-breeze fronts. Solitary wave production might proceed, as described above, through the formation of a soliton wave packet along the leading edge of a shallow sea-breeze current or simply through the evolution of the direct density current produced disturbance of the inversion layer. Insight into the nature of a new and probably more important mechanism is provided by the recent observations described by Simpson et al. (1977) of the formation of a horizontal vortex at the head of a sea-breeze front which separates from the sea-breeze shortly before sunset and continues to propagate as an independent phenomenon. The unusual stability of a propagating semi-elliptical horizontal atmospheric

vortex has been considered by Clarke (1965). Since closed circulation in the form of a propagating vortex is also a characteristic of large amplitude deep fluid solitary waves it is reasonable to assume that a sea-breeze generated vortex which interacts with the nocturnal inversion will eventually evolve into an internal atmospheric solitary wave.

This concludes the description and interpretation of atmospheric internal solitary waves which are observed in the arid interior of Australia. It is evident that further measurements of the properties of these waves are required if a full understanding of phenomena of this type is to be achieved. In particular, the evolution of the frontal zone of a shallow internal density current advancing into a deep stratified fluid and the role played by disturbances of this type in the production of solitary waves deserve further study. The experimental program at Warramunga is therefore being expanded to include further meteorological instrumentation. In addition, the infrasonic array is being enlarged, through the addition of portable array elements, to an aperture of about 100 km. With the completion of this program it should be possible to carry out a detailed investigation of the degree of wave coherence over large distances and to establish with certainty the source mechanisms responsible for the creation of waves of this type.

ACKNOWLEDGEMENTS

The authors wish to express their gratitude to Professor J.S. Turner for helpful comments on a first draft of this paper and to Dr. J.F. Gettrust for several stimulating discussions during the course of this research. We thank also an unknown reviewer for comments on an earlier draft of this paper. These comments have led to the inclusion of some data from more recent observations at Tennant Creek. In addition, we wish to thank Mr. David Daffen and Mr. Blair Lade for their efforts in operating and maintaining the Warramunga Seismic Station. This research was supported by the Air Force Office of Scientific Research under Contract No. AFOSR 75.2759A.

REFERENCES

Abdullah, A.J. 1949: Cyclogenesis by a purely mechanical process. J.Meteorology, 6, 86-97.

Abdullah, A.J. 1955: The atmospheric solitary wave. Bull.Amer.Met.Soc., 36. 511-518.

Abdullah, A.J. 1956: A note on the atmospheric solitary wave. J.Meteorology, 13, 381-387.

Ball, F.K. 1956: The theory of strong katabatic winds. Aust.J.Phys., 9, 373-386.

Ball, F.K. 1957: The katabatic winds of Adélie Land and King George V Land. Tellus, 9, 201-208.

Benjamin, T.B. 1966: Internal waves of finite amplitude and permanent form. J.Fluid Mech., 25, 241-270.

Benjamin, T.B. 1967: Internal waves of permanent form in fluids of great depth. J.Fluid Mech., 29, 559-592.

Bingham, C., Godfrey, M.D. and Tukey, J.W. 1967: Modern techniques of power spectrum estimation. Trans.IEEE AU-15, 2, 56-66.

Boussinesq, J. 1871: Théorie de l'intumescence liquide appelée onde solitaire ou de translation se propageant dans un canal rectangulaire. Inst.France, Acad.Sci.C.R., June 19, p.755.

Browning, K.A. and Ludlam, F.H. 1962: Airflow in convective storms. Quart.J.R.Met.Soc., 88, 117-135.

Brunt, D. 1927: The period of simple vertical oscillations in the atmosphere. Quart.J.R.Met.Soc., 53, 30-32.

Byatt-Smith, J.G.B. 1970: An exact integral equation for steady surface waves. Proc.Roy.Soc.Lond., A 315, 405-418.

Byatt-Smith, J.G.B. and Longuet-Higgins, M.S. 1976: On the speed and profile of steep solitary waves. Proc.R.Soc.Lond., A350, 175-189.

Chan, R.K.-C. 1974: A discretized solution for the solitary wave. J.Comput.Phys., 16, 32-48.

Charba, J. 1974: Application of gravity current model to analysis of squall-line gust front. Mon.Wea.Rev., 102, 140-155.

Clarke, R.H. 1965: Horizontal mesoscale vortices in the atmosphere. Austr.Met.Mag., 50, 1-25.

Clarke, R.H., Dyer, A.J., Brook, R.R., Reid, D.G. and Troup, A.J. 1971: The Wangara experiment: Boundary layer data. Tech. Paper No.19, Division of Meteor.Physics, CSIRO, Melbourne.

Clarke, R.H. 1972: The morning glory: an atmospheric hydraulic jump. J.Appl.Met., 11, 304-311.

Davis, R.E. and Acrivos, A. 1967: Solitary internal waves in deep water. J.Fluid Mech., 29, 593-607.

Fenton, J. 1972: A ninth-order solution for the solitary wave. J.Fluid Mech., 53, 257-271.

Friedrichs, K.O. 1948: On the derivation of the shallow water theory. Appendix to J.J. Stoker, The formation of breakers and bores, Comm.Pure Appl.Math., 1, 81-87.

Friedrichs, K.O. and Hyers, D.H. 1954: The existence of solitary waves. Comm.Pure Appl.Math., 7, 517-550.

Goff, R.C. 1976: Vertical structure of thunderstorm outflows. Mon.Wea.Rev., 104, 1429-1440.

Gossard, E.E. and Hooke, W.H. 1975: Waves in the Atmosphere. Elsevier, 456 pp.

Grimshaw, R. 1971: The solitary wave in water of variable depth. Part 2. J.Fluid Mech., 46, 611-622.

Hurdis, D.A. and Pao, H. 1975: Experimental observation of internal solitary waves in a stratified fluid. Phys.Fluids, 18, 385-386.

Jordan, A.R. 1972: Atmospheric gravity waves from winds and storms. J.Atmos.Sci., 29, 445-456.

Kanasewich, C.D., Hemmings, C.D. and Alpaslan, T. 1973: N-th root stack nonlinear multichannel filter. Geophysics, 38, 327-338.

Karpman, V.I. 1975: Non-linear Waves in Dispersive Media. Pergamon Press (trans. from Russian).

Keller, J.B. 1948: The solitary wave and periodic waves in shallow water. Comm.Pure Appl.Math., 1, 323-339.

Keulegan, G.H. 1953: Characteristics of internal solitary waves. J.Research Nat.Bur.Standards, 51, 133-140.

Korteweg, D.J. and de Vries, G. 1895: On the change of form of long waves advancing in a rectangular canal and on a new type of long stationary waves. Phil.Mag., 39 (5), 422-443.

Laitone, E.V. 1960: The second approximation to cnoidal and solitary waves. J.Fluid Mech., 9, 430-444.

Lamb, H. 1932: Hydrodynamics, 6th edn. Cambridge University Press, 423-426.

Lavrent'ev, M.A. 1947: On the theory of long waves. Akad.Nauk. Ukrain. RSR., Zbornik Prac.Inst.Mat., 1946, No.8, 13-69. (Trans. in Am.Math.Soc.Transl., Ser.1, 11, 273-321, 1962).

Lawson, T.J. 1971: Haboob structure at Khartoum. Weather, 26, 105-112.

Lenau, C.W. 1966: The solitary wave of maximum amplitude. J.Fluid Mech., 26, 309-320.

Lied, N.T. 1964: Stationary hydraulic jumps in a katabatic flow near Davis, Antarctica, 1961. Aust.Met.Mag., 47, 40-51.

Long, R.L. 1956a: Long waves in a two-fluid system. J. Meteorology, 13, 70-74.

Long, R.L. 1956b: Solitary waves in one- and two-fluid systems. Tellus, 8, 460-471.

Long, R.L. 1965: On the Boussinesq approximation and its role in the theory of internal waves. Tellus, 17, 46-52.

Long, R.L. 1972: The steepening of long, internal waves. Tellus, 24, 88-99.

Longuet-Higgins, M.S. and Fenton, J.D. 1974: On the mass, momentum, energy and circulation of a solitary wave. II. Proc.R.Soc.Lond. A 340, 471-493.

McAllister, L.G., Pollard, J.R., Mahoney, A.R. and Shaw, P.J.R. 1969: Acoustic sounding - a new approach to the study of atmospheric structure. Proc.IEEE, 57, 579-587.

McDonald, J.A. 1974: Naturally occurring atmospheric acoustical signals. J.Acoust.Soc.Am., 56, 338-351.

Muirhead, K.J. 1968: Eliminating false alarms when detecting seismic events automatically. Nature, 186, 704.

Muirhead, K.J. and Ram Datt 1976: The Nth root process applied to seismic array data. Geophys.J.Roy.Astr.Soc., 47, 197-210.

Peregrine, D.H. 1966: Calculations of the development of an undular bore. J.Fluid Mech., 25, 321-330.

Peters, A.S. and Stoker, J.J. 1960: Solitary waves in liquids having non-constant density. Comm.Pure Appl.Math., 13, 115-164.

Philips, D.H. 1976: A pressure jump and an associated seiche at Tobruk. Met.Mag., 105, 110-122.

Priestley, C.H.B. 1953: Buoyant motion in a turbulent environment. Aust.J.Phys., 6, 279-290.

Rayleigh, Lord, 1876: On waves. Phil.Mag., 1(5), 257-279.

Reynolds, R.M. and Gething, J.T. 1970: Acoustic sounding at Benalla, Victoria and Julia Creek, Queensland. Publ.No.17, Meteor.Department, University of Melbourne, Project EAR, Reports V-VII.

Scott-Russell, J. 1837: Report on Waves. British Association Reports, 417.

Scott-Russell, J. 1844: Report on Waves. British Association Reports, 311.

Shaw, N.A. 1971: Acoustic sounding of the atmosphere. Ph.D. thesis, Dept. of Physics, University of Melbourne, Melbourne.

Simpson, J.E., Mansfield, D.A. and Milford, J.R. 1977: Inland penetration of sea-breeze fronts. Quart.J.R.Met.Soc., 103, 47-76.

Smart, E. 1966: An examination of atmospheric pressure pulses recorded on microbarographs. M.Sc. thesis, Department of Physics, Colorado School of Mines, Golden, Colorado.

Spillane, K.T. and McCarthy, M.J. 1969: Downdraft of the organized thunderstorm. Aust.Met.Mag., 17, 3-24.

Stokes, G.G. 1880: On the theory of oscillatory waves. Mathematical and physical papers, 1, 197-229, 314. Cambridge University Press.

Strelkoff, T. 1971: An exact numerical solution of the solitary wave. Proc.2nd Int.Conf.Num.Methods Fluid Dyn., 441-446. Springer.

Turner, J.S. 1963: The motion of buoyant elements in turbulent surroundings. J.Fluid Mech., 16, 1-16.

Vliegenthart, A.C. 1971: On finite-difference methods for the Korteweg-de Vries equation. J.Eng.Maths., 5, 137-155.

Wallington, C.E. 1961: Observations of the effects of precipitation downdraughts. Weather, 16, 35-43.

Welch, P.D. 1967: The use of fast Fourier transforms for the estimation of power spectra; a method based on time averaging over short modified periodograms. Trans.IEEE AU-15, 2, 70-73.

Yamada, H. 1957: On the highest solitary wave. Rep.Res.Inst. Appl.Mech.Kyushu Univ., 5, 53-67.

Yamada, H. 1958: On approximate expressions of solitary wave. Rep.Res.Inst.Appl.Mech.Kyushu Univ., 6, 35-47.

Yamada, H., Kimura, G. and Okabe, J. 1968: Precise determination of the solitary wave of extreme height on water of a uniform depth. Rep.Res.Inst.Appl.Mech. Kyushu Univ., 16, 15-32.

Zabusky, N.J. and Kruskal, M.D. 1965: Interaction of "solitons" in a collisionless plasma and the recurrence of initial states. Phys.Rev.Lett., 15, 240-243.

TABLE 1. Measured properties of internal solitary atmospheric waves of elevation and corresponding theoretical estimates of the intensity and height of the temperature inversion and of the solitary wave amplitude based on Benjamin's first order approximation to the two-component deep-fluid solitary wave solution. The measured signal amplitude and full width of the profile at half maximum are obtained from array averages corrected for instrumental response.

Event	Day	Time (CST)	Velocity c ($m\ s^{-1}$)	Azimuth Θ (degrees)	Signal Amplitude ΔP ($dyn\ cm^{-2}$)	Full Width at Half Maximum $w_{½}$ (km)	Inversion Intensity ΔT (°C)	Inversion Height h (m)	Solitary Wave Amplitude $\alpha = a/h$
63-1-1233#	34	0216	4	20	50	0.47	6.8	55	0.32
76-2-1177#	140	0228	5	100	50	0.51	12.2	42	0.23
1-2-976	238	2146	4	340	80	0.39	3.6	88	0.61
80-1-487#	167	0920	7	20	300	1.30	2.2	390	0.83
51-2-1318#	315	0524	13	280	450	4.40	9.2	430	0.27
75-2-392	133	2258	16	280	1100	7.70	3.8	1400	0.49

Leading soliton in solitary wave group

FIGURE CAPTIONS

1. An example of a microbarograph array record section corresponding to the passage of an internal solitary wave of elevation. The azimuth noted for this wave is the source direction measured from true north.

2. Internal solitary wave surface pressure profiles corresponding to a 5^{o}C temperature inversion at the 980 mb level. The dimensionless amplitude, α, is chosen to be 0.5.

   (a) Classical internal solitary wave described by (2.1) with K = 1.

   (b) Internal solitary wave described by Benjamin's theory (2.11) for a fluid of great depth.

3. Configuration of the five-component microbarograph array.

4. Measured microbarograph amplitude response.

5. Computed microbarograph response to synthetic micropressure waveforms.

   (a) Solitary wave of elevation

   (b) Soliton wave packet ordered by amplitude

   (c) Solitary wave of depression

6. Variation in surface pressure derived from recorded microbarograph data through an inversion of the instrumental response specified by (3.1).

   (a) Solitary wave of elevation

   (b) Soliton wave packet

   (c) Solitary wave of depression

7. Examples of solitary waves of elevation observed at the Warramunga Seismic Station. Despite the relatively poor signal-to-noise ratio these waves are clearly defined in the infrasonic records. The deep fluid solitary wave signals shown in this figure are typical of the large number of small amplitude events of this type which have been observed.

8. Microbarometer array record sections which illustrate large amplitude solitary waves of elevation. Note the almost complete absence

of high frequency components in the micropressure spectrum corresponding to the wake of the wave shown in (a). Two smaller solitary waves preceed the unusually large amplitude event shown in (b).

9. Examples of unusual solitary wave characteristics.

(a) An evolving solitary wave of elevation.

(b) A solitary wave group consisting of 2 closely spaced large amplitude solitons.

10. Infrasonic array record sections containing isolated groups of well separated solitary waves of elevation.

11. Two examples of observations of large amplitude solitary wave packets.

12. Record sections which illustrate the signal characteristics of complex low amplitude solitary wave packets. In both of these examples the pronounced asymmetry of the differential signal indicates that the wave packet is formed from a family of well separated solitons.

13. Monthly frequency of observation of solitary waves of elevation.

14. Frequency of observation of deep fluid solitary waves as a function of time of day.

15. Occurrence of solitary waves of elevation as a function of source azimuth.

16. Microbarograph array observation of a large amplitude solitary wave of depression.

17. Microbarograph record and corresponding measurements of surface temperature, humidity, wind speed and wind direction, recorded at site 1, for the solitary wave of elevation which passed over the infrasonic array at 23.53 on the night of Dec. 2, 1976.

18. Some comparisons of the micropressure power spectral density ahead of and in the wake of isolated waves which illustrate the influence of the passage of internal solitary waves on the atmospheric spectrum. High frequency changes in the spectral estimates may be viewed as a

AD-A062 567 AUSTRALIAN NATIONAL UNIV CANBERRA RESEARCH SCHOOL OF--ETC F/G 4/1
RESEARCH ON LINEAR AND NONLINEAR ATMOSPHERIC WAVES.(U)
AUG 78 D R CHRISTIE, K J MUIRHEAD, A L HALES AFOSR-75-2759
UNCLASSIFIED 78-1 AFOSR-TR-78-1642 NL

2 OF 2
AD
A062567

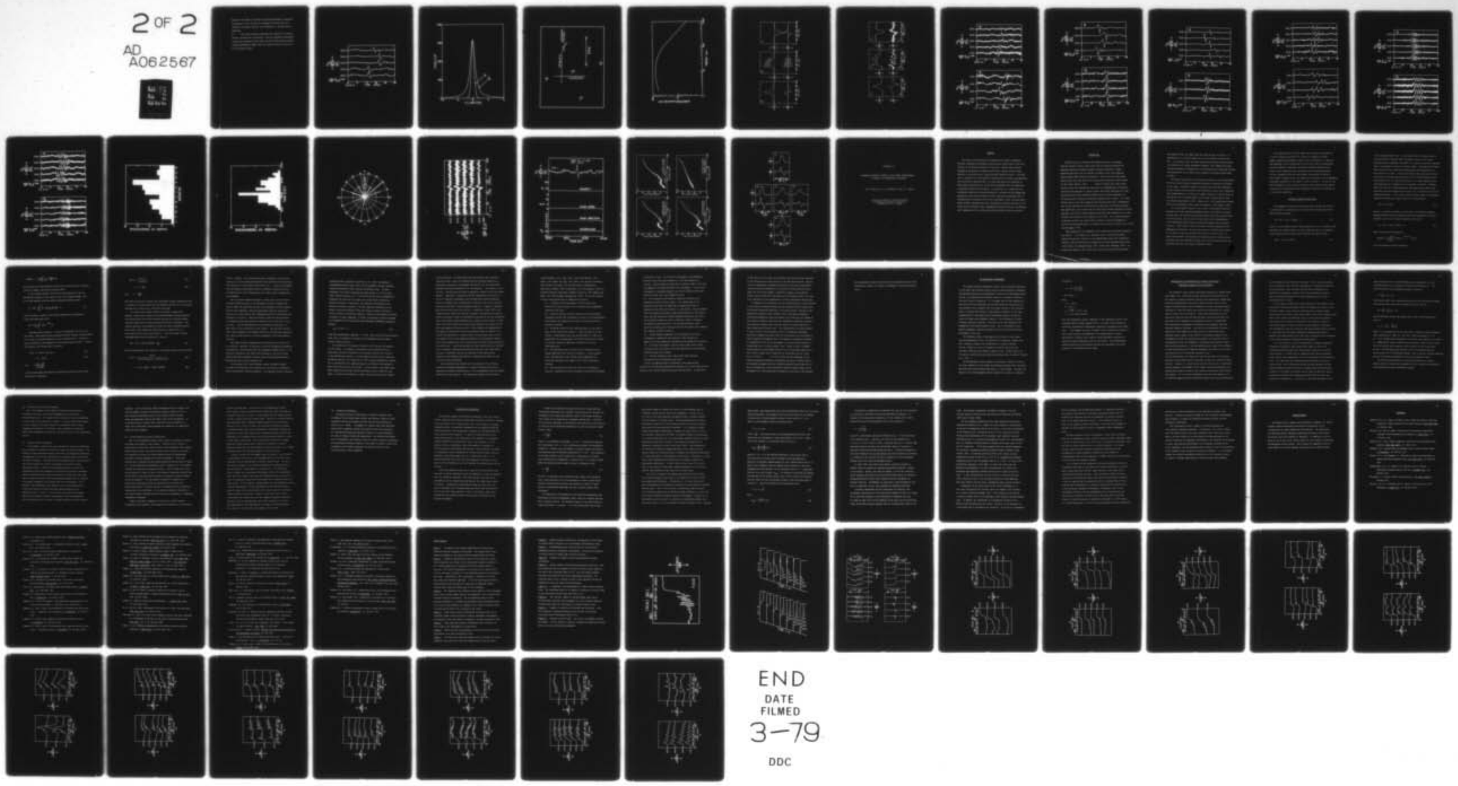

END
DATE
FILMED
3-79
DDC

measure of the degree of solitary wave-induced atmospheric turbulance. The analyses in (a), (b) and (c) correspond to solitary waves of elevation; the spectra shown in (d) correspond to a solitary wave of depression.

19. The surface pressure characteristics produced by an unusual evolving solitary wave of elevation. Both the recorded microbarograph solitary wave signature (lower trace) and the derived absolute surface pressure perturbation (upper trace) are shown in detail for each site of the intrasonic array.

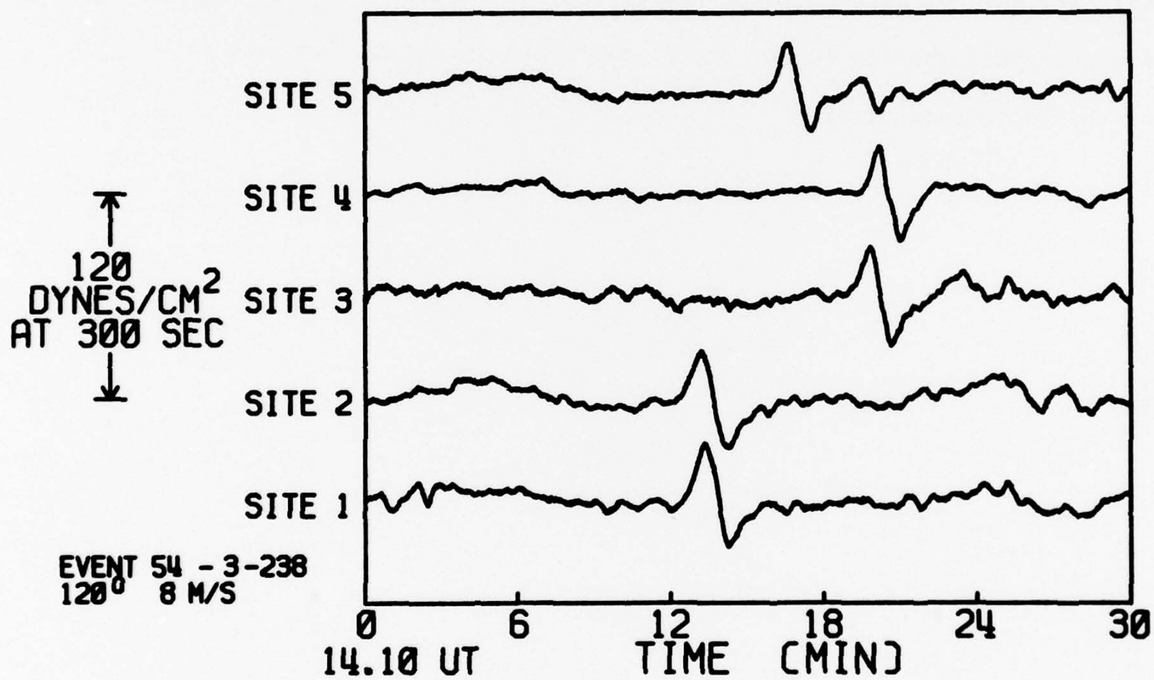
SITE 5
SITE 4
SITE 3
SITE 2
SITE 1
120
DYNES/CM2
AT 300 SEC
EVENT 54 - 3-238
120° 8 M/S
0
6
12
18
24
30
14.10 UT
TIME (MIN)

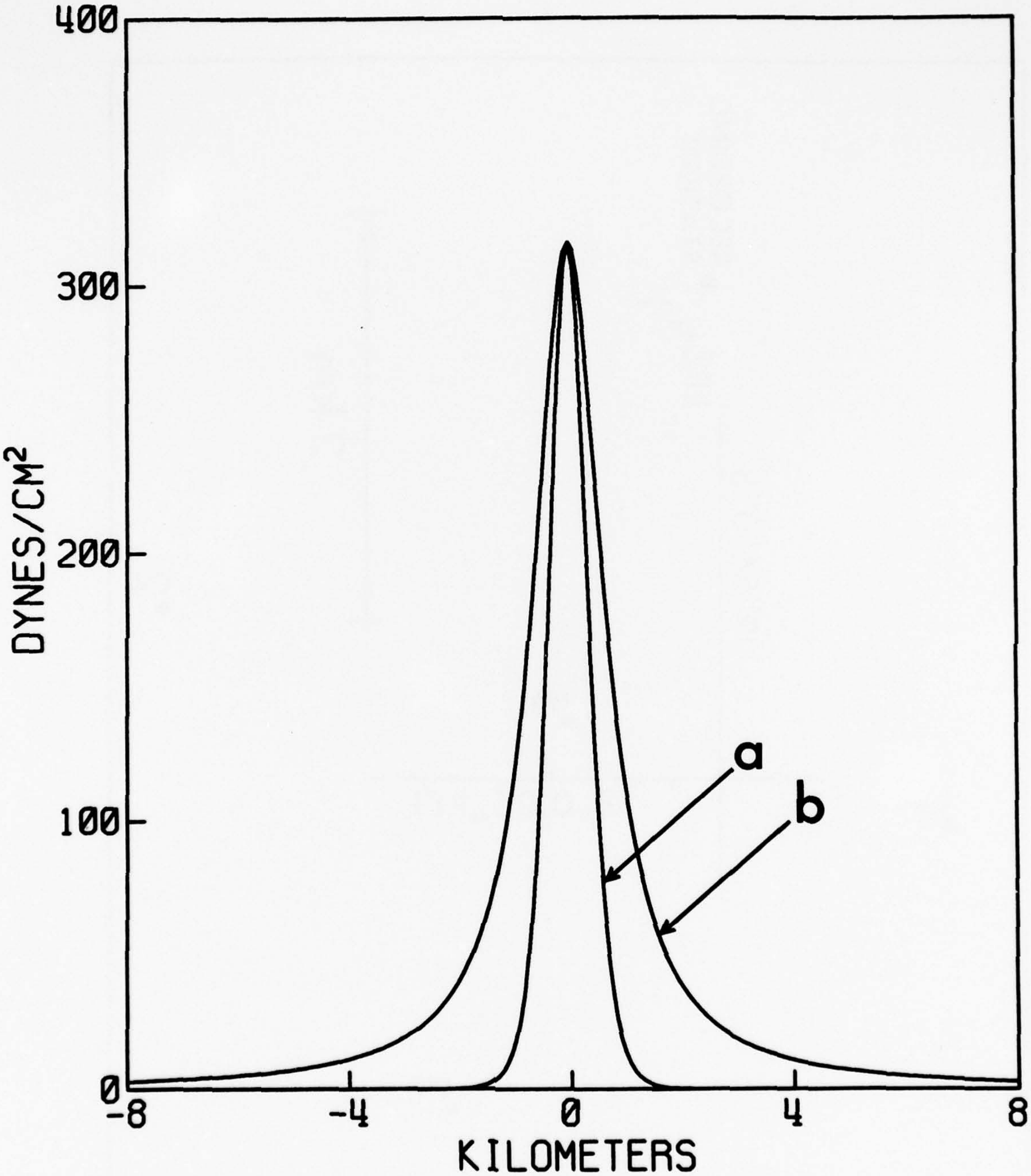

400
300
200
100
0
DYNES/CM²
a
b
-8
-4
0
4
8
KILOMETERS

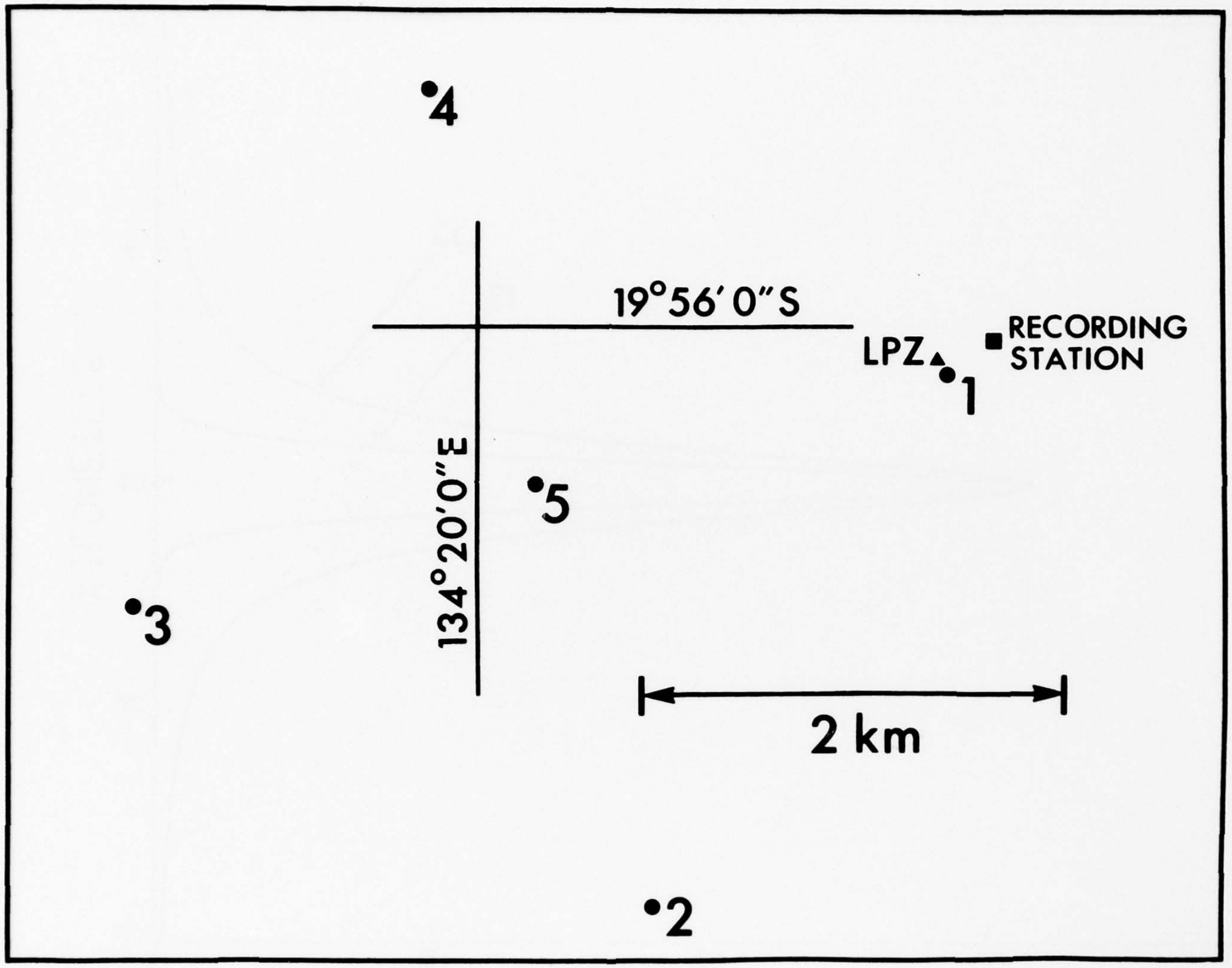

•4
19°56′0″S
LPZ
RECORDING STATION
•1
134°20′0″E
•5
•3
2 km
•2

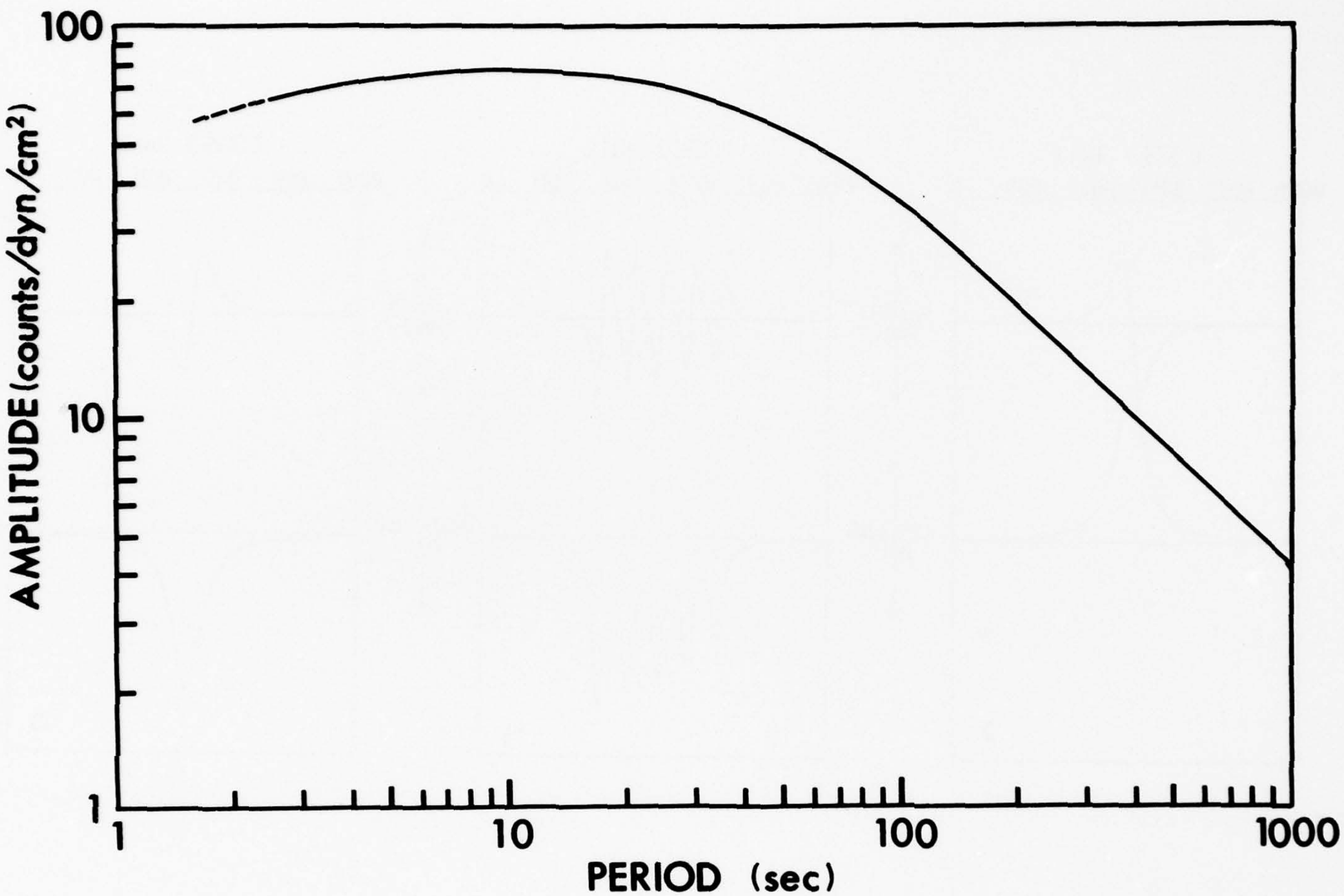

AMPLITUDE (counts/dyn/cm²)
100
10
1
1
10
100
1000
PERIOD (sec)

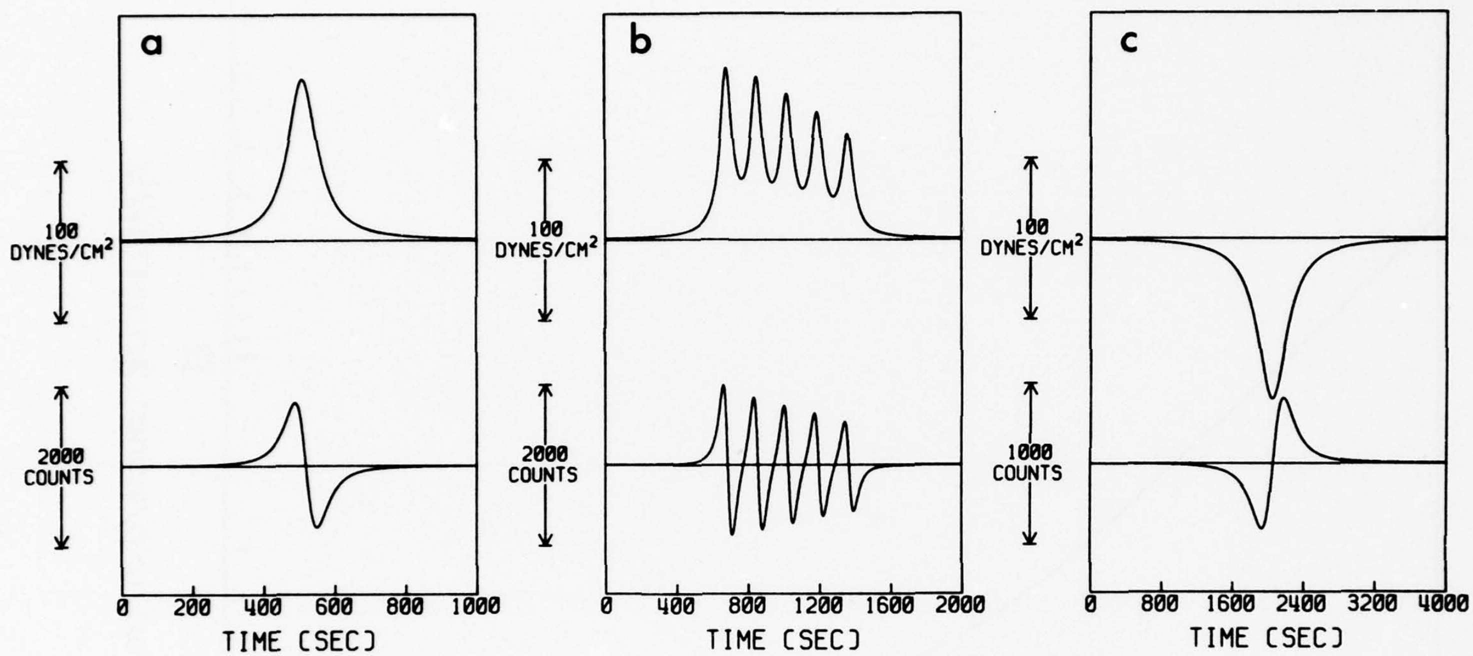

a
b
c
100 DYNES/CM²
2000 COUNTS
100 DYNES/CM²
2000 COUNTS
100 DYNES/CM²
1000 COUNTS
0 200 400 600 800 1000
0 400 800 1200 1600 2000
0 800 1600 2400 3200 4000
TIME (SEC)
TIME (SEC)
TIME (SEC)

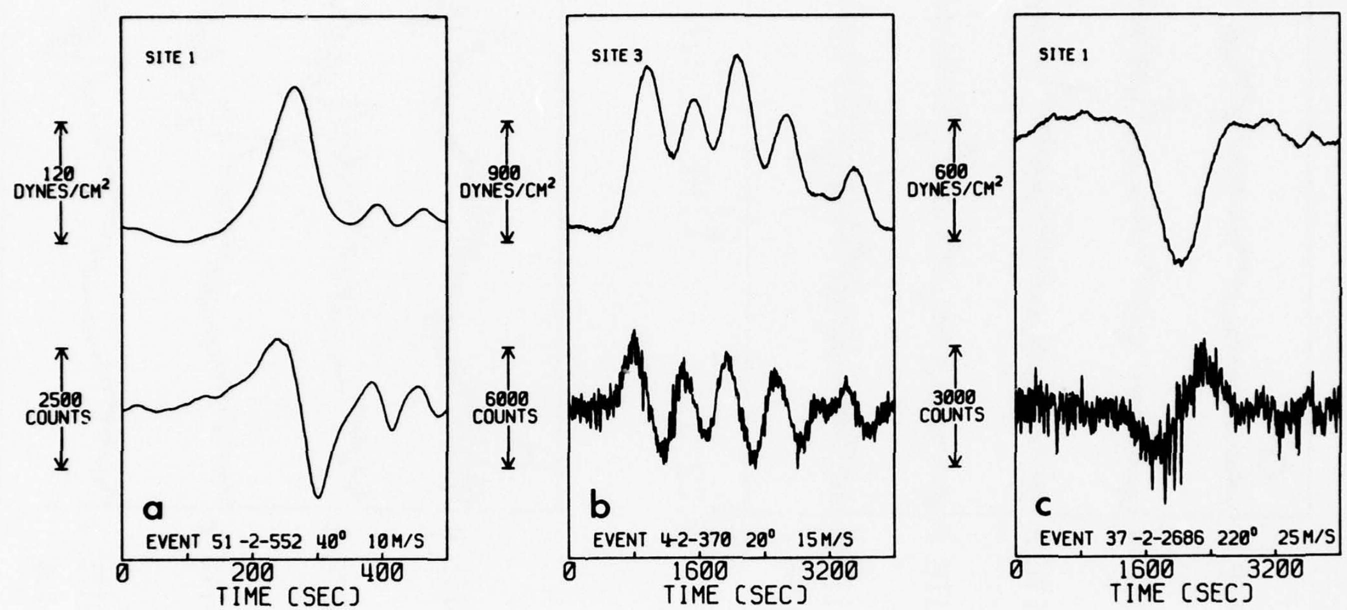

SITE 1
120 DYNES/CM²
2500 COUNTS
a
EVENT 51 -2-552 40° 10 M/S
0 200 400
TIME (SEC)
SITE 3
900 DYNES/CM²
6000 COUNTS
b
EVENT 4-2-370 20° 15 M/S
0 1600 3200
TIME (SEC)
SITE 1
600 DYNES/CM²
3000 COUNTS
c
EVENT 37 -2-2686 220° 25 M/S
0 1600 3200
TIME (SEC)

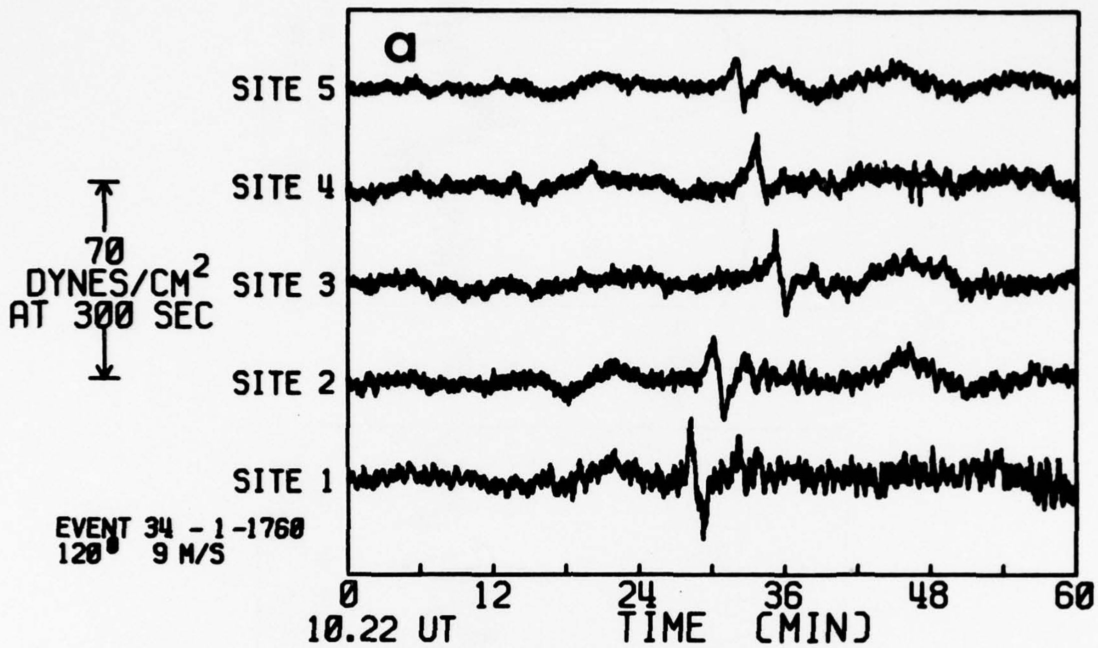
a
SITE 5
SITE 4
SITE 3
SITE 2
SITE 1
70
DYNES/CM^2
AT 300 SEC
EVENT 34 - 1-1760
120° 9 M/S
0 12 24 36 48 60
10.22 UT
TIME (MIN)

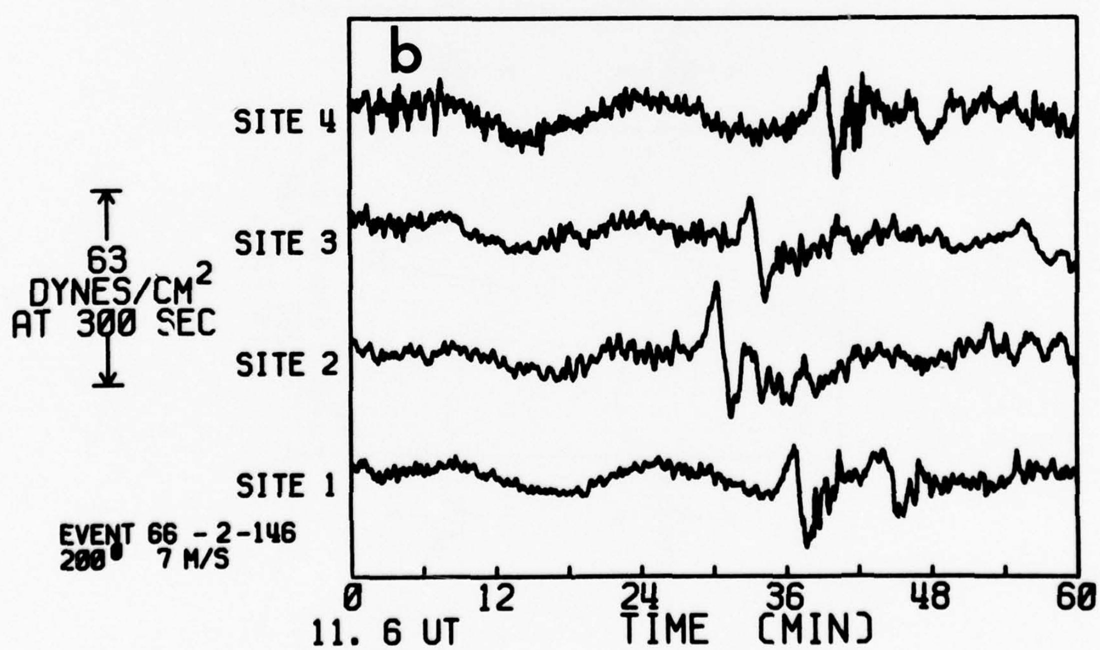
b
SITE 4
SITE 3
SITE 2
SITE 1
63
DYNES/CM^2
AT 300 SEC
EVENT 66 - 2-146
200° 7 M/S
0 12 24 36 48 60
11. 6 UT
TIME (MIN)

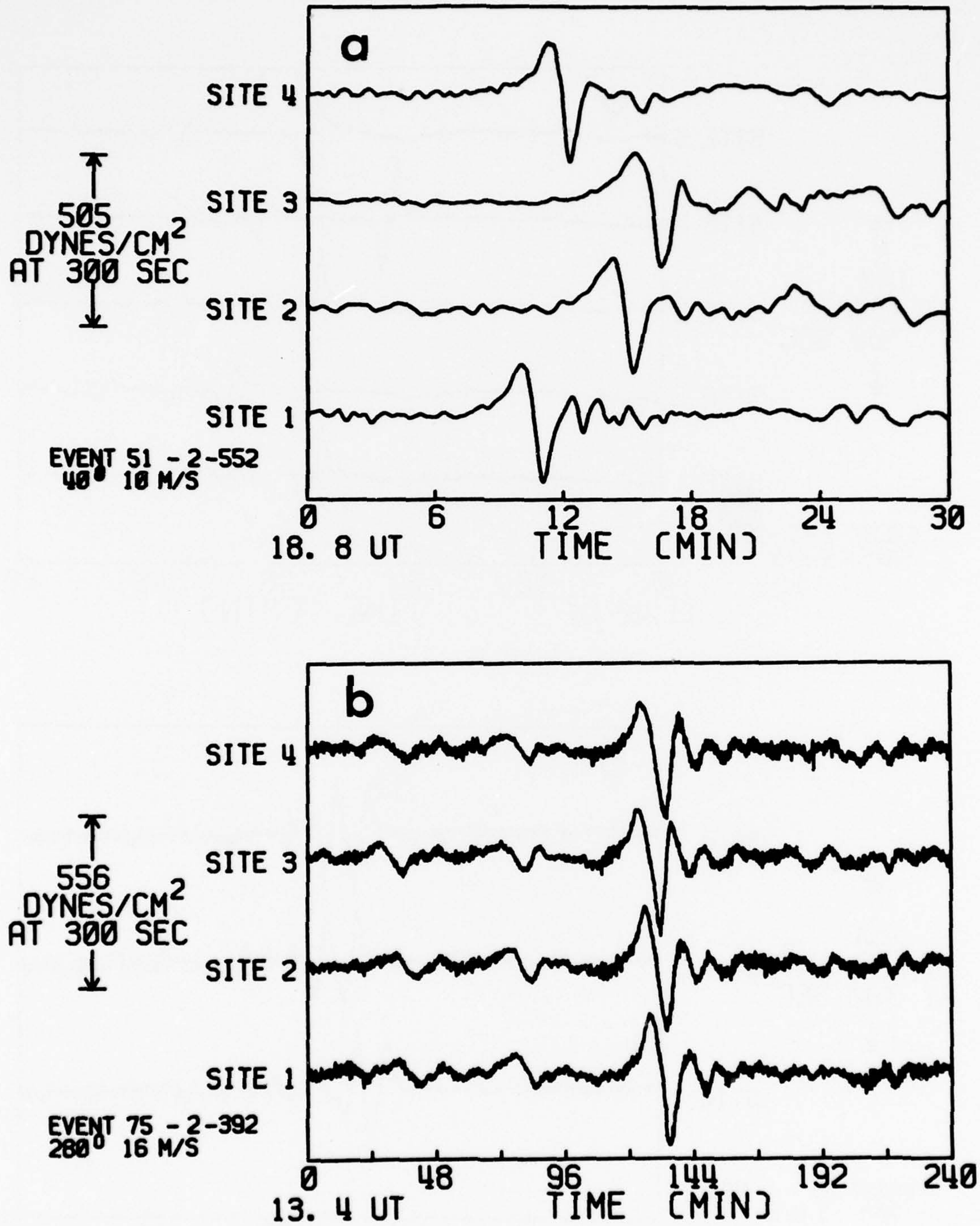
a
SITE 4
SITE 3
SITE 2
SITE 1
505
DYNES/CM2
AT 300 SEC
EVENT 51 - 2-552
40° 10 M/S
0
6
12
18
24
30
18. 8 UT
TIME (MIN)
b
SITE 4
SITE 3
SITE 2
SITE 1
556
DYNES/CM2
AT 300 SEC
EVENT 75 - 2-392
280° 16 M/S
0
48
96
144
192
240
13. 4 UT
TIME (MIN)

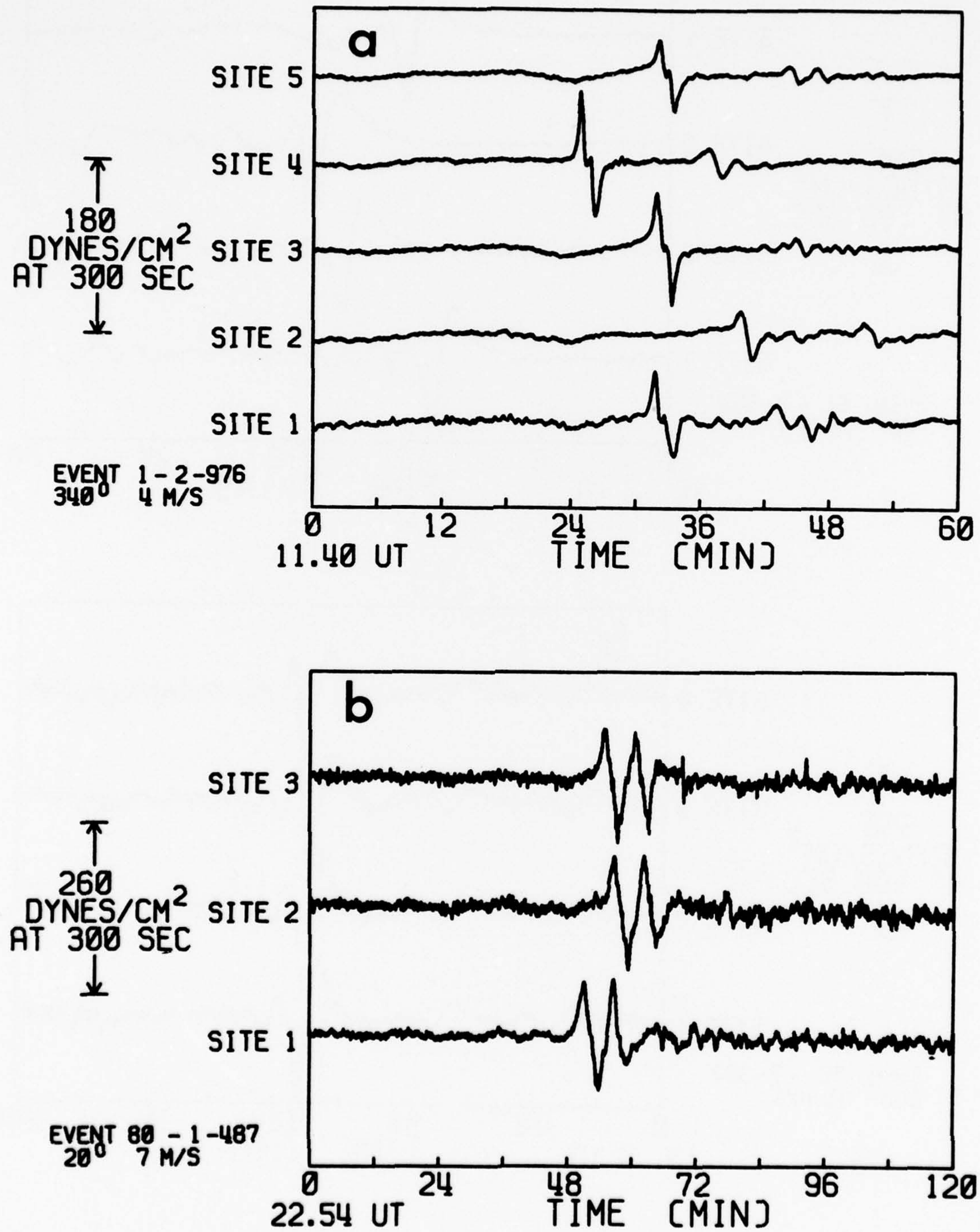

a
SITE 5
SITE 4
SITE 3
SITE 2
SITE 1
180 DYNES/CM2 AT 300 SEC
EVENT 1-2-976
340° 4 M/S
0 12 24 36 48 60
11.40 UT
TIME (MIN)
b
SITE 3
SITE 2
SITE 1
260 DYNES/CM2 AT 300 SEC
EVENT 80 - 1-487
20° 7 M/S
0 24 48 72 96 120
22.54 UT
TIME (MIN)

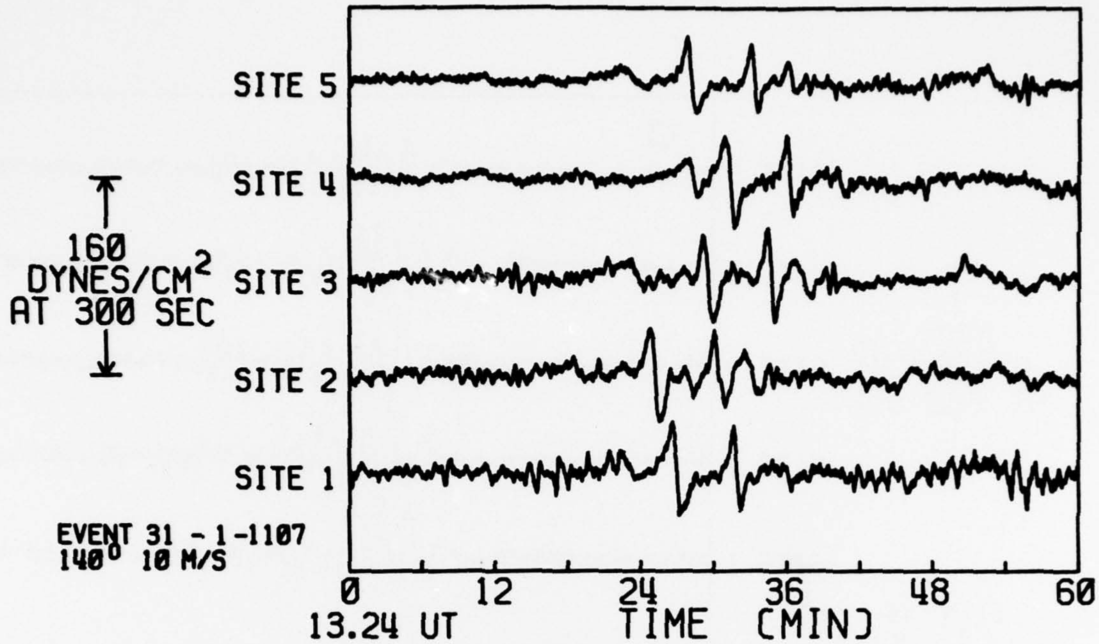
SITE 5
SITE 4
SITE 3
SITE 2
SITE 1
160
DYNES/CM2
AT 300 SEC
EVENT 31 - 1-1107
140° 10 M/S
0
12
24
36
48
60
13.24 UT
TIME (MIN)

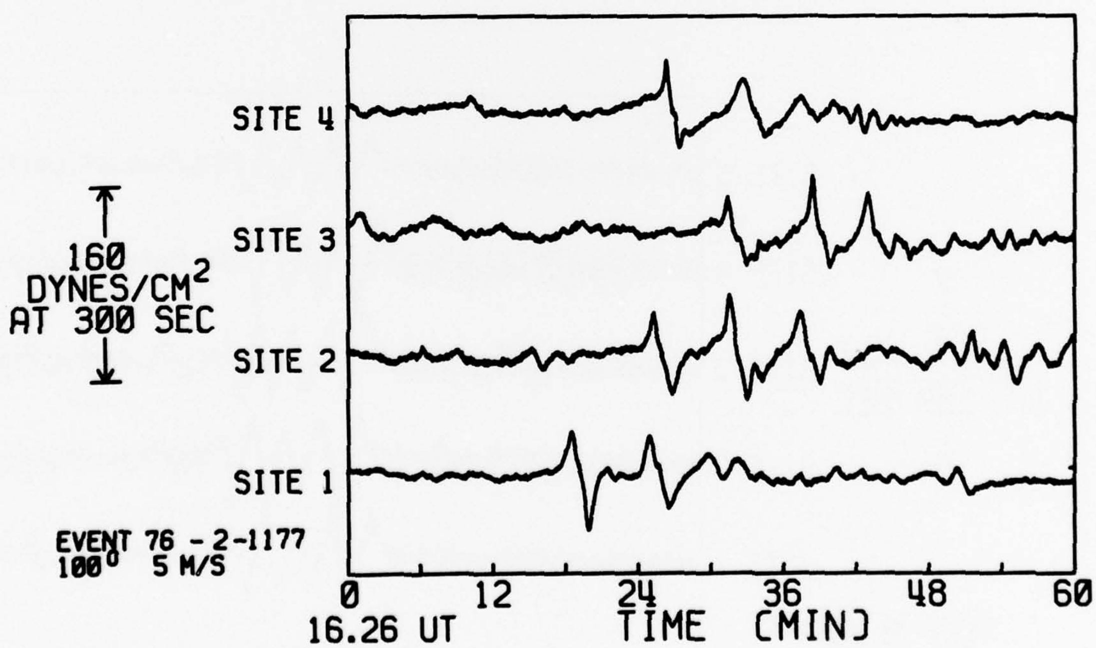
SITE 4
SITE 3
SITE 2
SITE 1
160
DYNES/CM2
AT 300 SEC
EVENT 76 - 2-1177
100° 5 M/S
0
12
24
36
48
60
16.26 UT
TIME (MIN)

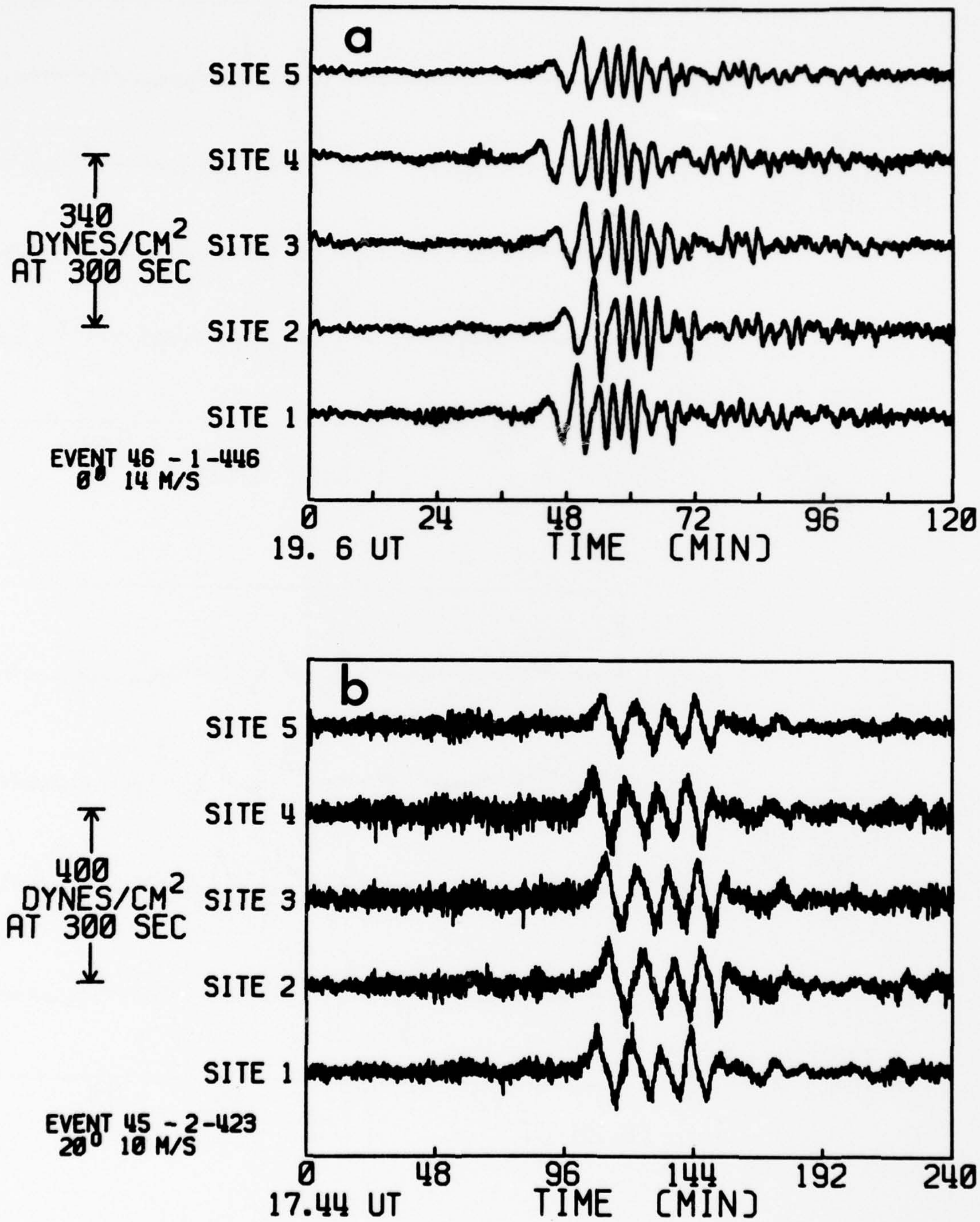
a
SITE 5
SITE 4
SITE 3
SITE 2
SITE 1
340
DYNES/CM2
AT 300 SEC
EVENT 46 - 1 -446
0° 14 M/S
0
24
48
72
96
120
19. 6 UT
TIME (MIN)
b
SITE 5
SITE 4
SITE 3
SITE 2
SITE 1
400
DYNES/CM2
AT 300 SEC
EVENT 45 - 2-423
20° 10 M/S
0
48
96
144
192
240
17.44 UT
TIME (MIN)

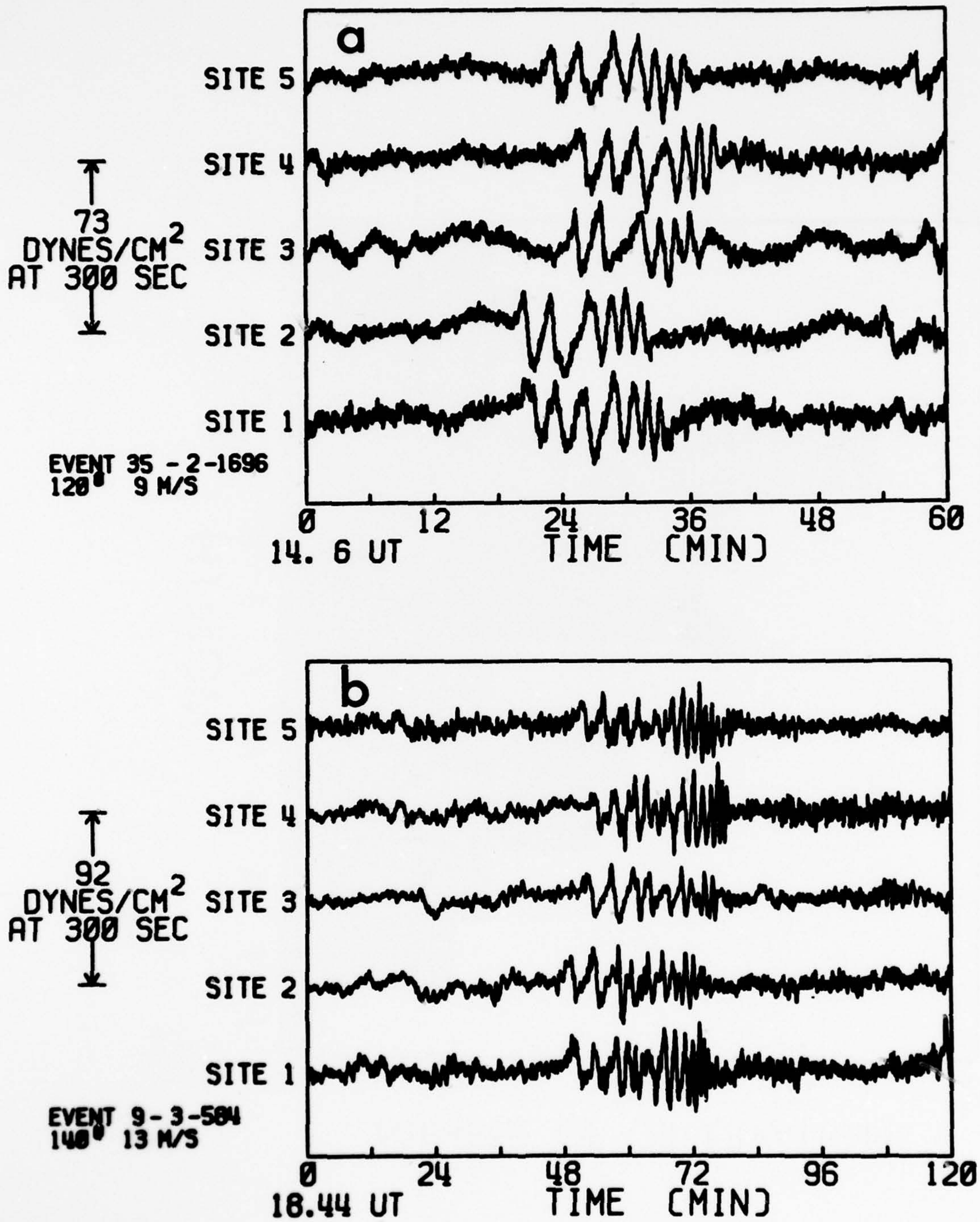

a
SITE 5
SITE 4
SITE 3
SITE 2
SITE 1
73
DYNES/CM2
AT 300 SEC
EVENT 35 - 2-1696
120° 9 M/S
0
12
24
36
48
60
14. 6 UT
TIME (MIN)
b
SITE 5
SITE 4
SITE 3
SITE 2
SITE 1
92
DYNES/CM2
AT 300 SEC
EVENT 9- 3-584
140° 13 M/S
0
24
48
72
96
120
18.44 UT
TIME (MIN)

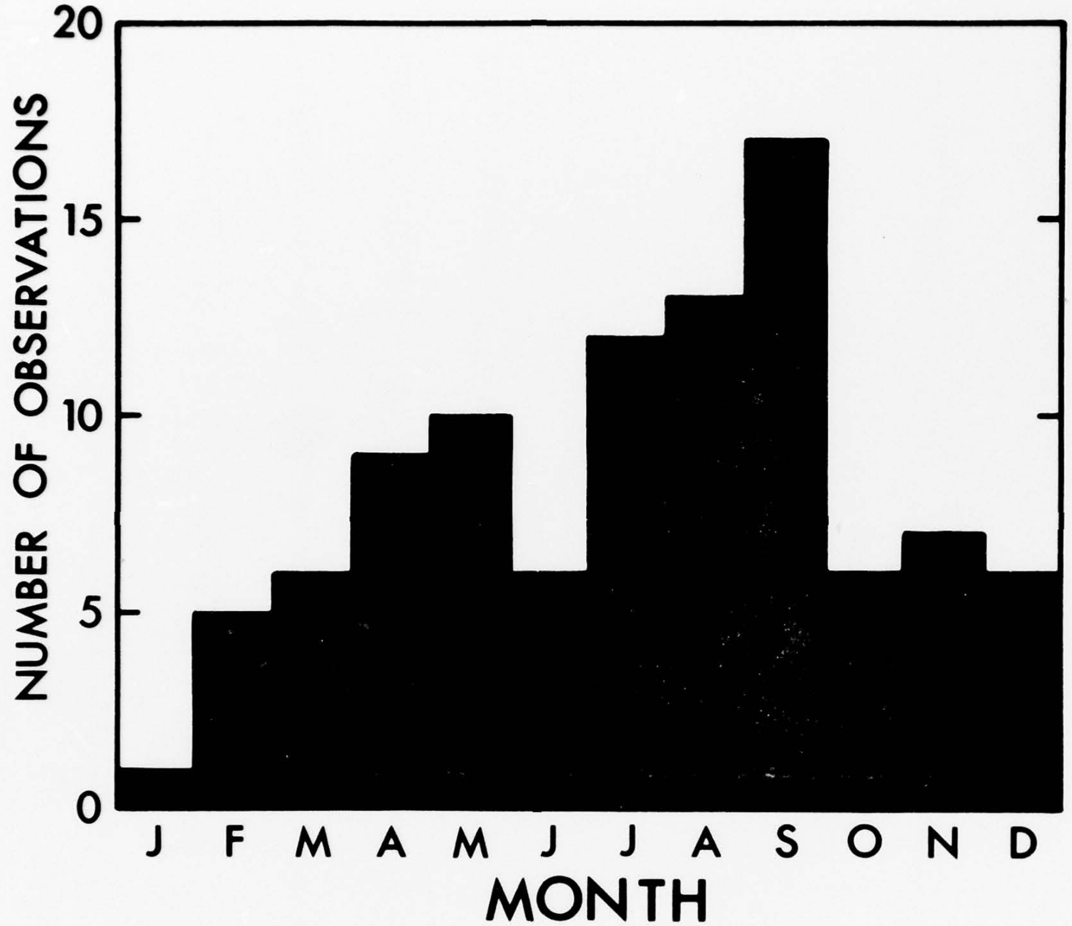

NUMBER OF OBSERVATIONS
20
15
10
5
0
J F M A M J J A S O N D
MONTH

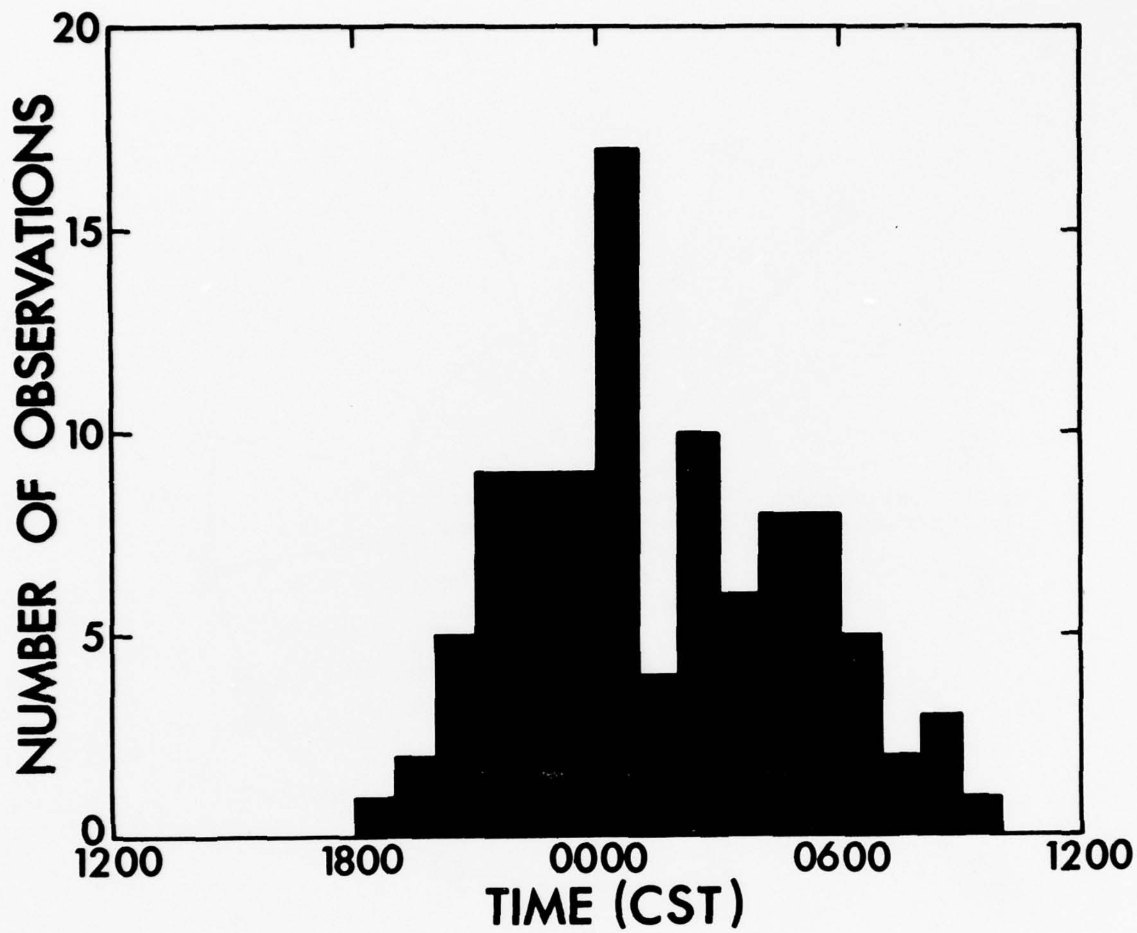
NUMBER OF OBSERVATIONS
20
15
10
5
0
1200
1800
0000
0600
1200
TIME (CST)

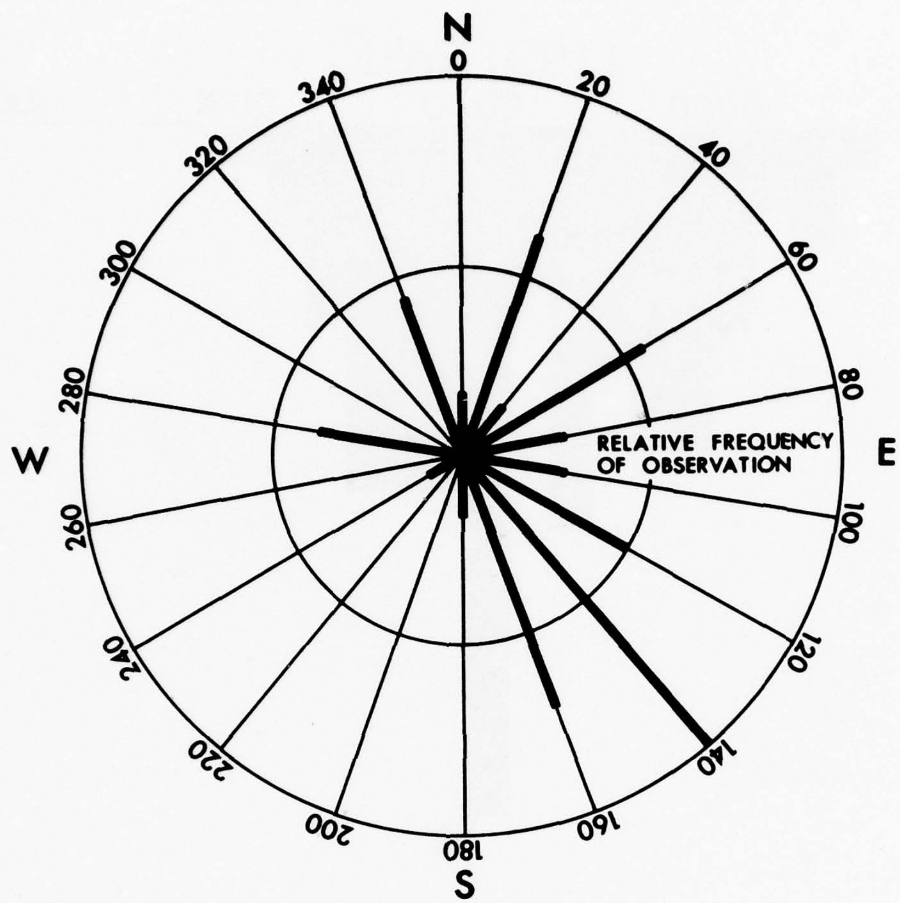
N
0
20
40
60
80
E
100
120
140
160
180
S
200
220
240
260
W
280
300
320
340
RELATIVE FREQUENCY
OF OBSERVATION

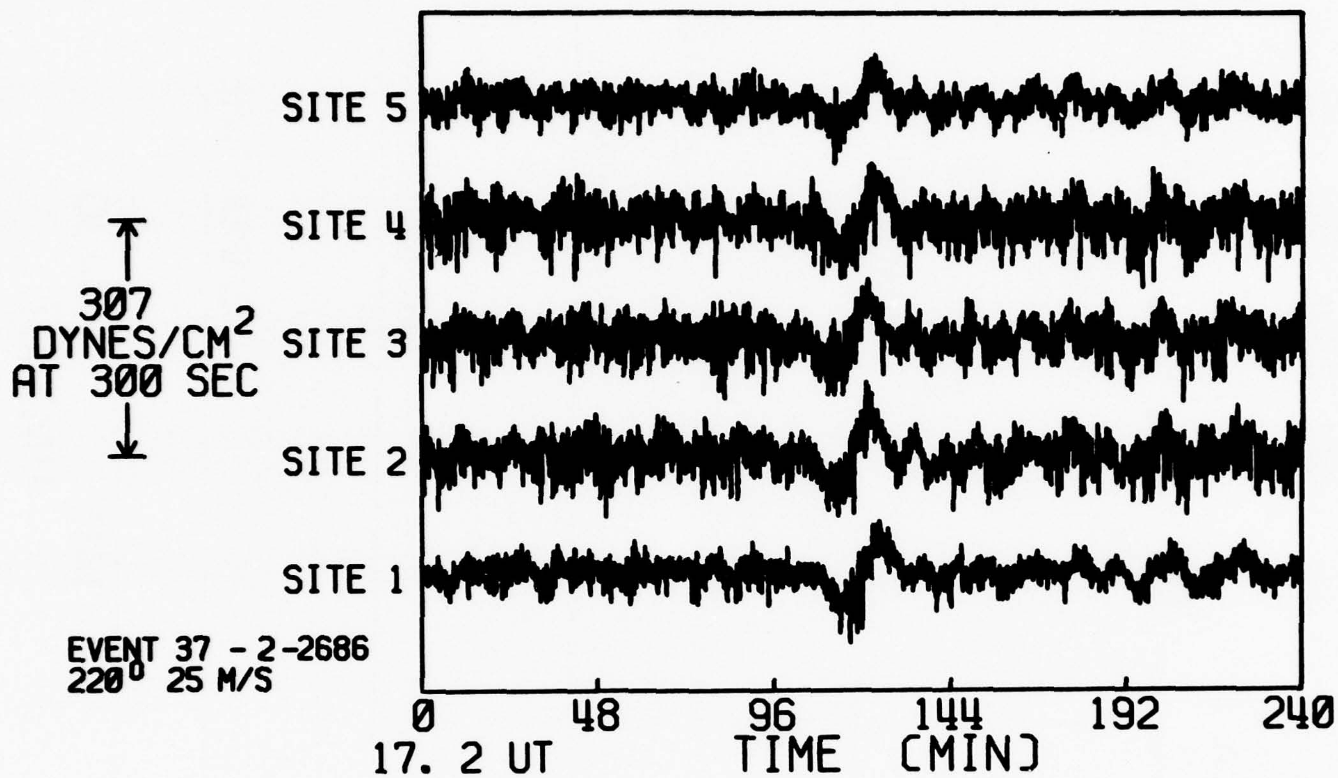

SITE 5
SITE 4
SITE 3
SITE 2
SITE 1
307
DYNES/CM²
AT 300 SEC
EVENT 37 - 2-2686
220° 25 M/S
0
48
96
144
192
240
17. 2 UT
TIME (MIN)

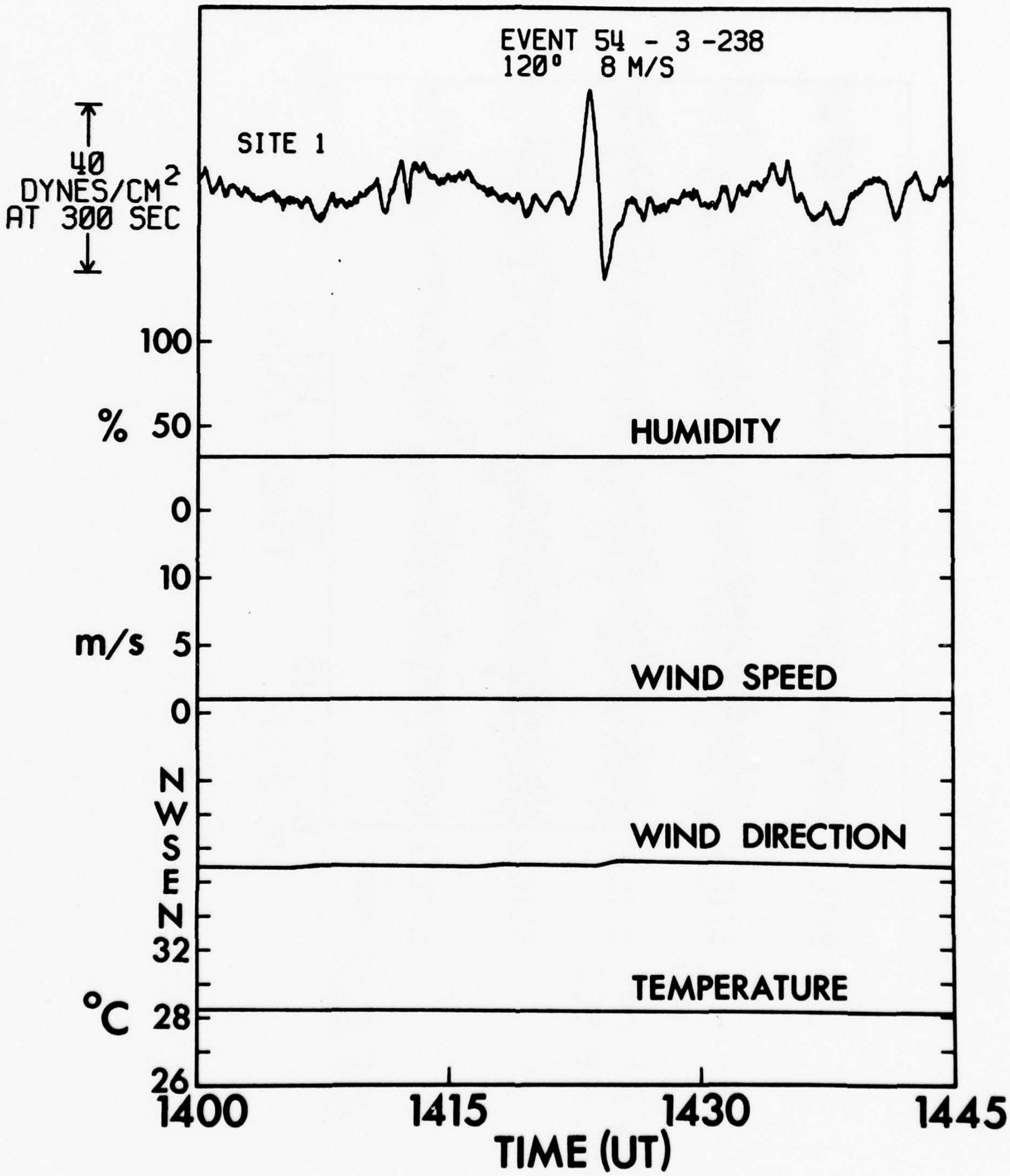

EVENT 54 - 3 -238
120° 8 M/S
SITE 1
40
DYNES/CM2
AT 300 SEC
100
%
50
HUMIDITY
0
10
m/s
5
WIND SPEED
0
N
W
S
E
N
WIND DIRECTION
32
TEMPERATURE
°C
28
26
1400
1415
1430
1445
TIME (UT)

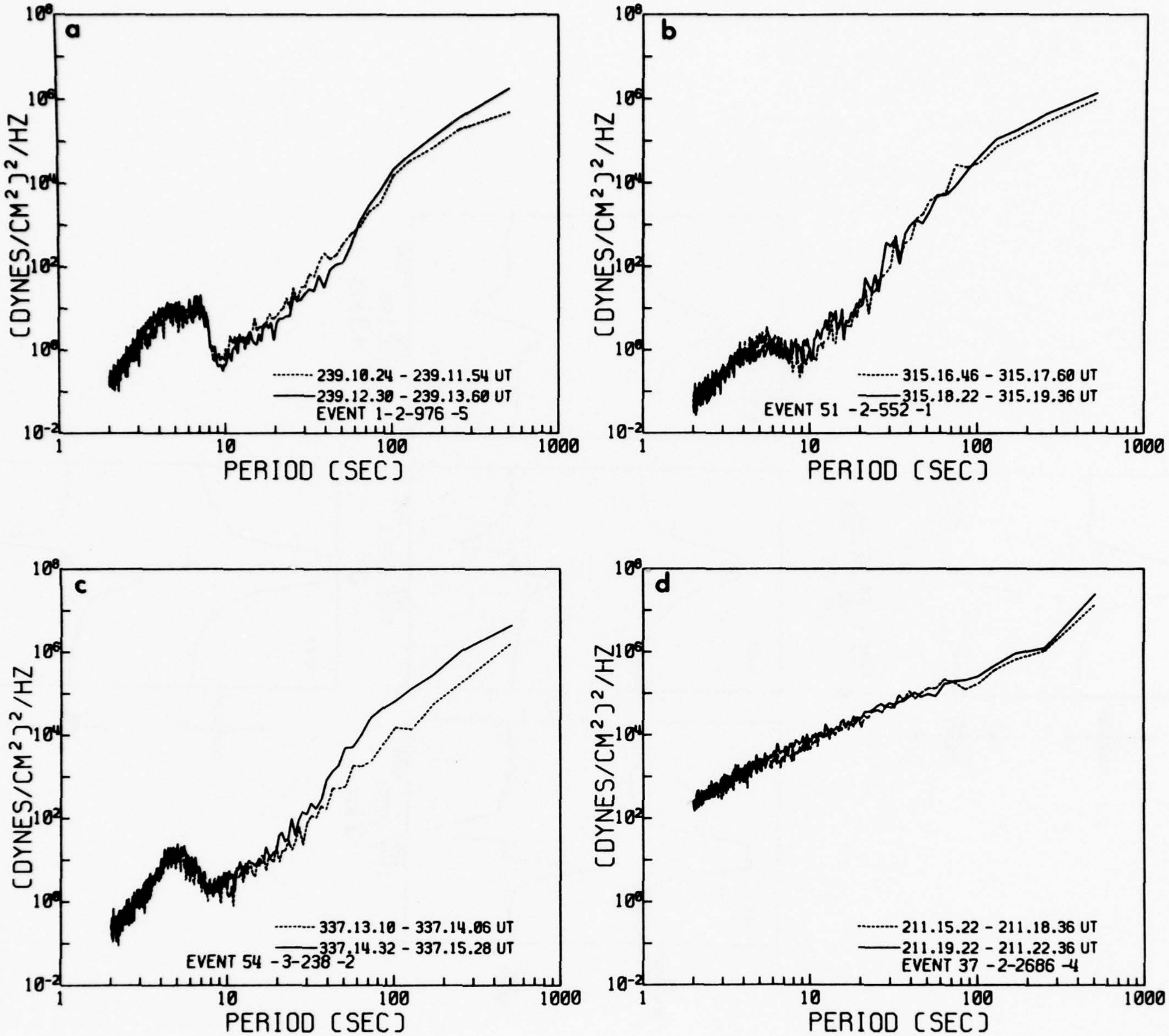

a
239.10.24 - 239.11.54 UT
239.12.30 - 239.13.60 UT
EVENT 1-2-976 -5
b
315.16.46 - 315.17.60 UT
315.18.22 - 315.19.36 UT
EVENT 51 -2-552 -1
c
337.13.10 - 337.14.06 UT
337.14.32 - 337.15.28 UT
EVENT 54 -3-238 -2
d
211.15.22 - 211.18.36 UT
211.19.22 - 211.22.36 UT
EVENT 37 -2-2686 -4
(DYNES/CM²)²/HZ
PERIOD (SEC)

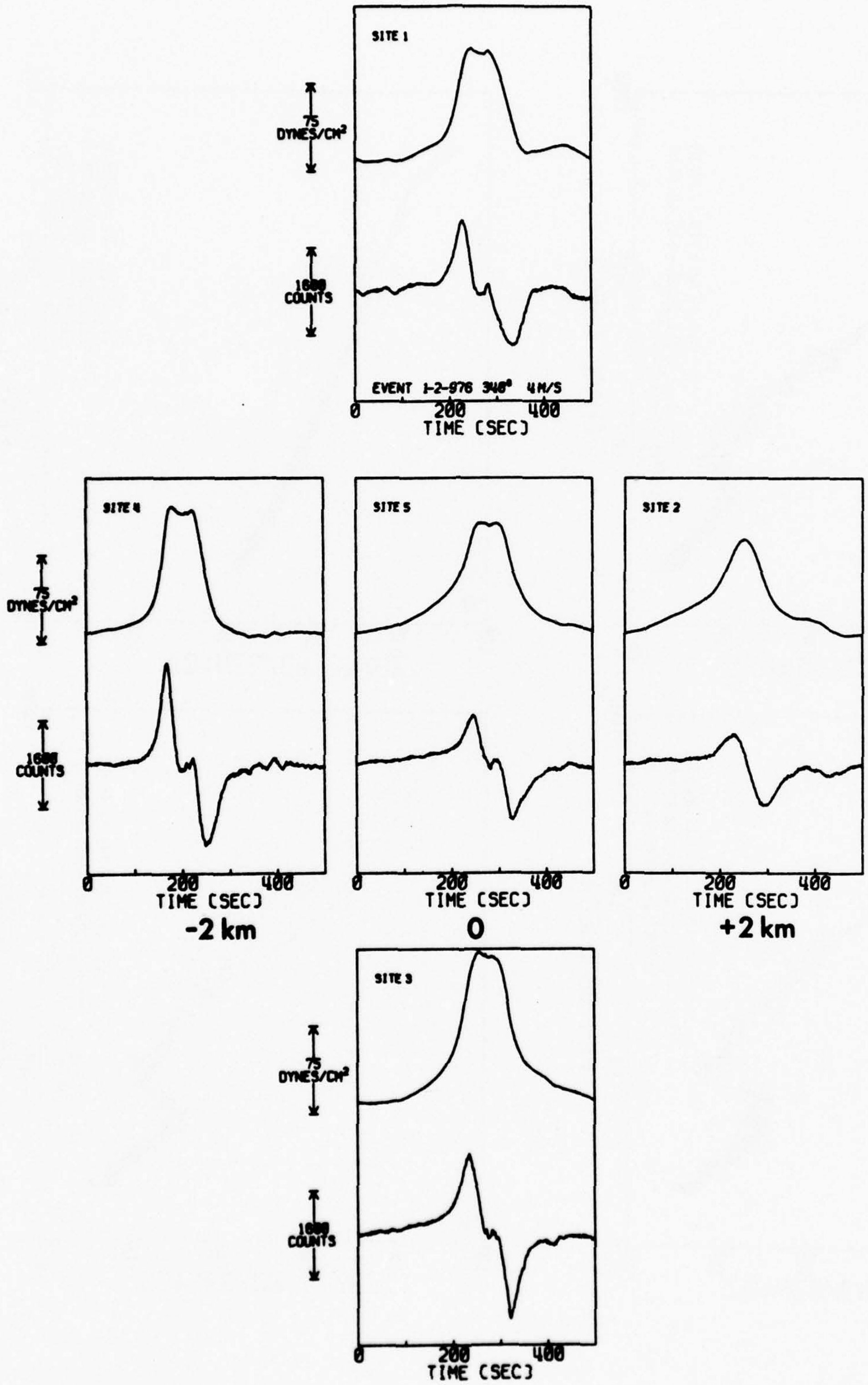

SITE 1
75 DYNES/CM²
1000 COUNTS
EVENT 1-2-976 340° 4 M/S
0
200
400
TIME [SEC]
SITE 4
SITE 5
SITE 2
-2 km
0
+2 km
SITE 3

APPENDIX B

INTRUSIVE DENSITY FLOWS IN THE LOWER TROPOSPHERE: A SOURCE OF ATMOSPHERIC SOLITONS

D.R. Christie, K.J. Muirhead, and A.L. Hales

Research School of Earth Sciences
Australian National University
Canberra, A.C.T., 2600.

ABSTRACT

This paper is concerned with the properties of complex propagating nonlinear tropospheric disturbances observed near Tennant Creek in the arid interior of the Northern Territory of Australia. Many of these unusual atmospheric disturbances resemble the well-known internal undular surges observed in the oceans and in inland stratified bodies of water. A description is presented of a wide variety of observations of solitary-wave-dominated evolving density intrusions and it is shown that many of the features of these unique disturbances are in qualitative agreement with the predictions of nonlinear dispersive wave theory. In particular, it is shown that the evolutionary behaviour of these disturbances is governed by the Benjamin-Ono equation and that intrusive motions of this type play an important role in the generation of boundary layer solitary atmospheric waves. Existing experimental evidence indicates that these disturbances originate primarily in the interaction of katabatic flows, propagating sea-breeze vortices, and "Morning Glory" phenomena with the stably-stratified nocturnal radiation inversion.

INTRODUCTION

Solitary waves are isolated finite-amplitude waves of permanent form and constant velocity which arise from an equilibrium between the competing processes of higher-frequency harmonic generation through amplitude dispersion and the transfer of energy to the lower-frequency modes through normal frequency dispersion. These waves have been widely studied ever since they were first observed and described by Scott Russell in 1837 (Scott Russell, 1837). However, despite this long history, solitary waves were regarded for many years as a mathematical and physical curiosity which appeared to require rather specialized conditions for their creation and which were therefore expected to be of minor importance in the initial-value problem for nonlinear dispersive wave systems. It is only recently that it has been recognized that solitary waves play a fundamental role in the evolution of a wide variety of physically interesting problems. More specfically, for a large class of physically relevant nonlinear evolution equations, the initial-value problem for arbitrary data condenses into a pure solitary wave solution in the asymtotic ($t \to \infty$) limit. For a good discussion of general solitary wave theory and an account of recent developments in the area the interested reader is referred to the reviews by Scott et al. (1973) and Cercignani (1977).

Many geophysical wave phenomena can be described by nonlinear dispersive wave theory. For example, on a planetary scale, solitary wave models explain the wavelike structure in the magnetosphere-solar wind interaction (Kikuchi, 1976) and describe the properties of finite-amplitude Rossby waves in the oceans and atmosphere (Long, 1964; Clarke, 1971; Redekopp, 1977). An interesting example of the latter type of wave has been given by Maxworthy

and Redekopp (1976) who suggest that the Great Red Spot of Jupiter is a manifestation of a solitary Rossby wave on a horizontally sheared zonal flow. On a smaller scale, nonlinear dispersive wave theory describes many of the features of tsunami propagation (Hammack, 1973; Hammack and Segur, 1978a) and provides the framework for the interpretation of nonlinear internal wave observations in the oceans and in thermally stratified inland bodies of water.

The latter observations are particularly relevant to the interpretation of the new type of complex propagating atmospheric disturbance considered in this paper. Nonlinear internal long water waves have been observed to occur as single isolated solitary wave disturbances (Gaul, 1961; Ziegenbein, 1970; Brekhovskikh et al., 1975) or as complex families of solitary waves in association with the leading edge of an evolving intrusive density flow or internal surge (Halpern, 1971; Thorpe et al., 1972; Hunkins and Fliegel, 1973; Lee and Beardsley, 1974; Ivanov and Konyayev, 1976; Gargett, 1976).

In a recent paper (Christie et al., 1978) we presented a detailed description of large amplitude atmospheric waves in the form of isolated solitary waves and isolated solitary wave packets which were observed over a two-year period, using an array of high sensitivity microbarometers, at the Warramunga Seismic Station located near Tennant Creek in central Australia. Three distinct types of isolated nonlinear atmospheric wave phenomena were observed: (a) large scale waves of elevation which belong to the class of classical shallow-fluid internal solitary waves, (b) large scale internal solitary waves of depression and (c) solitary waves associated with the atmospheric boundary layer which are described by the deep-fluid nonlinear wave theory of Benjamin (1967).

The primary objectives of this paper are to present a description of a series of unique observations of a variety of commonly occurring complex propagating atmospheric boundary layer disturbances, to show that the morphology of these disturbances is consistant with an interpretation with the framework of Benjamin's deep-fluid nonlinear dispersive wave theory, and to demonstrate that the genesis of the observed deep-fluid solitary atmospheric waves and wave packets may plausibly be traced to these complex intrusive flows. An example of the specific type of propagating disturbance considered in this paper is shown in Figure 1. It will be seen that disturbances of this type are similar in many respects to the complex solitary-wave-associated intrusive disturbances observed in the oceans and in stratified inland lakes.

NONLINEAR DISPERSIVE WAVE THEORY

The propagation of small-but-finite amplitude internal long waves in a shallow fluid is described by the classical KdV (Korteweg and de Vries, 1895) evolution equation,

$$\eta_t + c_0\eta_x + \alpha\eta\eta_x + c_0\beta\eta_{xxx} = 0 \qquad (1)$$

where c_0 is the maximum speed of infinitesimal waves, α is a constant which describes the nonlinear effects of finite amplitude and β is a parameter which characterizes the phase speed dispersion for shallow fluids,

$$c(k) = \omega/k = c_0(1-\beta k^2), \qquad (2)$$

in the long-wavelength limit. In an elegant study of internal waves in stratified fluids, Benjamin (1967) discovered a new class of finite-amplitude waves of permanent form which, in contrast to classical nonlinear waves, can propagate in fluids of infinite depth. The properties of these waves have also been studied both experimentally and theoretically by Davis and Acrivos (1967). Internal wave motions which belong to this new class occur in systems where the density of the stratified fluid varies significantly only in a region whose depth, h, is small compared to the total depth and small compared to the wavelength of the wave. Benjamin noted that the key to understanding the difference between shallow and deep-fluid nonlinear dispersive wave theory lies in the form of the linear dispersion relation. In the case of fluids of great depth, the dispersion relation for sufficiently small values of k is described by

$$c(k) = c_0(1-\gamma|k|), \tag{3}$$

where γ is a positive constant. On the basis of a heuristic argument Benjamin proposed that the infinitely-deep-fluid counterpart to the KdV equation is given by an evolution equation in the form

$$\eta_t + c_0\eta_x + \alpha\eta\eta_x - c_0\gamma\,\mathscr{F}(\eta_x) = 0 \tag{4}$$

where the operator $\mathscr{F}$ is defined by

$$\mathscr{F}(f(x)) = \frac{1}{2\pi}\int_{-\infty}^{\infty}\int_{-\infty}^{\infty} |k|f(x')e^{ik(x'-x)}\,dx'dk,$$

or by the equivalent Hilbert transform

$$\mathscr{F}(f(x)) = -\frac{1}{\pi}\mathscr{P}\int_{-\infty}^{\infty} \frac{1}{z-x}\left\{\frac{\partial f(z)}{\partial z}\right\} dz .$$

This equation has been rigourously derived by Ono (1975) and in a different context by Gargett (1976) and by Levikov (1977).

It may be shown (Joseph, 1977a) that the KdV equation (1) and the Benjamin-Ono equation (4) are special cases in the long-wavelength limit of the more general evolution equation proposed by Whitham (1967)

$$\eta_t + \alpha\eta\eta_x + \int_{-\infty}^{\infty} K(x-\xi)\eta_\xi(\xi,t)\,d\xi = 0 \tag{5}$$

where the kernel is given by the Fourier transform of the appropriate linear wave phase speed $c(k)$,

$$K(x) = \frac{1}{2\pi}\int_{-\infty}^{\infty} c(k)e^{ikx}\,dk.$$

The steady state solutions, $\eta = \eta(x-ct)$ of equations (1) and (4) are well known. Both equations have stationary periodic 'cnoidal' solutions which in the limit of long wavelength give rise to solitary waves. We shall be mainly interested in the properties of the solitary wave solutions. For the KdV equation, the solitary wave is given by

$$\eta(x,t) = \eta_o\, sech^2\,[\Delta(x-ct)] \tag{6a}$$

$$c = c_o + \frac{1}{3}\alpha\eta_o , \tag{6b}$$

with $\Delta = \left(\dfrac{\eta_o\alpha}{12c_o\beta}\right)^{1/2}$,

and for the Benjamin-Ono equation the spatially localized solution takes the form of a Lorentzian

$$\eta(x,t) = \frac{\eta_\circ \lambda^2}{(x-ct)^2+\lambda^2} \tag{7a}$$

$$c = c_\circ + \frac{1}{4}\alpha\eta_\circ \tag{7b}$$

with $\lambda = \dfrac{4c_\circ\gamma}{\alpha\eta_\circ}$.

Note that the classical solitary wave disturbance vanishes exponentially and is therefore of limited range while the Benjamin solitary wave, which decays algebraically, extends over a relatively long range.

In a recent study, Joseph (1977b) has obtained a simple exact internal solitary wave solution to the general Whitham evolution equation (5) which provides the natural connection between the classical shallow-fluid KdV theory and the infinitely-deep-fluid theory of Benjamin. This solution describes the propagation of small-but-finite amplitude solitary waves along a thin thermocline characterized by a depth scale h in a two-layer fluid of total finite depth D. For this system, the long wavelength phase velocity dispersion is given by

$$c(k) = c_\circ[1 - \frac{1}{2} kh \ (coth(kD) - \frac{1}{kD})] \tag{8}$$

and the corresponding exact solution to the Whitham equation takes the form

$$\eta(x,t) = \frac{\Delta^2\lambda^2\eta_\circ}{\Delta^2\lambda^2 cosh^2[\Delta(x+ct)] + sinh^2(\Delta(x-ct))} \tag{9a}$$

$$c = c_\circ \left[1 + \frac{h}{2D}\ [1 - 2\Delta D cot\ (2\Delta D)]\right], \tag{9b}$$

with $\lambda\Delta = \cot(\Delta\mathcal{V})$. This solution converges to Benjamin's solitary wave solution (7) in the infinitely-deep-fluid limit ($\Delta\to 0$) and to the classical KdV solution (6) in the shallow-fluid limit ($\lambda\to\infty$). It must be anticipated that this general finite-depth solution to Whitham's equation will play an important role in the interpretation of a wide variety of geophysical wave phenomena.

One of the most important advances in recent years in the study of nonlinear dispersive waves is the remarkable discovery of Zabusky and Kruskal (1965) who found that solitary waves governed by the KdV equation preserve their amplitude, shape and speed under nonlinear interaction. Solitary waves which exhibit this independent particle-like behaviour are referred to as solitons. When two solitons collide the faster particle is advanced and the slower particle retarded with the result that, asymtotically, the only manifestation of the nonlinear interaction is a phase shift in the trajectories of the solitons. The fact that solitons form a major component in the general solution to the nonlinear dispersive wave initial-value problem is a direct consequence of this extraordinary stability.

This paper is mainly concerned with the nonstationary solutions of the evolution equations; in particular, since the propagating disturbances considered here are associated with the atmospheric boundary layer, we are primarily interested in the form of the solutions to the initial-value problem described by Whitham's equation near the infinitely-deep-fluid Benjamin-Ono limit given by equation (4).

At the present time, three different general systematic methods are known for finding the exact solution of a wide variety of nonlinear partial differential evolution equations: the ingeneous inverse scattering

transform method originated by Gardiner et al. (1967), the Bäckland transformation method (Lamb, 1974), and the dependent variable transform technique developed by Hirota (Hirota and Satsuma, 1976). Of these techniques, the inverse scattering transform method is by far the most widely studied (Ablowitz et al., 1974) and has been used to determine the properties and solutions of a large class of physically interesting problems including, in particular, the properties and solution to the general KdV evolution equation. The most important achievement of the inverse scattering transform is that the original problem of solving a nonlinear partial differential equation is reduced to the problem of solving a sequence of linear equations. In brief, the nonlinear problem is reduced to an examination of an associated time-independent Schrödinger eigenvalue problem,

$$\psi_{xx} + (\lambda + u)\psi = 0, \tag{10}$$

where the nondimensional amplitude $u = \alpha\eta/c_0$ plays the role of the potential term, and to the problem of solving the corresponding linear Gel'fand-Levitan integral equation.

The properties of the general solution to the classical KdV equation are well known. In contrast, at the present time relatively little is known about the precise behaviour of the general nonstationary solutions to the Benjamin-Ono equation. It would appear that the inverse scattering transform technique is not applicable to this integral-differential equation. Let us consider first the important question of whether or not Benajmin's deep fluid solitary waves are solitons. At first glance, since these waves decay algebraically and thus interact nonlinearly over a relatively long range, it would seem reasonable to suspect that these waves may not exhibit

soliton behaviour. If indeed these waves are unstable under nonlinear interaction then it must be concluded that the evolution properties of disturbances governed by the Benjamin-Ono equation will be significantly different from those described by the KdV equation. This however, is not the case. Recently there has been an upsurge in interest in this particular problem. Maxworthy (T. Maxworthy, private communication) has shown in a series of laboratory experiments that nonlinear deep fluid disturbances evolve in a manner which is qualitatively similar to that of the classical problem; in particular, these experiments show that, in general, Benjamin's deep fluid solitary waves are solitons. In addition, Joseph (1977a) and Joseph and Egri (1978) have recently succeeded in obtaining pure N-soliton analytic solutions to both the Benjamin-Ono equation and the thin thermocline form of the general Whitham equation for a system of finite depth. In both cases, exact two-solitary wave solutions are explicitly given which verify that true algebraic solitons do exist. These results are complemented by the numerical calculations of Meiss and Pereira (1978) who examine a two-soliton collison process, a three-soliton collision process and, as well, more general initial-value problems governed by the Benjamin-Ono equation which evolve asymtotically into a pure soliton state and a small dispersing oscillatory tail. From these calculations, Meiss and Pereira also conclude that, in general, Lorentzian deep-fluid solitary waves are stable under nonlinear interaction and that the behaviour of the nonstationary solutions of the Benjamin-Ono equation is qualitatively similar to that of the classical KdV problem.

We can therefore gain insight into the properties of an evolving nonlinear disturbance propagating in a stably-stratified deep fluid by examining the general characteristics of the corresponding classical problem defined by the KdV equation. The mathematical problem has been widely

studied (Gardner et al., 1967, 1974; Berezin and Karpman, 1967; Hirota, 1971; Wadati and Toda, 1972; Segur, 1973; Ablowitz and Newell, 1973; Ablowitz and Segur, 1977) and the results confirmed both numerically (Zabusky, 1967; Vliegenthart, 1971) and through a series of detailed laboratory experiments (Zabusky and Galvin, 1971; Hammack and Segur, 1974, 1978b; Weidman and Maxworthy, 1978). The salient features of these investigations may be summarized as follows:

(a) A general initial disturbance of finite extent will evolve into a finite discrete set of solitons and an independent dispersive wave train.

(b) Each real negative discrete eigenvalue of the associated Schrödinger problem (10) contributes a soliton to the nonstationary KdV solution; the dispersive wave state is associated with the continuous spectrum.

(c) The group velocity of the dispersing waves is less than or equal to the critical wave speed c_0. Since the speed c of each soliton is supercritical and since the deviation of c from c_0 is proportional to wave amplitude, the solution evolves into a family of solitons, ordered by amplitude, followed by a train of dispersing waves.

(d) The amplitude of the solitons will not exceed twice the maximum amplitude of the initial disturbance. In the asymtotic state, the amplitude of the loading soliton approaches the theoretical maximum as the length of the initial disturbance increases.

(e) The existence of at least one soliton in the asymtotic solution is guaranteed if the net volume of the initial disturbance

is positive or zero. If the initial disturbance is predominantely positive, most of the wave energy goes into the production of solitons. Soliton production when the net initial volume is less than zero depends on the detailed form of the disturbance. If the initial disturbance is everywhere negative, no solitons emerge and thus the solution evolves into a pure dispersive state.

(f) The structure of the asymtotic dispersive solution may be separated into four distinct regions: the leading edge of the dispersive state where the amplitude is exponentially small, a leading wave zone where the solution is self-similar, a dissipationless shock layer where the solution changes from monotonic to oscillatory, and a trailing subcritical complex modulated oscillatory wave train. The oscillatory dispersive state is basically linear in character and exhibits normal dispersion. The leading wave decays faster than the oscillating wave train and thus the oscillatory waves dominate the asymtotic dispersive solution.

(g) A high frequency component in the spectrum of the initial disturbance is absorbed by the dispersive state and does not appear to have any significant influence on the production of solitons.

(h) An initial disturbance of finite extent cannot excite either a solution with two solitons of the same amplitude nor the stationary periodic cnoidal wave solution.

(i) Solitons experience only a phase shift under nonlinear interaction with the dispersive wave state.

It must be emphasized that the behaviour of the nonstationary solutions to the deep-fluid Benjamin-Ono equation will be only qualitatively similar to the classical behaviour pattern outlined above. In particular,

we note that little is known at the present time about the exact behaviour of the dispersing wave train portion of the deep-fluid solution. However, since the atmospheric disturbances described in this paper correspond to initially positive disturbances in the form of intrusive density flows, almost all of the wave energy is expected to appear in the asymtotic soliton state and thus the exact nature of the dispersive state is of only minor importance in the interpretation of these experimental observations.

To summarize this discussion, the well-known properties of the solutions to the classical nonlinear dispersive wave evolution problem coupled with the presently understood behaviour of the nonstationary solutions of the Benjamin-Ono equation clearly indicate that a long smooth atmospheric disturbance propagating along the boundary layer inversion will steepen in the regions of negative slope under the influence of amplitude dispersion and eventually condense into a distinct family of solitary waves and a small dispersing oscillatory tail. This characteristic evolution pattern is shown in detail in the extensive series of laboratory experiments described by Hammack and Segur (1974) on the evolution of a wide range of finite amplitude disturbances and in the numerical calculations presented by Vleigenthart (1971) of the development of a soliton family along the leading edge of an initially smooth bore. Figure 2 shows a schematic representation of the principal features in the evolutionary behaviour of both a finite length wave of elevation and the frontal zone of a long wave at elevation. It will be shown that the morphology of the complex propagating atmospheric disturbances observed at Tennant Creek is in reasonable agreement with this predicted behaviour pattern and thus it may be concluded that these observations represent various stages in the development of a finite-amplitude disturbance as described by the Benjamin-

Ono evolutionary equation, and that the final asymtotic form of these disturbances consists of a family of independent solitary atmospheric waves.

THE EXPERIMENTAL ARRANGEMENT

The complex nonlinear atmospheric gravity wave disturbances described in this paper were observed using an array of National Bureau of Standards designed high-sensitivity microbarometers located at the Warramunga Seismic Station, 37 kilometers SSE of Tennant Creek, at a latitude of 19°56'S in the arid interior of Australia. It is thought that the high frequency of observation of these nonlinear waves and the excellent resolution of the wave patterns result primarily from the unique location of the infrasonic array, a location which favours a high degree of stability in the lower atmosphere due to the absence of the perturbing influence of both the oceans and large-scale orographic features. The development of intense nocturnal radiation inversions - which provide an ideal medium for the propagation of nonlinear dispersive waves - may be attributed to this unusual atmospheric stability coupled with the low latitude semi-desert environment of the array.

The infrasonic array is configured in the form of a five-element centered quadrilateral with a net aperture of 4 kilometers. Signals from the 5 infrasonic channels are transmitted to a central recording station, sampled at a rate of 2 samples per second, digitized, and recorded in IBM compatable format on magnetic tape. Further details of the digital recording and data processing techniques may be found in Christie et al. 1978.

The microbarometer array elements are designed to effectively filter out those components in the surface micropressure spectrum which lie beyond the useful pass-band extending from about 1 to 1000 seconds. The phase and modulus of the microbarograph transfer function R are given as a function

of period by

$$\phi = tan^{-1} \frac{T^2 - T_o^2}{(T_1 + T_2)T} \quad ,$$

$$|R| = A\cos\phi \quad ,$$

where

$T_1 = 1.95\ s$,

$T_1 = 48.7\ s$,

$T_o = \sqrt{T_1 T_2} = 9.7\ s$ and

$A = 77.9$ counts/dyne/cm^2

Since the fundamental spectral components of the atmospheric gravity waves considered here are large compared with T_o, the array records provide an essentially differential micropressure signature of propagating wave phenomena. *Two examples are given in Figure 3 which* illustrate inversions of array record sections corresponding to the leading edge of a fairly smooth density intrusion and a complex soliton-dominated disturbance to provide the true micropressure trace at the surface. The microbarograph transfer function has been deconvolved from all experimental array data presented in the remainder of this paper.

OBSERVATIONS AND INTERPRETATION OF COMPLEX PROPAGATING ATMOSPHERIC BOUNDARY LAYER DISTURBANCES

The infrasonic array has been operating continuously at Tennant Creek since August 1975. During this period observations have been made of a wide variety of unusual nocturnal nonlinear wave disturbances ranging from extensive perturbations in the form of smooth intrusive density flows, complex evolving nonlinear wave disturbances, and fully developed undular intrusions to localized soliton wave packets and observations of isolated single solitary waves of elevation. Since these disturbances are only observed at night and since the observed phase speeds and amplitudes are consistent with a boundary layer disturbance it may be concluded that these observations correspond to disturbances that propagate along the nocturnal radiation inversion. As noted in the introduction, the major objectives of this paper are to show that all of these observations represent various stages in the evolution of nonlinear dispersive wave disturbances and that the observed wave patterns are consistent with an interpretation within the framework of the Benjamin-Ono infinitely-deep-fluid evolution equation. A detailed meteorological study of the influence of these disturbances on the ambient atmospheric flow field has also been carried out and will be published separately along with the implications of a statistical study of the diurnal and seasonal frequency of observation, and the variations in amplitude, azimuth and phase velocity. However, it is worth noting here that the azimuthal distribution and the frequency of occurrence of the complex nonlinear disturbances are qualitatively similar to those of the isolated solitary waves and solitary wave packets. It is also worth remarking on the fact that almost all of the observed complex intrusive disturbances produce only minor perturbations

in the atmospheric flow field at the surface. Thus it may be concluded that the energy of these intrusive disturbances is concentrated near the nocturnal boundary layer interface and that these disturbances are therefore the atmospheric analog of the soliton-producing interfacial density intrusions observed on the ocean thermocline and in inland stratified bodies of water.

At this point we would like to draw attention to the important study described by Reynolds and Gething (1970) of transient disturbances on the nocturnal boundary layer which were observed, using an acoustic radar, during the month of June at Julia Creek, 800 km to the east of Tennant Creek. Some of these complex perturbations occur as 'spike-like' disturbances associated with an increase in the depth of the radiation inversion while others appear to take the form of isolated familes of nonlinear waves propagating along the relatively undisturbed boundary layer interface. It seems clear that the unusual atmospheric phenomena described by Reynolds and Gething belong to the same class of nonlinear wave disturbance as the soliton-dominated disturbances considered here.

Let us now examine a series of observations of complex propagating atmospheric disturbances whose morphologies appear to exhibit the evolutionary pattern predicted by the nonlinear dispersive wave theory outlined above. It should first be emphasized that these disturbances do not usually evolve appreciably over the 4 km aperture of the infrasonic array; the individual array observations must therefore be viewed as various stages in the evolutionary process and thus agreement with the predicted behaviour pattern can only be inferred from the observations. A measure of the degree of evolution over an array of aperture A may be obtained by considering two Lorentzian deep-fluid solitary waves with dimensionless amplitudes $a_1 = \eta_o^1/h$ and $a_2 = \eta_o^2/h$ which propagate in the

same direction along a nocturnal boundary layer represented, in a two-fluid description, by an inversion of depth h and intensity ΔT. The relative speed of the two Benjamin solitons is given by

$$s \simeq \frac{3}{8} c_0 \, (a_2 - a_1),$$

the relative shift in the centroidal positions of the solitary waves during the traverse of the array may be expressed to first order by

$$\Delta x \simeq \frac{sA}{c_0} = \frac{3}{8} A(a_2 - a_1)$$

and the effective soliton wave lengths (full width at half maximum) are given by

$$w = 2\lambda = \frac{8}{3} (1 + \frac{\Delta T}{T}) \frac{h}{a} ,$$

where T is the temperature of the lower fluid. Assuming a typical boundary layer specified by $T = 300K$, $\Delta T = 5K$, and $h = 300m$ and taking $a_1 = 0.2$, $a_2 = 0.4$ as representative amplitudes, the soliton wave lengths are $w_1 \simeq 4000\ m$, $w_2 \simeq 2000m$ and the relative shift Δx over the array is 300 m, which is about 10% of the spatial shift required to fully resolve the two-soliton wave pattern. The individual array observations do not therefore provide a direct measure of the evolutionary pattern; they do however, provide sufficient data for an accurate determination of the wave propagation vector.

The following observations are therefore presented in an ordered sequence which is in qualitative agreement with the theoretically predicted finite-amplitude long wave evolutionary pattern.

(a) Soliton-free intrusive disturbances.

Only a few examples of long smooth solitary-wave-free intrusive disturbances have been observed at Warramunga over the three-year observational period. Two examples which illustrate the typical morphology of these events are illustrated in Figure 4. As can be seen, there appears to be no evidence for soliton formation in the frontal zones of these propagating disturbances; it therefore seems reasonable to assume that these smooth disturbances correspond to the initial state in the evolutionary process.

(b) Initial soliton development.

A large number of observations have been made of intrusive disturbances whose structure is indicative of the early stages of soliton formation. Two examples of large amplitude intrusive flows with weak long-period undulations corresponding to the initial condensation of large amplitude solitary waves are shown in Figure 5. The form of these disturbances may be contrasted with that of the smaller-scale events illustrated in the record sections presented in Figure 6. Both of the disturbances shown in Figure 6 are interesting in that they propagate at low velocities and thus a noticeable degree of evolution occurs over the 4 km array. The relatively weak event shown in Figure 6a provides direct observational evidence for the influence of nonlinear steepening in the frontal zone of the disturbance. This unusually slow disturbance first appears at site 1 and then proceeds to traverse the array as a planar wave front directed along the axis defined by sites 1, 5 and 3. As can be seen, the slope of the leading edge of the disturbance increases continuously as the wave progresses over the array and at site 3 there is primary evidence for initial soliton

formation. The two relatively simple disturbances shown in Figure 7 and the more complex intrusions illustrated in Figure 8 appear to be in a more advanced evolutionary state in that several distinct solitary waves are beginning to form in the frontal zone of the disturbance. It is possible, but by no means clear, that some of the oscillations in these early evolutionary states represent the formation of a subcritical dispersive wave component.

(c) Soliton-dominated intrusive disturbances.

Most of the propagating boundary layer intrusive disturbances observed at Tennant Creek belong to this category. Consider first a series of observations of relatively localized short-lived disturbances with a spatial extent of about 20 km. The record sections shown in Figure 9 are chosen to illustrate the process of soliton formation along the leading edge of clearly localized propagating intrusive disturbances. These wave patterns may be compared with the expected behaviour pattern shown in Figure 2a. The more complicated disturbances shown in Figures 10 to 12 illustrate a number of interesting evolutionary features. The fact that none of the soliton patterns in Figure 10 and 11 are ordered by amplitude indicates that these actively evolving waveforms probably originated in unusually complex initial disturbances. The wave pattern illustrated in Figure 11a is particularly interesting in that an essentially pure solitary wave packet consisting of 6 distinct solitons has condensed out well behind the leading edge of the disturbance. The essentially asymtotic character of this soliton family indicates that the wave packet originated in a completely independent disturbance.

Figure 12 provides a comparison of two fairly similar intrusive disturbances whose asymtotic states apparently correspond to the excitation

of three solitary waves. As can be seen, the morphologies of these events differ in that the profiles of the solitons in event 43-1-1894 are flattened at the crest; in fact, it might appear that the leading soliton is about to fission into two solitary waves. However, an isolated solitary wave disturbance with a similarly distorted profile has been observed (Christie et al., 1978) to evolve into the normal Lorentzian waveform; it therefore seems likely that the disturbance illustrated in Figure 12a represents a fairly early stage in the evolutionary process and that this disturbance will eventually evolve into a soliton pattern which is similar to that shown in Figure 12b. This distortion of the profile of higher amplitude leading solitary waves, which may be related to a form of amplitude instability, has been observed on several occasions (e.g., Figures 6b and 8b) and will be discussed briefly in the next section.

Finally, consider the six examples shown in Figures 1, 3b, 13 and 14, of observations of extensive, well developed families of solitary waves associated with the leading edge of intrusive density flows. As can be seen from the diagrams, all of these disturbances are characterized by the excitation of a large number of solitary waves. The observation shown in Figure 13a is particularly noteworthy in that this disturbance, which took over 3 hours to pass over the infrasonic array, consists of at least 17 individual solitary waves and extends over a spatial distance of about 130 km. At first glance, it might appear that the morphology of these extended disturbances is in good agreement with the behaviour pattern shown in Figure 2b for the evolution of the frontal zone of an initially smooth long wave of elevation. However, in the case of all of these observations the solitary waves are not completely ordered by amplitude and thus it may be concluded that, while these patterns are in fairly good agreement with the representation of Figure 2, these disturbances have apparently evolved from a more complex initial state.

(d) Asymtotic disturbances.

An extensive series of observations of asymtotic boundary layer disturbances in the form of pure solitary wave packets, families of well-separated solitons and isolated solitary waves has been described by Christie et al. (1978). An example of a typical large scale amplitude-ordered pure 6-component solitary wave packet and an event consisting of 2 low-amplitude spatially-separated solitons on a noisy background are shown in Figures 15a and 15b respectively. The solitary wave packet may be interpreted as the asymtotic state of a fairly extensive dissipating soliton-dominated intrusion similar to those shown in Figures 14 while the 2-component soliton family represents the asymtotic form of a more localized smaller scale disturbance.

DISCUSSION AND CONCLUSIONS

The detailed sequence of observations presented in the last section clearly indicates that initially smooth long propagating atmospheric boundary layer disturbances evolve asymtotically into a finite number of solitary atmospheric waves, in qualitative agreement with the predicted behaviour pattern predicted by the nonstationary solutions of the Benjamin-Ono nonlinear dispersive wave equation. It should be noted that none of the observations provide a clear indication of the formation of a prominant coherent dispersive oscillatory wave train. This, however, is to be expected since, as noted above, these waves appear to originate in initially positive disturbances and therefore the wave energy is expected to go primarily into the production of solitons with the result that the dispersive state should appear only as a second order effect. It is certainly possible that some of the weak irregular oscillations in the wake of these disturbances do in fact represent the dispersing part of the solution.

It has been emphasized that only a relatively few observations have been made of soliton-dominated intrusive disturbances in which the solitary waves are ordered by amplitude. This then indicates that the initial disturbances are more complicated than those of the simple models shown in Figure 2. Alternatively, perturbations along the propagation path such as variations in the inversion depth may lead to the excitation of new solitary waves (Kaup and Newell, 1978; Ko and Kuehl, 1978) and a distortion of the original pattern, thus masking the structure of the original disturbance.

It might seem reasonable to expect that for very large amplitude disturbances nonlinearity will dominate over dispersion and therefore the disturbance will steepen and eventually break in the forward direction, thus leading to the formation of a turbulent internal bore. A measure of the relative importance of nonlinearity and dispersion in the evolution of classical finite amplitude disturbances is given by the Ursell number (Ursell, 1953),

$$\mathcal{U} = \frac{N_o \lambda^2}{h^3} \tag{11}$$

where λ is the effective wavelength. If $\mathcal{U} \gg 1$, nonlinearity dominates the fluid motion; if $\mathcal{U} \ll 1$, the evolutionary character is determined by dispersion. Solitary waves correspond to a balance between nonlinearity and dispersion and are therefore represented by $\mathcal{U} = O(1)$. This definition of the Ursell number is only suitable for a description of classical finite-amplitude wave propagation in shallow fluids. For fluids of great depth the equivalent Ursell number is given by (Benjamin, 1967),

$$\mathcal{U} = \frac{N_o \lambda}{h^2} . \tag{12}$$

The fact, as reflected in this modified Ursell number, that dispersion plays a more important role in the propagation of waves in deep fluids indicates that deep-fluid solitary wave motions are stable to higher values of dimensionless amplitude than their classical shallow fluid counterpart.

An examination of the properties of the deep-fluid propagating wave disturbances observed at Warramunga reveals values of $\mathcal{U}$ ranging from near unity to greater than 20. One therefore expects to see some evidence of strong nonlinearity in the data. It is worth noting that none of these

observations appear to indicate the onset of a wave-breaking type of instability in the frontal zone of the disturbance. In fact, even in the case of very large amplitude disturbances there is primary evidence for the formation of solitary waves. The only manifestation of strong nonlinearity appears to be the peculiar distorted solitary wave profiles associated with large amplitude disturbances. It is premature without further experimental observations to examine the nature of these unusual wave patterns in detail but the effect is probably related to the presence of a closed circulation cell in the developing streamline pattern of large-amplitude solitary waves as shown in the numerical calculations and laboratory observations of Davis and Acrivos (1967). This breakdown of the uniform flow pattern at higher amplitudes into a pattern with an enclosed region of circulating fluid is probably the principal manifestation of strong nonlinearity in fluid motions of this type. Nevertheless, in some cases a more complicated flow pattern may be required to explain the experimental observations. It does, however, seem clear at this point that, in the absence of wind shear, strong nonlinearity will not lead to internal wave breaking in these deep fluid solitary waves.

Very little is known at the present time about the precise nature of the source mechanism which leads to the production of these solitary wave generating disturbances. Nevertheless, it is clear that many of these disturbances must originate at distances of several hundred kilometers from the array. This can be seen from the following simple estimates of the distance required for an initially smooth disturbance to evolve into the extensive asymtotic waveforms observed at Warramunga. Suppose that a long smooth wave of elevation is created on an established boundary layer inversion at time $t = 0$, at a distance X from the infrasonic array. Ignoring

phase shifts, and assuming that the initial perturbation evolves over X into an ordered disturbance, the minimum arrival time at the array of the leading solitary wave in the disturbance is given to first order by $t_1 = X/c$ where c is the Benjamin solitary wave phase speed,

$$c = c_0 \; (1 + K), \tag{13}$$

with $K = \frac{3}{8}a$. The arrival time of the minimum amplitude solitary wave produced by the disturbance is given approximately by $t_2 = X/c_0$. Hence, a first order estimate of the minimum source distance is

$$X_{min} = \left(\frac{1 + K}{K}\right) c_0 \Delta t, \tag{14}$$

where $\Delta t = t_2 - t_1$ is the observed difference in the arrival time at the array of the solitary waves of mimimum and maximum amplitude. Equation (14) probably underestimates the true source distance since it is based on the assumption that the leading soliton observed at the array propagates over the distance X at the constant velocity c. A rough upper bound on the source distance, X_{max}, can therefore be obtained by assuming the amplitude of the leading solitary wave varies linearly with distance from the origin and thus the maximum estimate of the wave speed used to calculate t_1 should be replaced by the minimum mean value

$$\bar{c} = c_0 \; (1 + \frac{K}{2}) \tag{15}$$

Hence,

$$X_{max} = (\frac{2 + K}{K}) \; c_0 \Delta t. \tag{16}$$

Consider now an application of equations (14) and (16) to observations of extensive well developed solitary-wave-dominated disturbances. An estimate of the dimensionless amplitude a of the leading soliton may be obtained from the two-fluid boundary layer inversion model as

$$a = \frac{\Delta P}{\rho c^2 - \frac{3}{4}\Delta P} ,$$

where ΔP is the measured pressure perturbation and ρ is the mean density of the boundary layer. Typically, the values of the parameters are $a = 0.6$, $c_o = 10$ m/s, and $\Delta t = 6000$ s and hence some of the observed large amplitude extensive solitary wave disturbances appear to originate at distances between 330 and 590 km from the array. It should be emphasized that these estimates are only approximate and that considerable uncertainty is introduced by the possibility that the properties of the atmospheric boundary layer vary along the propagation path.

It seems likely that some of the density intrusions observed at Tennant Creek are produced by thunderstorm-generated downdraft outflows at the surface. However, this does not appear to be the most important source mechanism since many of the soliton-associated events are observed during periods when totally clear conditions prevail throughout the Northern Territory. Furthermore, as noted above, these disturbances only occur at night and, as well, they originate in preferred directions.

A possible explanation for the large number of relatively weak disturbances which arrive at the array from an azimuth of 140° (e.g. Figure 7b) is that they originate in the interaction of katabatic flow from the range of small hills to the southeast of the array with the developing stably-stratified nocturnal boundary layer on the featureless plane to the

north. The possible significance of katabatic drainage in the low-latitude regions of Australia has been discussed by Reynolds and Gething (1970) and by Clarke (1972).

The most probable explanation of the large amplitude solitary wave-dominated disturbances (e.g., Figure 13) which originate in the direction of the Gulf of Carpentaria, 550 km to the north, is that they are generated in the interaction of a sea-breeze vortex or in the interaction of the "Morning Glory" phenomenon with the boundary layer radiation inversion. The Morning Glory is a spectacular propagating isolated roll cloud formation which is frequently observed along the southern and eastern coasts of the Gulf of Carpentaria. It has been suggested that this unusual phenomenon may represent a propagating katabatic-produced internal hydraulic jump (Clarke, 1972), a travelling sea-breeze vortex (R.H. Clarke, private communication quoted in Neal et al., 1977) or an orographically-produced propagating gravity wave disturbance (Neal et al., 1977). In view of the observations presented in this paper, it seems very likely that the Morning Glory phenomenon is in fact a manifestation of a fairly well-developed large amplitude isolated solitary wave or group of solitary waves. In this interpretation the roll clouds are associated with the closed circulation cells in the streamline pattern of large amplitude deep-fluid internal solitary waves propagating along a marine inversion.

Irregardless of the exact nature of the source disturbance it is clear that the production of solitary waves will depend on the existence of a suitably stratified boundary layer. This accounts for the failure to observe solitary waves in the thoroughly mixed turbulent daytime boundary layer. In general, the interaction of a propagating intrusion with a density-stratified deep fluid will result, initially, in the formation of a long smooth wave at the head of the intrusion; this wave will subsequently

evolve according to the Benjamin-Ono equation. A significant portion of the energy of the intrusion is therefore dissipated directly into the production of long waves and into the production of closed circulation cells in the larger amplitude solitons. In the asymtotic state, all trace of the original intrusive fluid body is lost and the disturbance is reduced to a finite number of stable, independent, solitary atmospheric waves.

The main conclusion of this investigation is that intrusive density flows in the atmosphere provide a primary source of solitary atmospheric waves. It should be noted however, that other types of disturbances (Maxworthy, 1978) may play an equally important role in soliton production. For example solitary waves may evolve from the disturbance associated with the dissipation of a Kelvin-Helmholtz instability or the collapse of standing eddies and lee waves induced by a sudden variation in the properties of the flow over an orographic feature.

It is evident that the atmospheric solitary-wave-dominated intrusive disturbances described in this paper bear a strong resemblence to the well-known soliton-associated internal surges observed in the oceans and in inland stratified bodies of water. Since the density profile and shear structure of the thermocline differ from those of the nocturnal inversion, it must be expected that the characteristics of the marine form of these nonlinear wave disturbances will differ in detail from the characteristics of the equivalent atmospheric disturbances. Neverthelss, all of these disturbances belong to the same fundamental class of fluid motions and thus the basic properties of these large scale waves may be profitably studied in either the marine or atmospheric environment. In this regard, it is worth noting that it is easier to obtain accurate detailed experimental

observations of these disturbances in the atmospheric boundary layer. Moreover, it should be possible, through the use of portable microbarograph array elements, to examine the complete evolutionary pattern of these atmospheric disturbances.

This investigation leaves a number of interesting geophysical fluid dynamical problems unanswered. In particular, very little is known about the detailed form of the source mechanisms that excite these disturbances, the exact nature of the role played by strong nonlinearity, the relative importance of topographic perturbations, the influence of the passage of these large amplitude disturbances on the dynamical structure of the lower troposphere, and the mechanisms which eventually lead to the destruction of the extremely stable asymtotic solitary wave component. It is therefore evident that further experimental observations will be required in order to achieve a thorough understanding of these nonlinear wave phenomena.

ACKNOWLEDGEMENTS

The authors wish to express their gratitude to Professor J.S. Turner for many valuable discussions and perceptive observations on the interpretation of complex geophysical fluid motions. The authors have also benefited greatly from many stimulating discussions on the nature of solitary waves with Professor T. Maxworthy. In addition, we wish to thank Mr. Blair Lade and Mr. Phillip Taylor for their efforts in operating the Warramunga Seismic Station. This research was supported by the Air Force Office of Scientific Research under Contract No. AFOSR-75.2759A.

REFERENCES

Ablowitz, M.J., D.J. Kaup, A.C. Newell, and H. Segur, The inverse scattering transform - Fourier analysis for nonlinear problems, Stud. Appl. Math., 53, 249-315, 1974.

Ablowitz, M.J. and A.C. Newell, The decay of the continuous spectrum for solutions of the Korteweg-de Vries equation, J. Math. Phys., 14, 1277-1284, 1973.

Ablowitz, M.J., and H. Segur, Asymptotic solutions of the Korteweg-de Vries equation, Stud. Appl. Math., 57, 13-44, 1977.

Benjamin, T.B., Internal waves of permanent form in fluids of great depth, J. Fluid Mech., 29, 559-592, 1967.

Berezin, Yu. A., and Karpman, V.I., Nonlinear evolution of disturbances in plasmas and other dispersive media, Sov. Phys. JETP, 24, 1049-1056, 1967.

Brekhovskikh, L.M., K.V. Konjaev, K.D. Sabinin, and A.N. Serikov, Short-period internal waves in the sea, J. Geophys. Res., 80, 856-864, 1975.

Cercignani, C., Solitons. Theory and applications, Riv. Nuovo Cimento, 7, 429-469, 1977.

Christie, D.R., K.J. Muirhead, and A.L. Hales, On solitary waves in the atmosphere, J. Atmos. Sci., 35, 805-825, 1978.

Clarke, R.A., Solitary and cnoidal planetary waves, Geophys. Fluid Dyn., 2, 343-354, 1971.

Clarke, R.H., The morning glory : an atmospheric hydraulic jump, J. Appl. Met., 11, 304-311, 1972.

Davis, R.E., and A. Acrivos, Solitary internal waves in deep water, J. Fluid Mech., 29, 593-607, 1967.

Gardner, C.S., J.M. Greene, M.D. Kruskal, and R.M. Miura, Method for solving the Korteweg-de Vries equation, Phys. Rev. Lett., 19, 1095-1097, 1967.

Gardner, C.S., J.M. Greene, M.D. Kruskal, and R.M. Miura, Korteweg-de Vries equation and generalizations. VI. Methods for exact solution, Comm. Pure Appl. Math., 27, 97-133, 1974.

Gargett, A.E., Generation of internal waves in the Strait of Georgia, British Columbia, Deep Sea Res., 23, 17-32, 1976.

Gaul, R.D., Observations of internal waves near Hudson Canyon, J. Geophys. Res., 66, 3821-3830, 1961.

Halpern, D., Observations on short-period internal waves in Massachusetts Bay, J. Marine Res., 29, 116-132, 1971.

Hammack, J.L., A note on tsunamis : their generation and propagation in an ocean of uniform depth, J. Fluid Mech., 60, 769-799, 1973.

Hammack, J.L. and H. Segur, The Korteweg-de Vries equation and water waves. Part 2. Comparison with experiments, J. Fluid Mech., 65, 289-314, 1974.

Hammack, J.L. and H. Segur, Modelling criteria for long water waves, J. Fluid Mech., 84, 359-373, 1978a.

Hammack, J.L. and H. Segur, The Korteweg-de Vries equation and water waves. Part 3. Oscillatory waves, J. Fluid Mech., 84, 337-358, 1978b.

Hirota, R., Exact solution of the Korteweg-de Vries equation for multiple collisions of solitons, Phys. Rev. Lett., 27, 1192-1194, 1971.

Hirota, R., and J. Satsuma, N-soliton solutions of model equations for shallow water waves, J. Phys. Soc. Japan, 40, 611-612, 1976.

Hunkins, K., and M. Fliegel, Internal undular surges in Seneca Lake : A natural occurrence of solitons, J. Geophys. Res., 78, 539-548, 1973.

Ivanov, V.A. and K.V. Konyayev, A bore on the thermocline, Izv. Akad. Nauk SSSR Fiz. Atmos. Okeana, 12 (4), 416-423, 1976. (Izv. Acad. Sci. USSR Atmos. Ocean Phys., Engl. Transl. 12 (4), 251-255, 1976).

Joseph, R.I., Multi-soliton-like solutions to the Benjamin-Ono equation, J. Math. Phys., 18, 2251-2258, 1977a.

Joseph, R.I., Solitary waves in a finite depth fluid, J. Phys. A : Math Gen., 10, L225-227, 1977b.

Joseph, R.I., and R. Egri, Multi-soliton solutions in a finite depth fluid, J. Phys. A : Math. Gen., 11, L97-102, 1978.

Kaup, D.J. and A.C. Newell, Solitons as particles, oscillators, and in slowly changing media: a singular perturbation theory, Proc. R. Soc., 361A, 413-446 (1978).

Kikuchi, H., Shocks, Solitons and the plasmapause J. Atmos. Terr. Phys., 38, 1055-1060, 1976.

Ko, K., and H.H. Kuehl, Korteweg-de Vries soliton in a slowly varying medium, Phys. Rev. Lett., 40, 233-236, 1978.

Korteweg, D.J., and G. de Vries, On the change of form of long waves advancing in a rectangular canal and on a new type of long stationary waves, Phil. Mag., Ser. 5, 39, 422-443, 1895.

Lamb, Jr., G.L., Bäcklund transformations for certain nonlinear evolution equations. J. Math. Phys., 15, 2157-2165, 1974.

Lee, C.-Y., and R.C. Beardsley, The generation of long nonlinear internal waves in a weakly stratified shear flow, J. Geophys. Res., 79, 453-462, 1974.

Levikov, S.P., Nonstationary and slightly nonlinear internal waves in a deep ocean, Oceanology, 16, 551-554, 1977.

Long, R., Solitary waves in the westerlies, J. Atmos. Sci., 21, 197-200, 1964.

Maxworthy, T., On the formation of internal solitary waves from the gravitational collapse of mixed regions in two and three dimensions, To be submitted for publication, 1978.

Maxworthy, T., and L.G. Redekopp, A solitary wave theory of the Great Red Spot and other observed features of the Jovian atmosphere, Icarus, 29, 261-271, 1976.

Meiss, J.D. and N.R. Pereira, Internal wave soliton, Phys. Fluids, 21, 700-702, 1978.

Neal, A.B., I.J. Butterworth, and K.M. Murphy, The Morning Glory, Weather, 32, 176-183, 1977.

Ono, H., Algebraic solitary waves in stratified fluids, J. Phys. Soc. Japan, 39, 1082-1091, 1975.

Redekopp, L.G., On the theory of solitary Rossby waves, J. Fluid Mech., 82, 725-745, 1977.

Reynolds, R.M. and J.T. Gething, Acoustic sounding at Benalla, Victoria and Julia Creek, Queensland, Publ. No. 17, Meteor. Department, University of Melbourne, Project EAR, Rep. V-VII, 1970.

Scott, A.C., F.Y.F. Chu, and D.W. McLaughlin, The soliton : A new concept in applied science, Proc. IEEE, 61, 1443-1483.

Scott Russell, J., Report on waves, Meeting of the British Association for the Advancement of Science, 417-496, 1837.

Segur, H., The Korteweg-de Vries equation and water waves. Solutions of the equation. Part 1., J. Fluid Mech., 59, 721-736.

Thorpe, S.A., A. Hall, and I. Crofts, The internal surge in Loch Ness, Nature, 237, 96-98, 1972.

Ursell, F., The long-wave paradox in the theory of gravity waves, Proc. Camb. Phil. Soc., 49, 685-694, 1953.

Vliegenthart, A.C., On finite-difference methods for the Korteweg-de Vries equation, J. Eng. Math., 5, 137-155, 1971.

Wadati, M., and M. Toda, The exact N-soliton solution of the Korteweg-de Vries equation, J. Phys. Soc. Japan, 32, 1403-1411, 1972.

Weidman, P.D. and T. Maxworthy, Experiments on strong iteractions between solitary waves, J. Fluid Mech., 85, 417-431, 1978.

Whitham, G.B., Variational methods and applications to water waves, Proc. R. Soc., 299A, 6-25, 1967.

Zabusky, N.J., A synergetic approach to problems of nonlinear dispersive wave propagation and interaction, Proc. Symp. on Nonlinear Partial Differential Equations, (W.F. Ames, ed.), Academic Press, New York, 223-258, 1967.

Zabusky, N.J. and Galvin, C.J., Shallow-water waves, the Korteweg-de Vries equation and solitons, J. Fluid Mech., 47, 811-824, 1971.

Zabusky, N.J. and Kurskal, M.D., Interaction of "solitons" in a collisionless plasma and the recurrence of initial states, Phys. Rev. Lett., 15, 240-243.

Ziegenbein, J., Spatial observations of short internal waves in the Strait of Gibraltar, Deep-Sea Res., 17, 867-875, 1970.

Figure Captions

Figure 1. An example of the typical morphology of a solitary-wave-dominated intrusive atmospheric disturbance. The azimuth noted in this diagram corresponds to the source direction measured from true north.

Figure 2. Schematic representation, based on the predictions of non-linear dispersive wave theory, of the evolutionary behaviour pattern of (a) a finite-length wave of elevation and (b) the leading edge of a long wave. The initial disturbance in (a) evolves into a supercritical solitary wave family followed by a weak dispersing subcritical oscillatory wave train. Asymtotically, this disturbance is reduced to 4 solitary waves which are ordered by amplitude. In (b) the evolutionary pattern is characterized by the formation of a long train of amplitude-ordered solitary waves along the leading edge of the disturbance.

Figure 3. Two examples of the inversion (lower figures) of microbarograph array record sections (upper figures) corresponding to (a) a solitary-wave-dominated intrusive disturbance. The site numbering shown in these diagrams corresponds to a centered quadrilateral array configuration where the 4 sites on the perimeter are numbered in the clockwise direction from the north and the fifth site is located at the center.

Figure 4. Array record sections illustrating the frontal zone of two relatively smooth solitary-wave-free intrusive atmospheric disturbances. Disturbances of this type appear to represent a primary evolutionary state.

Figure 5. Large amplitude intrusive disturbances which illustrate an early stage in the development of solitary waves.

Figure 6. Record sections corresponding to two relatively weak evolving disturbances in an early evolutionary state.

Figure 7. Two relatively simple disturbances which illustrate the initial formation of solitary waves along the leading edge of intrusive flows.

Figure 8. Surface pressure perturbations corresponding to the passage of complex density intrusions in an intermediate developmental stage.

Figure 9. Microbarograph array record sections of two localized propagating intrusive atmospheric disturbances. Solitary wave formation is evident along the leading edge of these intrusions.

Figure 10. Examples of complex solitary-wave-dominated intrusive disturbances.

Figure 11. Unusual complex soliton-associated density intrusions. Note the essentially pure six-component solitary wave family which appears in the wake of the disturbance shown in (a). This wave packet probably represents the asymtotic state of an independent disturbance. The intrusion shown in (b) is unusual in that a large amplitude soliton has condensed out near the center of the disturbance.

Figure 12. A comparison of the morphologies of simple intrusive density flows. The disturbance shown in (a) appears to represent an earlier stage in the evolutionary process than that shown in (b).

Figure 13. Two excellent examples of microbarograph array record sections which illustrate the development of a very extensive family of solitary waves along the leading edge of intrusive density flows.

Figure 14. Examples of extensive soliton-dominated intrusions. Note the low degree of amplitude ordering in the solitary wave pattern associated with the disturbance shown in (a).

Figure 15. Asymtotic soliton states. (a) A pure six-component solitary wave packet. (b) Two asymtotic, spatially separated low amplitude solitary waves on a noisy micropressure background.

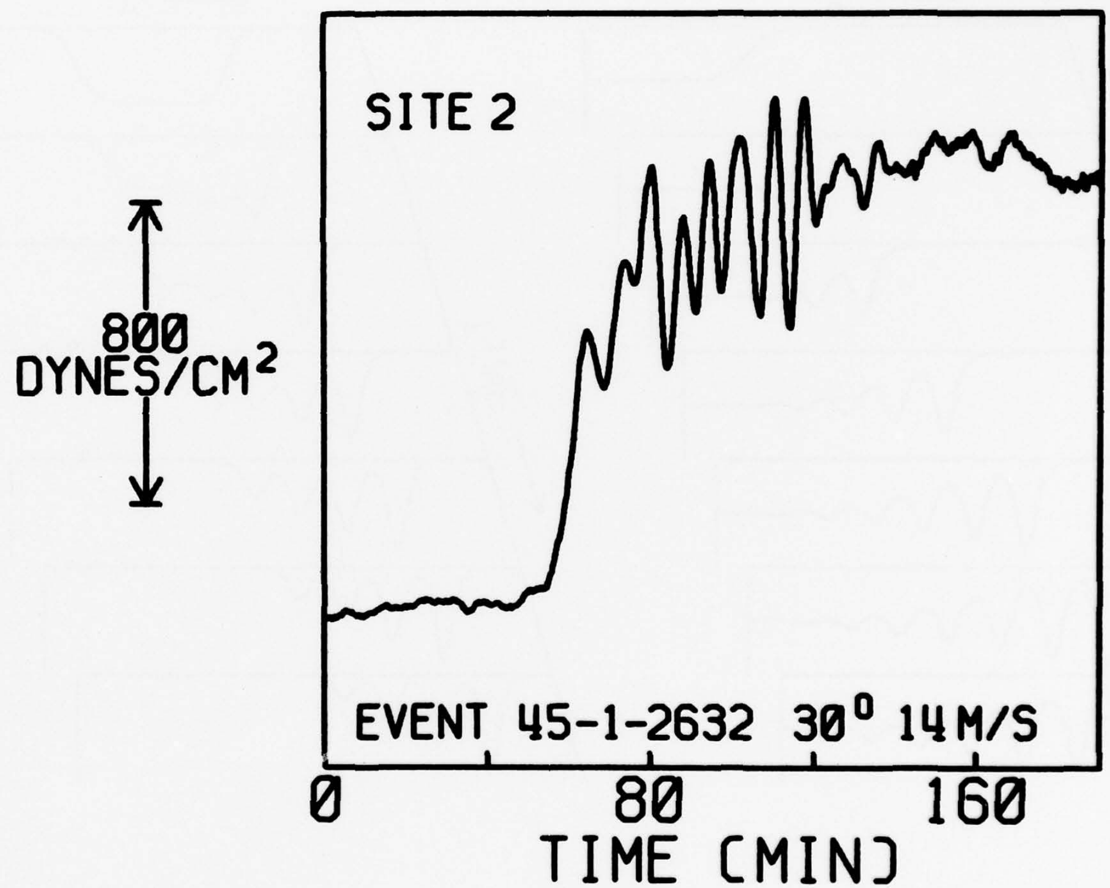
SITE 2
800
DYNES/CM²
EVENT 45-1-2632 30° 14M/S
0
80
160
TIME (MIN)

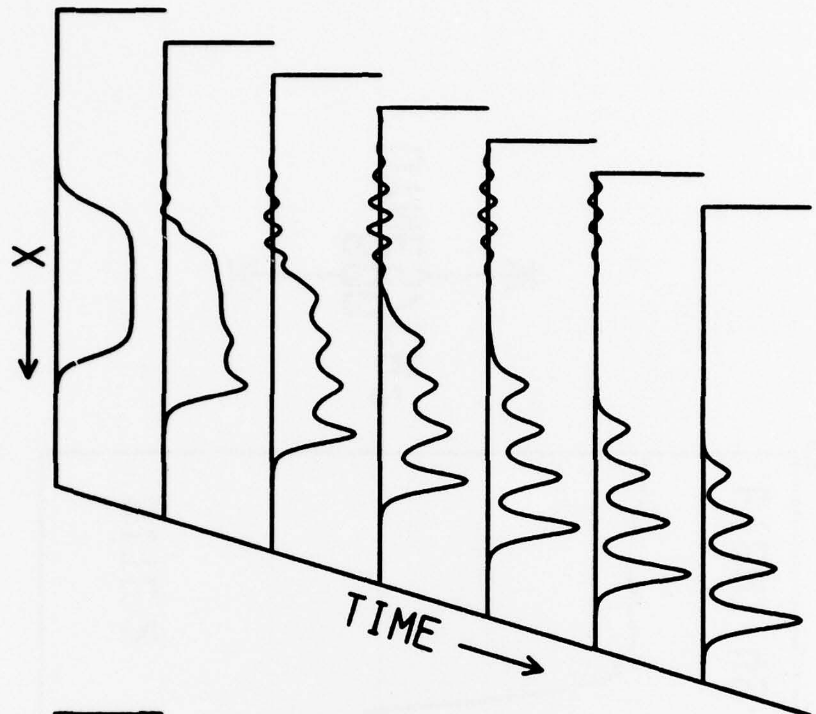
X
TIME

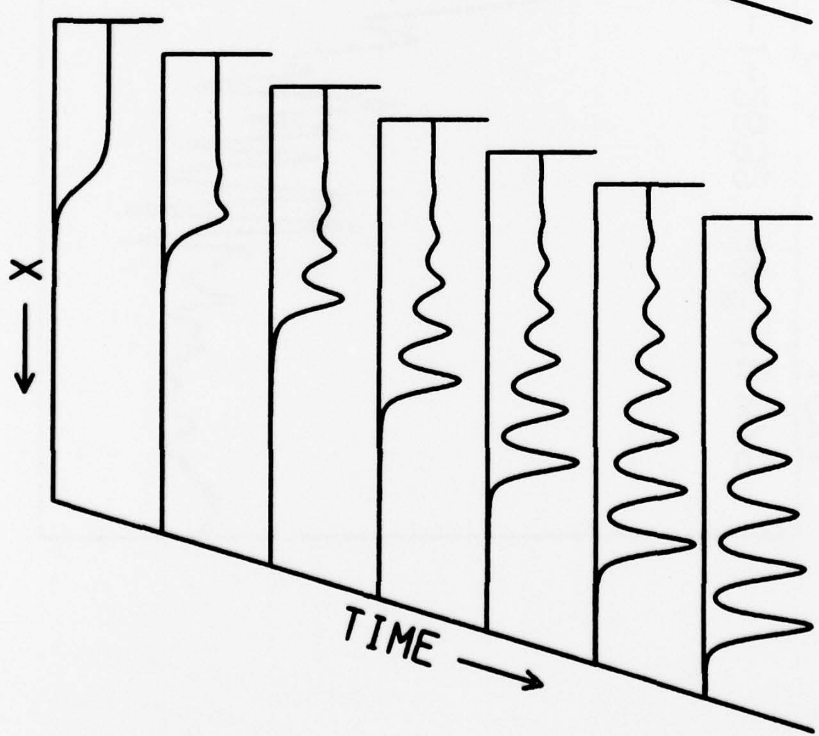
X
TIME

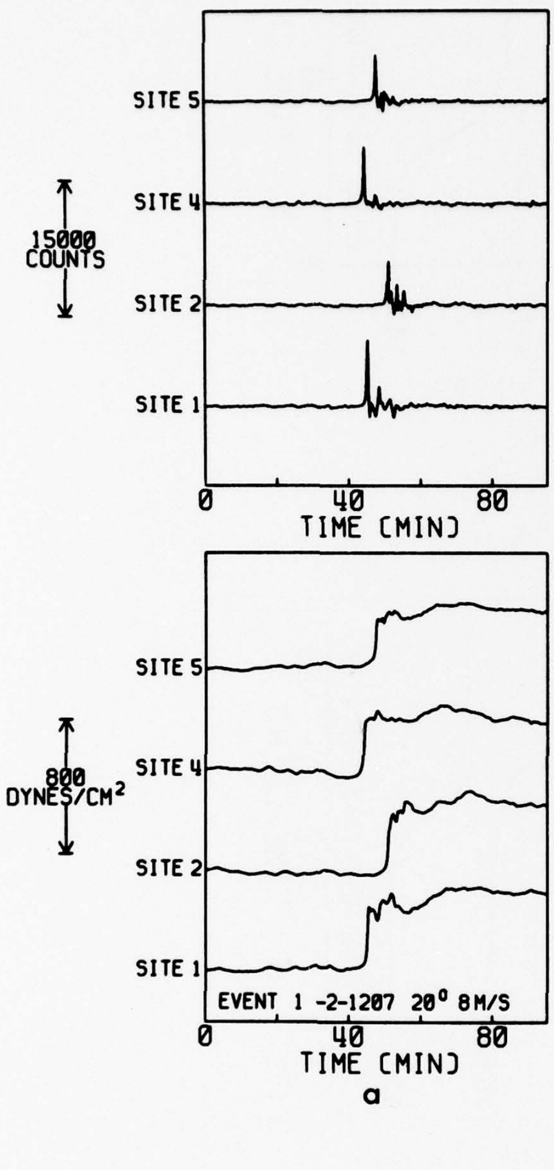
SITE 5
SITE 4
SITE 2
SITE 1
15000 COUNTS
0
40
80
TIME (MIN)
SITE 5
SITE 4
SITE 2
SITE 1
800 DYNES/CM^2
EVENT 1 -2-1207 20° 8M/S
0
40
80
TIME (MIN)

a

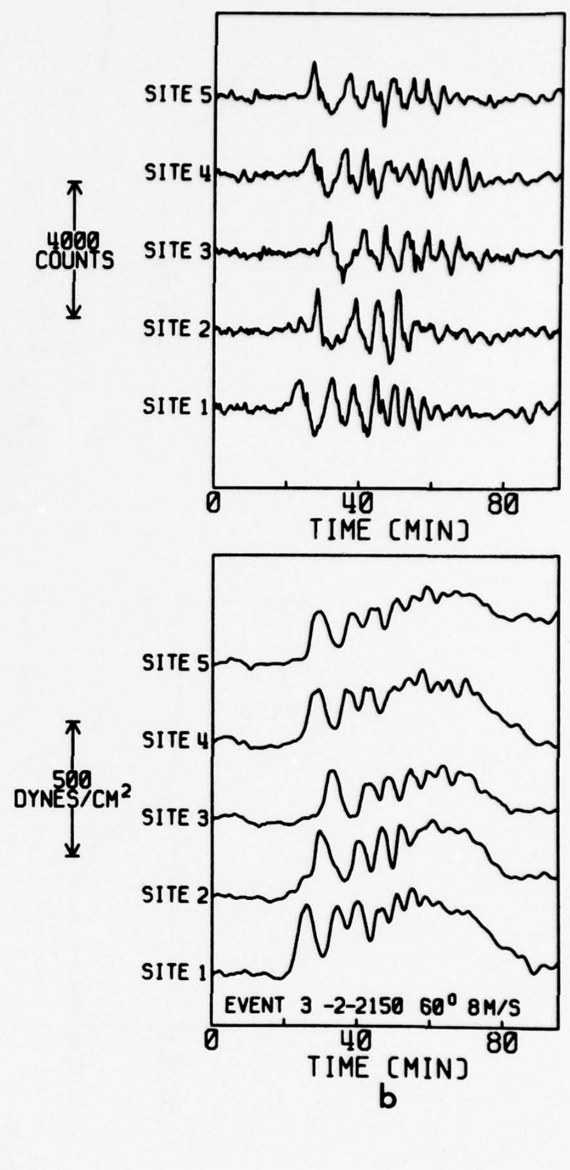
SITE 5
SITE 4
SITE 3
SITE 2
SITE 1
4000 COUNTS
0
40
80
TIME (MIN)
SITE 5
SITE 4
SITE 3
SITE 2
SITE 1
500 DYNES/CM^2
EVENT 3 -2-2150 60° 8M/S
0
40
80
TIME (MIN)

b

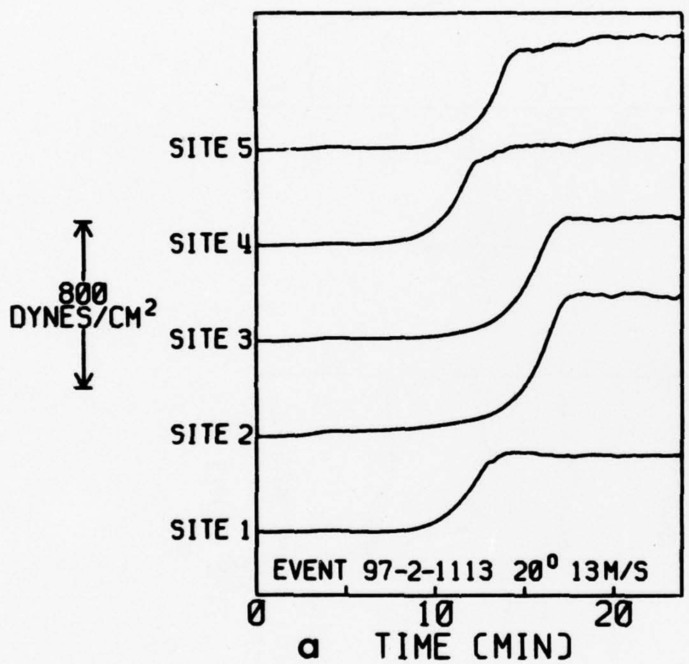
800
DYNES/CM²
SITE 5
SITE 4
SITE 3
SITE 2
SITE 1
EVENT 97-2-1113 20° 13M/S
0
10
20
TIME (MIN)

a

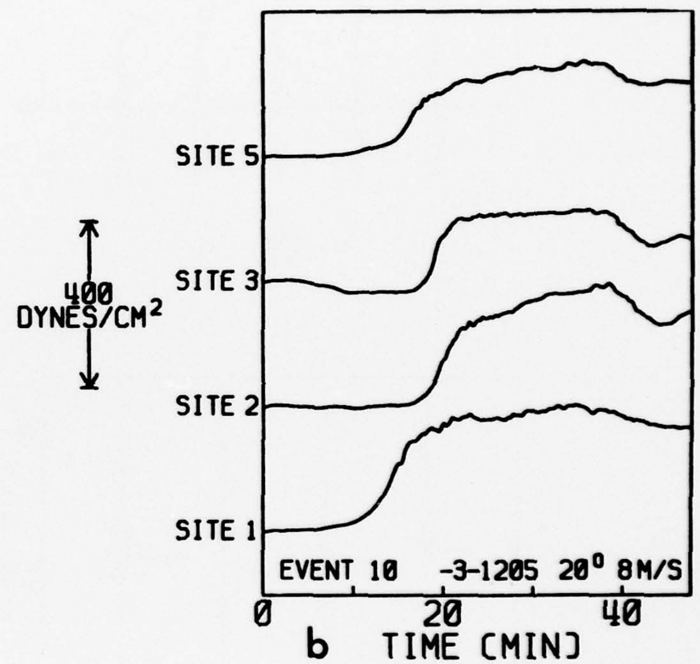
400
DYNES/CM²
SITE 5
SITE 3
SITE 2
SITE 1
EVENT 10 -3-1205 20° 8M/S
0
20
40
TIME (MIN)

b

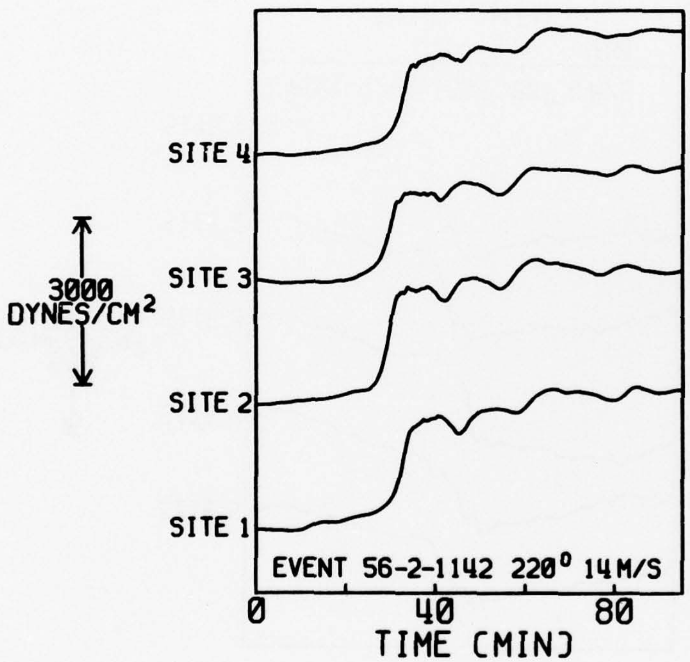
3000
DYNES/CM²
SITE 4
SITE 3
SITE 2
SITE 1
EVENT 56-2-1142 220° 14M/S
0
40
80
TIME (MIN)
a

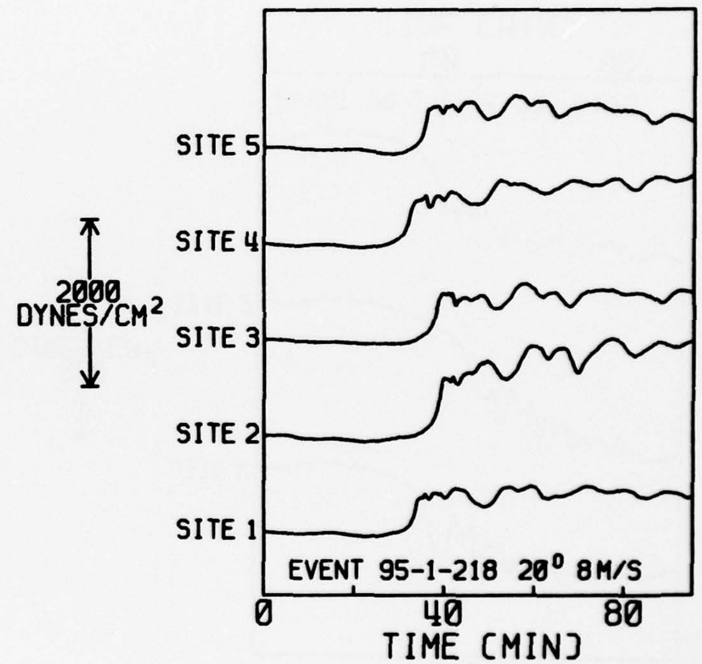
2000
DYNES/CM²
SITE 5
SITE 4
SITE 3
SITE 2
SITE 1
EVENT 95-1-218 20° 8M/S
0
40
80
TIME (MIN)
b

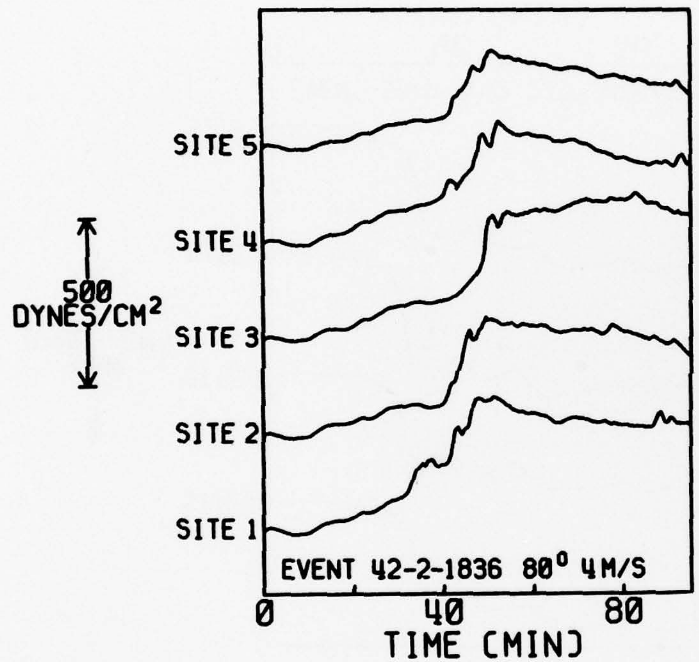
500
DYNES/CM²
SITE 5
SITE 4
SITE 3
SITE 2
SITE 1
EVENT 42-2-1836 80° 4M/S
0
40
80
TIME (MIN)
a

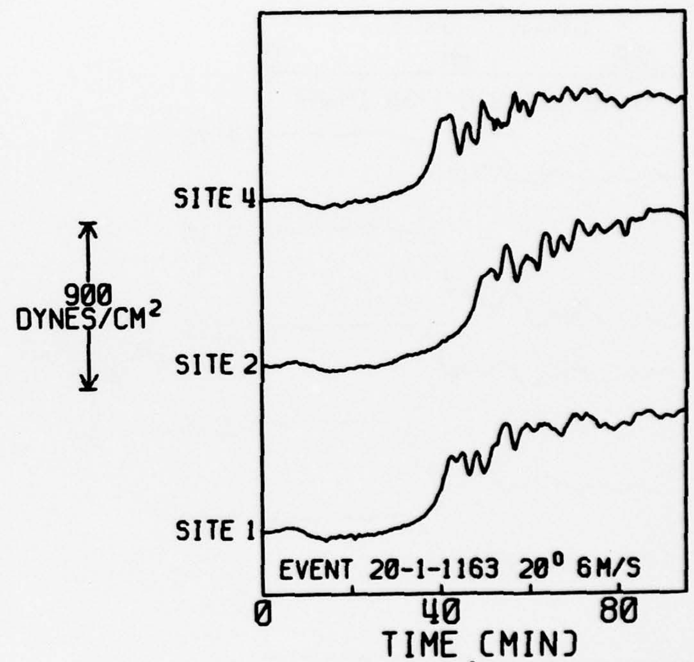
900
DYNES/CM²
SITE 4
SITE 2
SITE 1
EVENT 20-1-1163 20° 6M/S
0
40
80
TIME (MIN)
b

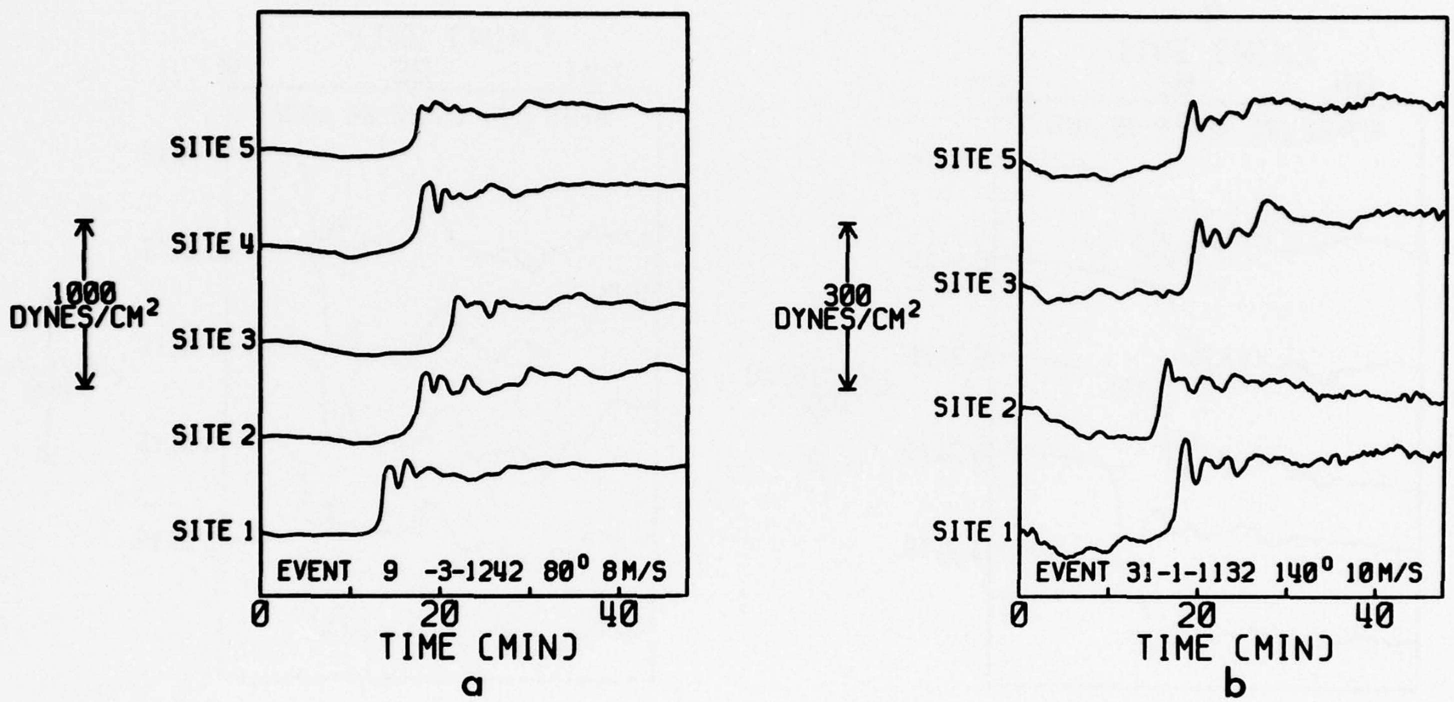
1000
DYNES/CM²
SITE 5
SITE 4
SITE 3
SITE 2
SITE 1
EVENT 9 -3-1242 80° 8M/S
0
20
40
TIME (MIN)
a
300
DYNES/CM²
SITE 5
SITE 3
SITE 2
SITE 1
EVENT 31-1-1132 140° 10M/S
0
20
40
TIME (MIN)
b

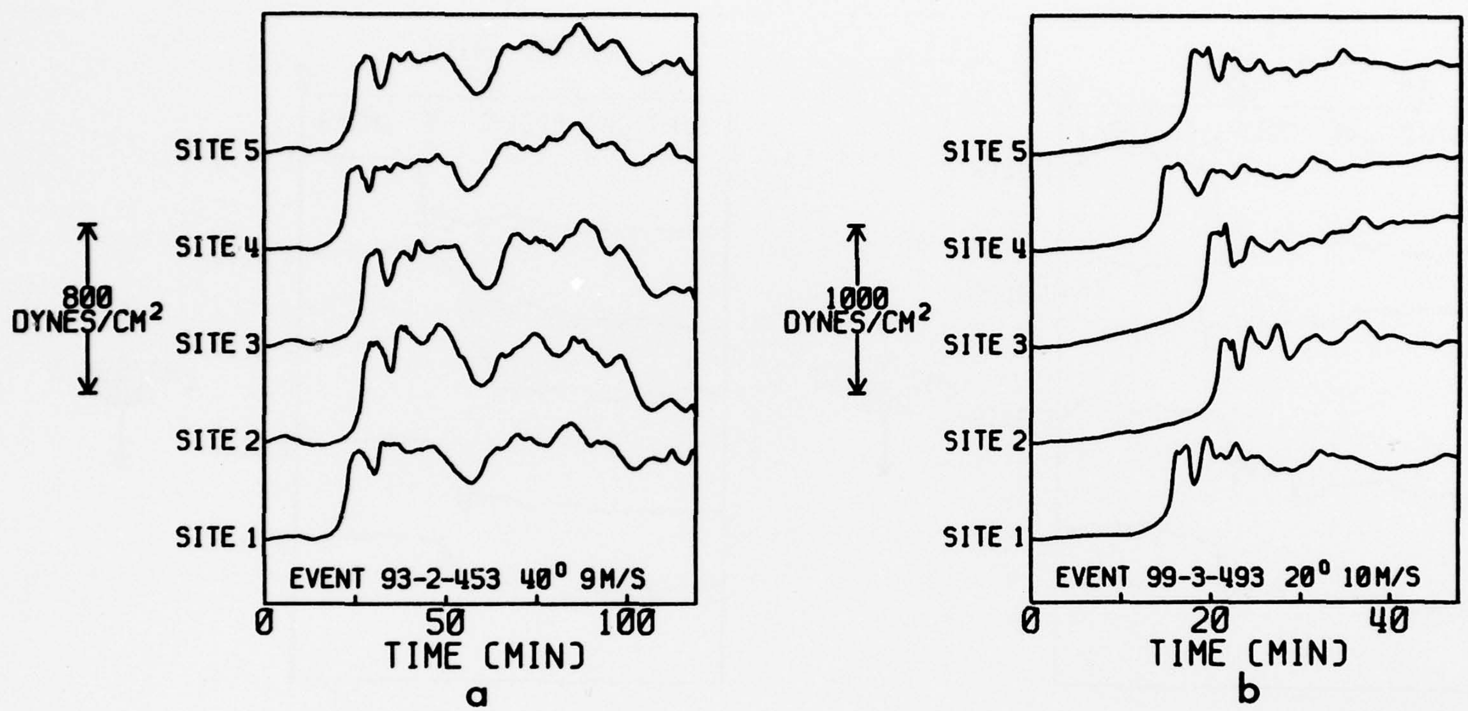

800
DYNES/CM²
SITE 5
SITE 4
SITE 3
SITE 2
SITE 1
EVENT 93-2-453 40° 9M/S
0
50
100
TIME (MIN)
a
1000
DYNES/CM²
SITE 5
SITE 4
SITE 3
SITE 2
SITE 1
EVENT 99-3-493 20° 10M/S
0
20
40
TIME (MIN)
b

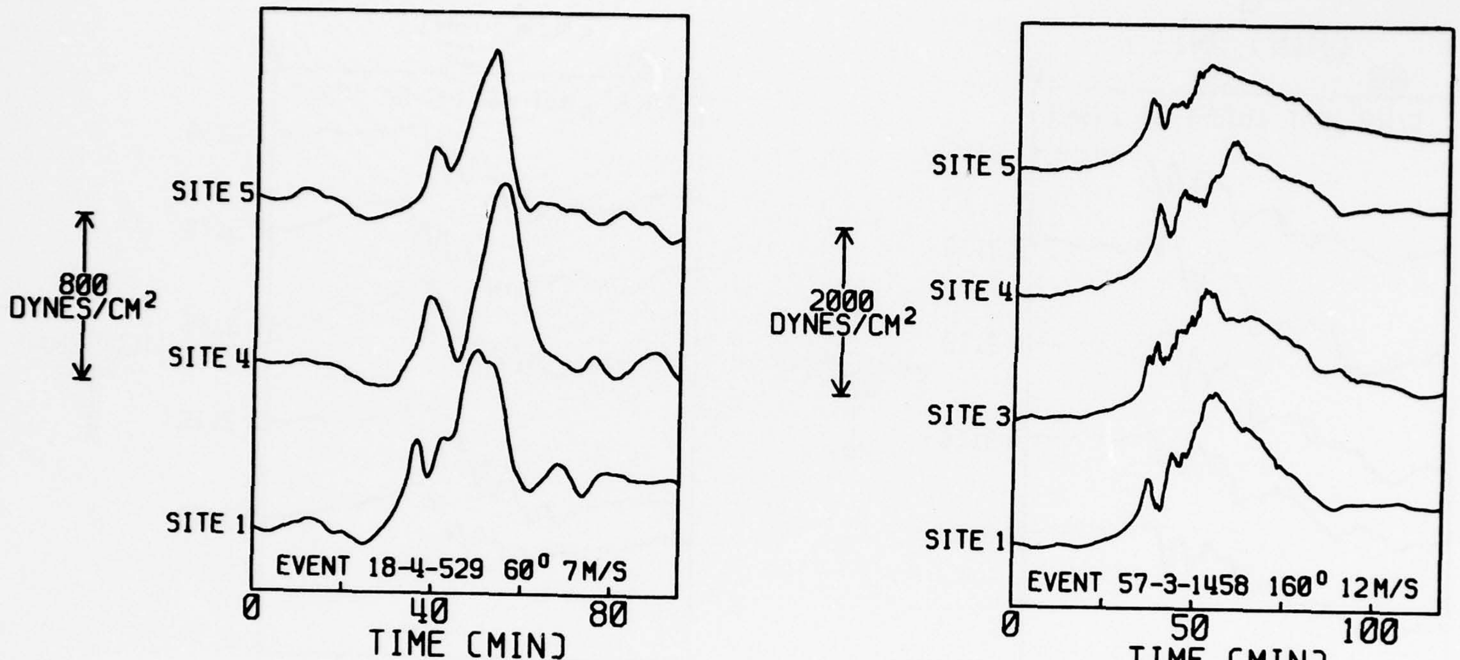
800
DYNES/CM²
SITE 5
SITE 4
SITE 1
EVENT 18-4-529 60° 7M/S
0
40
80
TIME (MIN)
2000
DYNES/CM²
SITE 5
SITE 4
SITE 3
SITE 1
EVENT 57-3-1458 160° 12M/S
0
50
100
TIME (MIN)

a

b

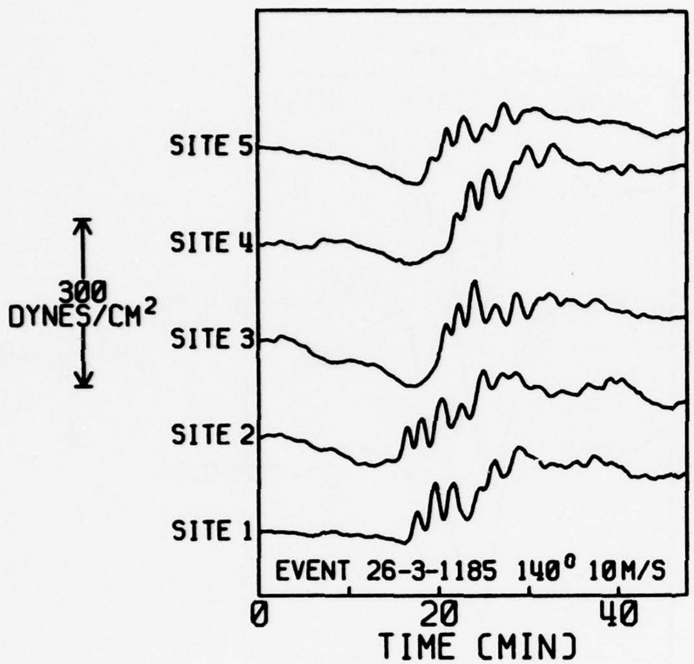

300
DYNES/CM²
SITE 5
SITE 4
SITE 3
SITE 2
SITE 1
EVENT 26-3-1185 140° 10M/S
0
20
40
TIME (MIN)

a

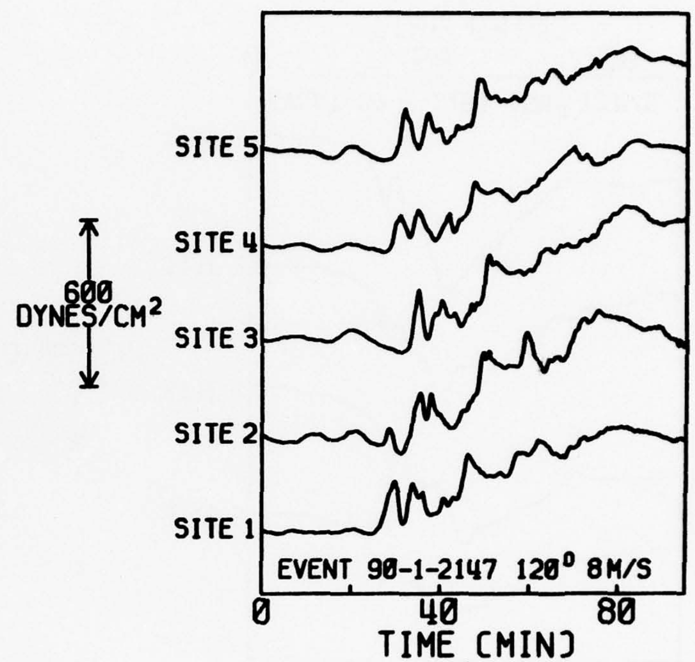

600
DYNES/CM²
SITE 5
SITE 4
SITE 3
SITE 2
SITE 1
EVENT 90-1-2147 120° 8M/S
0
40
80
TIME (MIN)

b

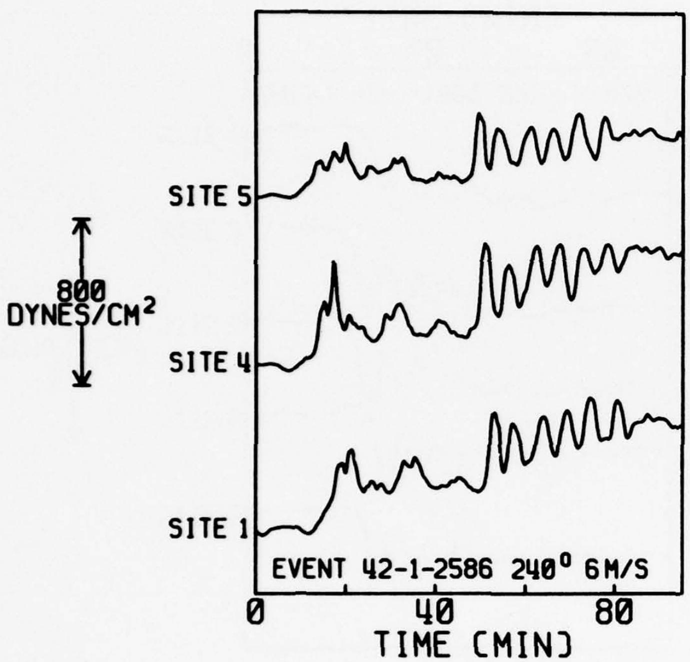

800
DYNES/CM²
SITE 5
SITE 4
SITE 1
EVENT 42-1-2586 240° 6M/S
0
40
80
TIME (MIN)

a

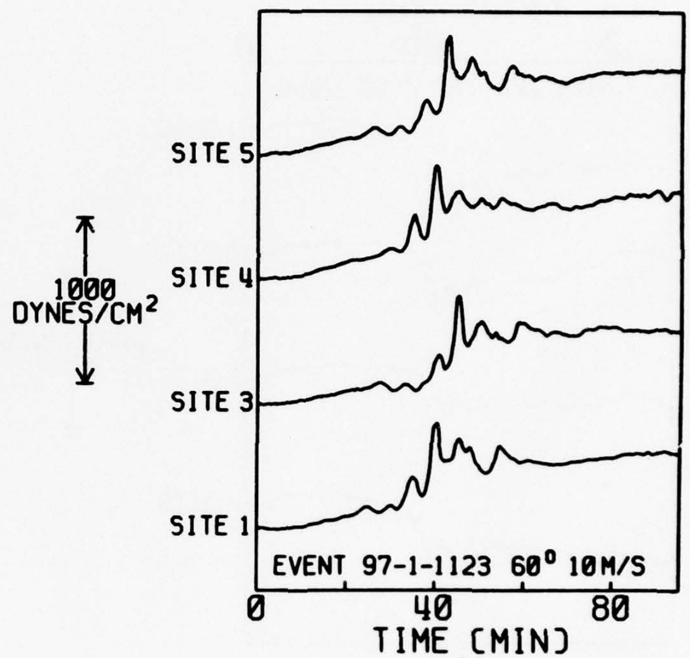

1000
DYNES/CM²
SITE 5
SITE 4
SITE 3
SITE 1
EVENT 97-1-1123 60° 10M/S
0
40
80
TIME (MIN)

b

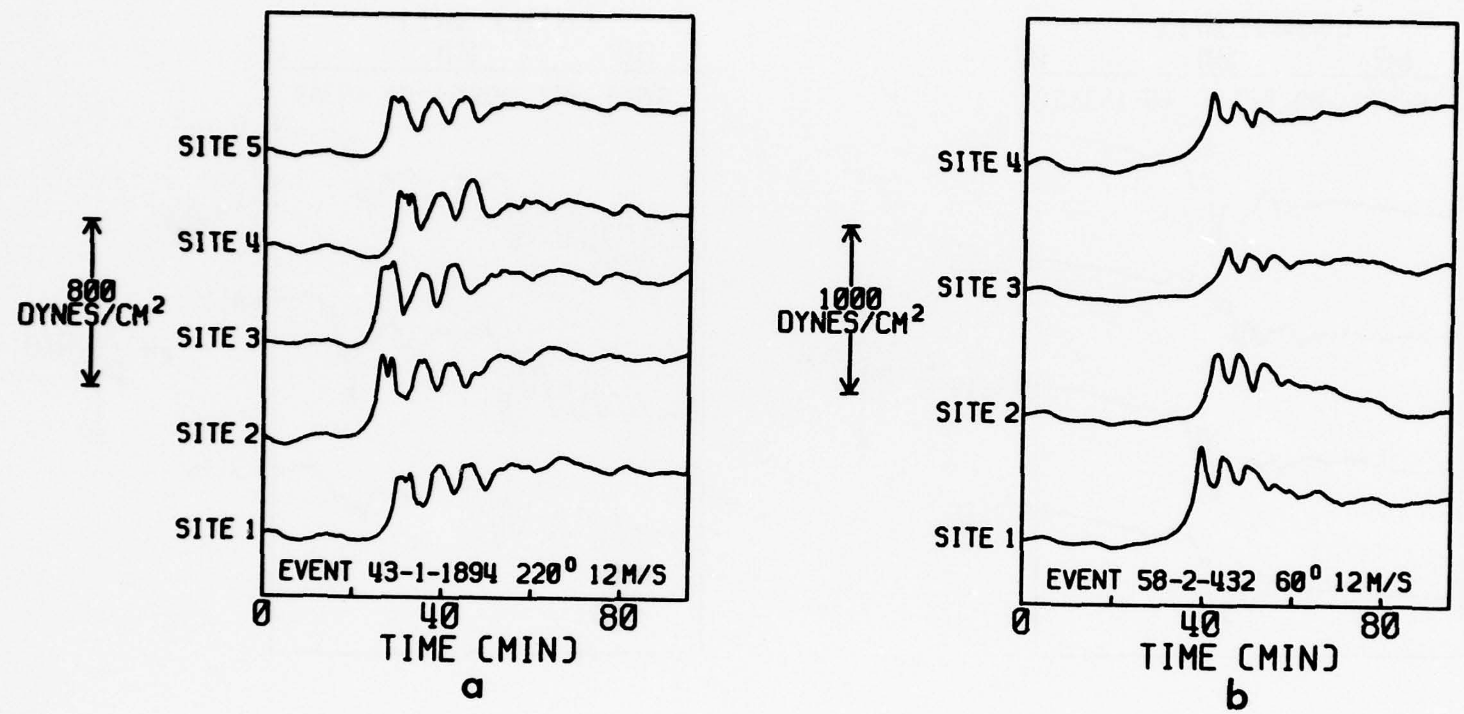
800
DYNES/CM²
SITE 5
SITE 4
SITE 3
SITE 2
SITE 1
EVENT 43-1-1894 220° 12M/S
0
40
80
TIME (MIN)
a
1000
DYNES/CM²
SITE 4
SITE 3
SITE 2
SITE 1
EVENT 58-2-432 60° 12M/S
0
40
80
TIME (MIN)
b

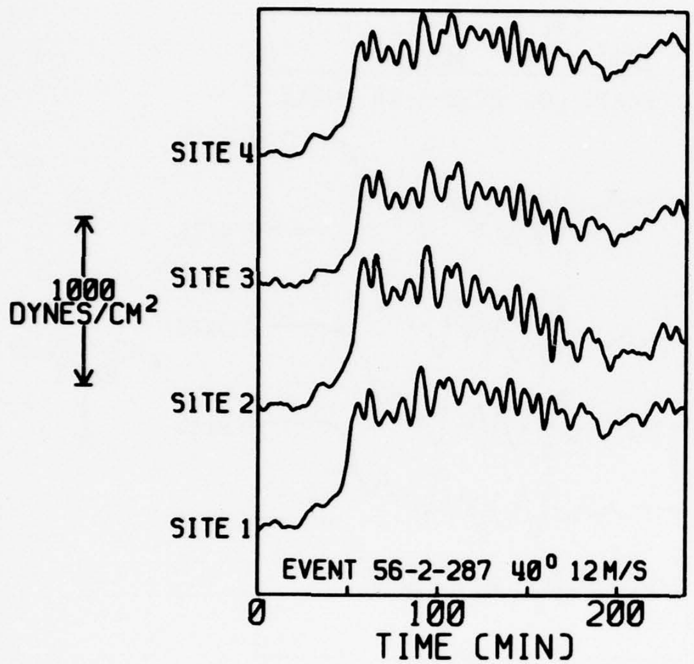
1000
DYNES/CM²
SITE 4
SITE 3
SITE 2
SITE 1
EVENT 56-2-287 40° 12M/S
0
100
200
TIME (MIN)

a

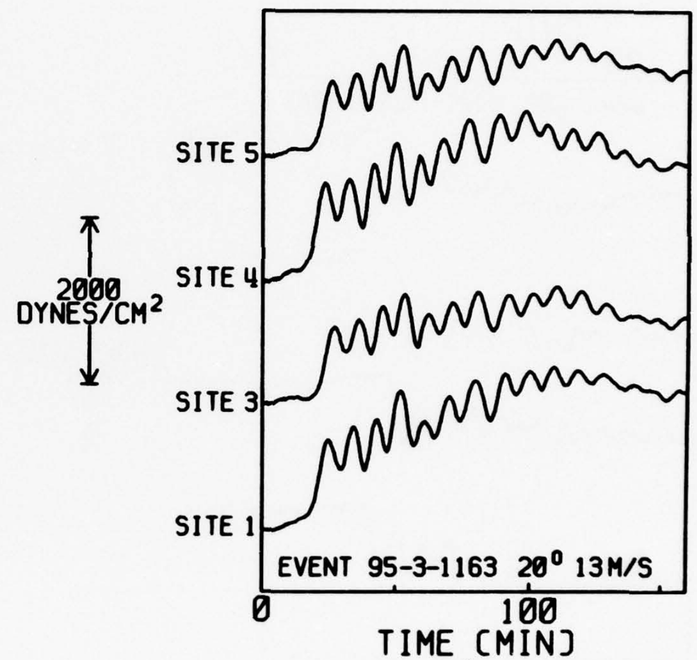
2000
DYNES/CM²
SITE 5
SITE 4
SITE 3
SITE 1
EVENT 95-3-1163 20° 13M/S
0
100
TIME (MIN)

b

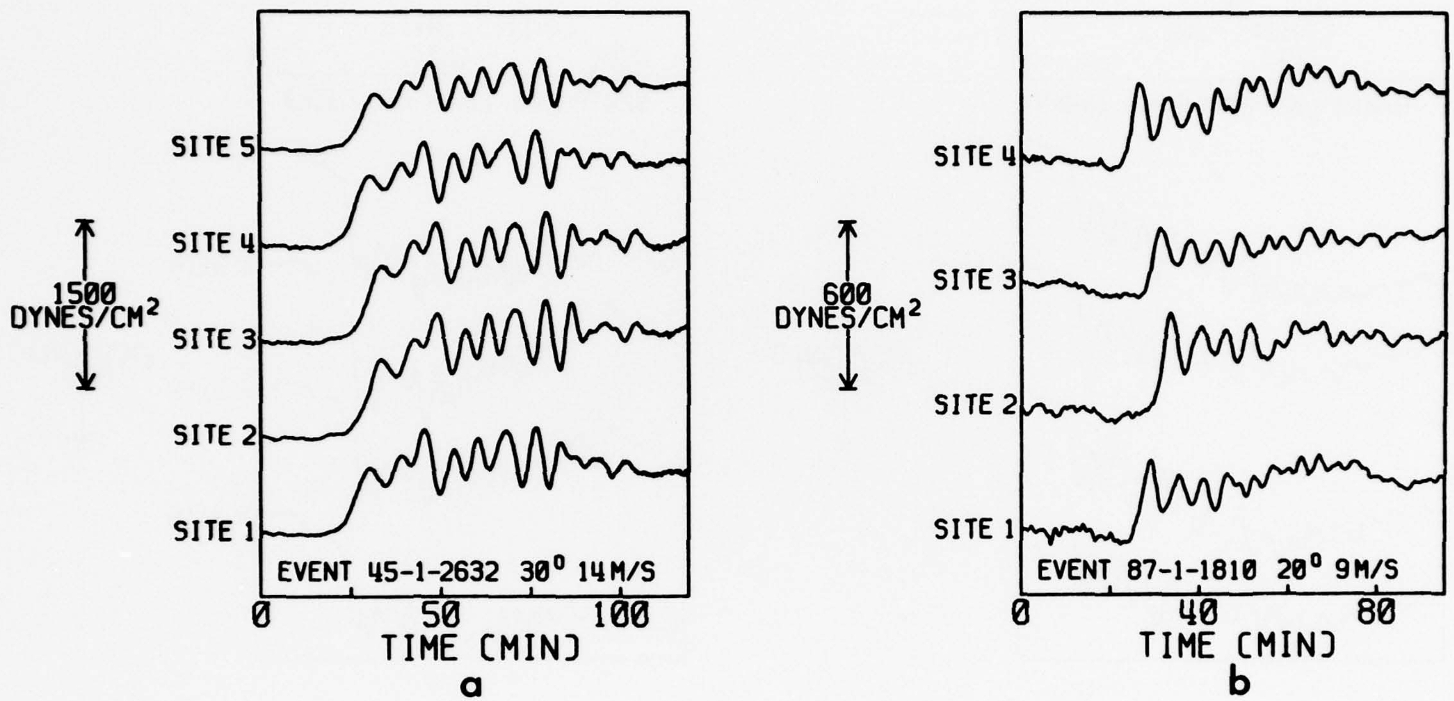
1500
DYNES/CM²
SITE 5
SITE 4
SITE 3
SITE 2
SITE 1
EVENT 45-1-2632 30° 14M/S
0
50
100
TIME (MIN)
a
600
DYNES/CM²
SITE 4
SITE 3
SITE 2
SITE 1
EVENT 87-1-1810 20° 9M/S
0
40
80
TIME (MIN)
b

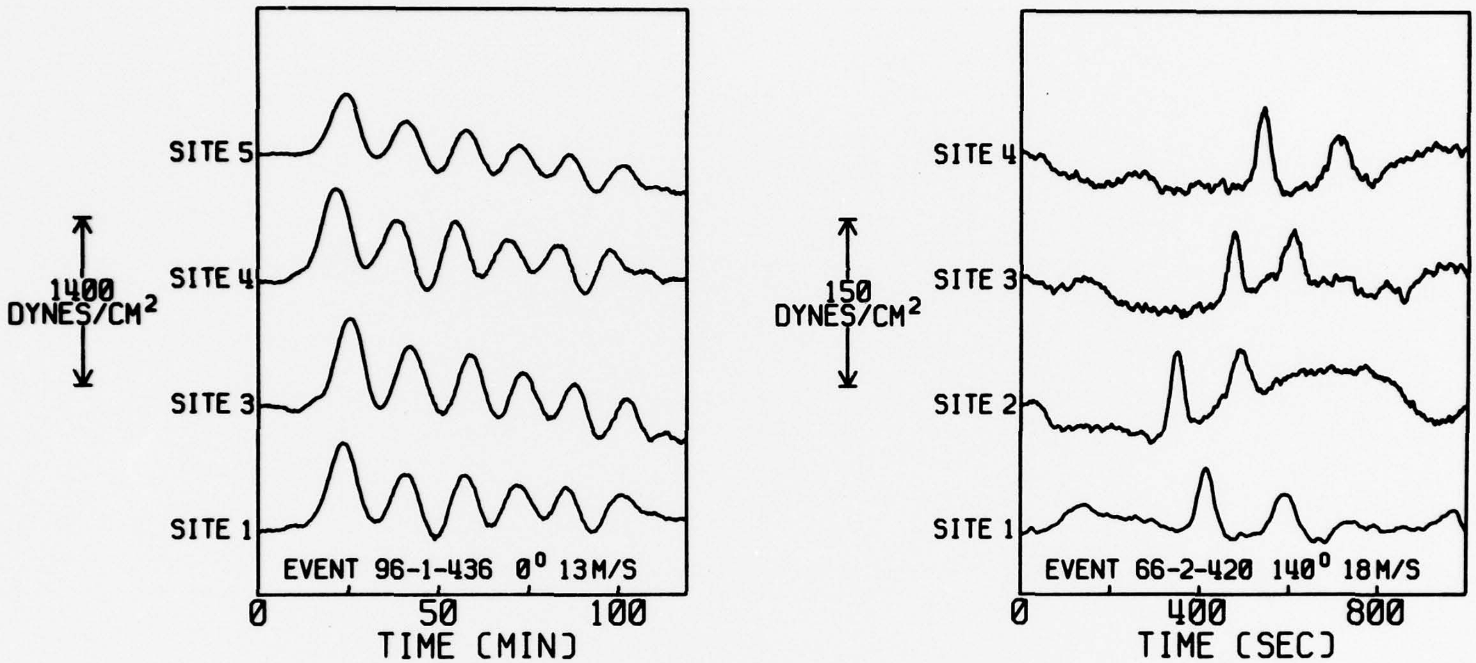

1400
DYNES/CM²
SITE 5
SITE 4
SITE 3
SITE 1
EVENT 96-1-436 0° 13M/S
0
50
100
TIME (MIN)
150
DYNES/CM²
SITE 4
SITE 3
SITE 2
SITE 1
EVENT 66-2-420 140° 18M/S
0
400
800
TIME (SEC)

a

b